SYNAPTIC TRANSMISSION IN THE FERRET LATERAL GENICULATE NUCLEUS IN VITRO: MODULATION BY MEMBRANE VOLTAGE AND NEUROTRANSMITTERS

by

MANUEL ESGUERRA

B. A. Biology / Psychology, Columbia University 1984

Submitted to the Department of Brain and Cognitive Sciences in partial fulfillment of the requirements for the degree of

DOCTOR OF PHILOSOPHY

at the

MASSACHUSETTS INSTITUTE OF TECHNOLOGY
June, 1991

Signature of Author.....
Manuel Esguerra
Department of Brain and Cognitive Sciences
May 8, 1991

Certified by.....
Mriganka Sur
Associate Professor of Neuroscience
Thesis Supervisor

Accepted by.....
Emilio Bizzi
Chairman
Department of Brain and Cognitive Sciences

SYNAPTIC TRANSMISSION IN THE FERRET LATERAL GENICULATE NUCLEUS IN VITRO: MODULATION BY MEMBRANE VOLTAGE AND NEUROTRANSMITTERS

by

MANUEL ESGUERRA

Submitted to the Department of Brain and Cognitive Sciences
on May 1, 1991 in partial fulfillment of the
requirements for the degree of Doctor of Philosophy in
Neuroscience

ABSTRACT

This thesis tested the hypothesis that a specific extraretinal projection to the lateral geniculate nucleus (LGN) can increase the efficacy of retinal transmission by activating the NMDA receptor class of excitatory amino receptors at sites of retinogeniculate input. I used intracellular recordings and afferent stimulation in slices of the ferret lateral geniculate nucleus maintained in vitro to test the effects of membrane potential, neurotransmitter blockade, and electrical stimulation on excitatory potentials elicited by stimulation of the retinogeniculate and corticogeniculate afferent pathways to LGN. The investigation was accomplished in four stages.

I first studied the effects of membrane voltage on action potential output of LGN cells maintained in vitro. This study confirmed that ferret LGN cells can fire action potentials in several modes, depending on the membrane potential. At hyperpolarized voltages, LGN cells responded to depolarizing inputs with high frequency bursts of action potentials elicited by low-threshold calcium spikes. At depolarized potentials, LGN cells responded to stimulation with continuous trains of action potentials whose frequency was linearly related to the membrane potential. I also observed a novel "mixed" firing mode, in which cells showed characteristics of both burst and tonic firing.

In the second study, I investigated the role of NMDA receptors at sites of retinal input. I found that pharmacological blockade of NMDA receptors attenuated all components of the retinogeniculate EPSP. Furthermore, membrane depolarization led to nonlinear enhancement of the EPSP by activation of NMDA receptors at sites of retinogeniculate input.

In the third study, I examined the postsynaptic responses observed in LGN cells after stimulation of the corticogeniculate feedback projection. I found that cortical afferents can elicit both direct excitatory and indirect inhibitory influences on LGN cells. The excitatory response to corticofugal stimulation was sensitive to magnesium

concentration and d-APV, suggesting that NMDA receptors participate in synaptic responses to activity in this projection as well. However, the optic radiations-evoked EPSP was largely insensitive to depolarization at the cell body, suggesting that these sites are located at sites that are electrically distant from cell body.

In the final study, I examined whether the depolarization by excitatory components of the corticofugal feedback projection could activate NMDA receptors at sites of retinogeniculate input. Concurrent stimulation of the retinogeniculate and corticogeniculate pathways led to several types of responses, including nonlinear summation and enhancement of retinogeniculate EPSP amplitude. This enhancement was due in part to activation of NMDA receptors at sites of retinogeniculate input. Thus corticogeniculate feedback can indeed enhance the gain of retinogeniculate transmission by voltage-dependent regulation of NMDA receptors at retinogeniculate synapses.

Thesis supervisor: Dr. Mriganka Sur
Title: Associate Professor of Neuroscience

ACKNOWLEDGMENTS

I am deeply indebted to these people who have put up with me over the years:

Mriganka Sur, who as my friend and adviser has taught me above all that science should be fun, despite the occasional pitfalls that seem so inevitable in this field. Mriganka has been an endless source of clear-headed enthusiasm and crazy enlightenment over our 7 years together in New Haven and Cambridge.

David McCormick, for being so generous with his time, lab, and wizardry. These experiments would have foundered and sunk 2 years ago without David's expertise and encouragement.

Peter Schiller and Ann Graybiel, for their advice and insights on planning and writing this thesis.

Jong-On Hahm, Young Kwon, Anna Roe, and Diana Smetters, for listening and laughing and moving big desks.

Preston Garraghty, for sharing with me The Two Most Important Things You Need to Survive Graduate School - "Organization and perseverance, bub."

Sarah Pallas, Cheryl White, and Sacha Nelson, for egging me on through the worst of times, and convincing me that postdocs can actually be way-cool.

My teachers and colleagues at the Section of Neurobiology at Yale University, for my first two years of graduate training.

Nori Geary, for instilling in me a respect for the wonderful intricacies of the nervous system.

I dedicate this dissertation to my wife Loren, whose love and confidence have sustained me through the years, and especially in these last months of my graduate study.

I was supported by a National Science Foundation Minority Graduate Fellowship a Whitaker Health Sciences Fund Fellowship, and EY07023 to Mriganka Sur for the duration of this research.

TABLE OF CONTENTS

Chapter 1

Introduction and General Methods

INTRODUCTION

Our view of the role of the thalamus in processing of sensory information has undergone a radical transformation in the past 2 decades. The early investigations on the lateral geniculate nucleus (LGN), the major visual center in the thalamus, reinforced the early view that sensory thalamic nuclei are simply relays between the sensory epithelia and their cortical targets. Hubel and Wiesel (1961) reported that the visual responses of LGN cells in anesthetized cats and monkeys differed little from the visual responses of retinal ganglion cells. Their recordings from single LGN neurons revealed concentric, roughly circular receptive fields in which either light offset or onset elicited strong responses. The major finding reported was that antagonistic surround mechanisms appeared to be slightly stronger in the LGN cell receptive fields than in those of retinal ganglion cells. They proposed that the role of the thalamic visual nuclei was to sharpen the retinal receptive fields so that they could be used for construction of various sorts of feature detectors, which at that time were being discovered and described with great success for the visual cortex.

The discovery of parallel channels for visual processing (e.g. Enroth-Cugell and Robson, 1966) in the retina led to a search for similar organization in the LGN. It was found that LGN cells carry the X/Y and ON/OFF channels with little alteration of their properties (Sherman and Spear, 1982). Subsequent studies, all performed in anesthetized animals, described transformations of retinal information by the LGN that resemble receptive fields in the visual cortex, although with poor tuning. These

included slight orientation biases (Leventhal et al., 1985) and length tuning (Murphy and Sillito, 1987). However, most descriptions of LGN cell physiology continued to maintain the view that the representation of the visual field in the LGN is a slightly sharper version of the array of circular receptive fields arriving from the retinal ganglion cells. Mastronarde's description (1987) of the "lagged" and "nonlagged" classes of X cells in cat LGN proposed receptive field properties that appeared to be an emergent feature of LGN circuitry and possibly intrinsic properties of LGN cells themselves. These classes of LGN cells add a significant phase delay to the retinal input, without changing the spatial properties of the receptive field. Mastronarde originally proposed that this delay is produced by inhibitory circuits within the LGN.

These studies of the role of LGN in vision were made against the background of an extensive literature on the role of the thalamus in arousal and sleep. Electroencephalogram and evoked-potential studies indicated that most thalamic nuclei change their behavior dramatically as the animal's state of arousal shifts from fully waking through the various stages of sleep. These neural behaviors appear as synchronized or desynchronized waves of activity within the thalamus. They are dependent on ascending influences from the brainstem, particularly noradrenergic, serotonergic, and cholinergic projections from the locus coeruleus, raphe, reticular formation, and basal forebrain (reviewed by Steriade and Deschenes, 1984).

In addition to the diffuse modulatory projections from the brainstem and basal forebrain, the other major extraretinal projection to the LGN arises in layer 6 of

the visual cortex. Counts of the numbers of layer 6 pyramidal cells labeled after tracer injection into the LGN suggest that the visual cortex sends a larger number of axons back to the LGN than the nucleus receives from the retina; some studies have estimated that the cortical feedback projection is 10 to 40 times larger than the retinal projection (Updyke, 1975; Robson, 1983). Thus the primary target of LGN relay cell axons must have a profound influence on its own input, by activity in this large projection.

Studies that have investigated the possible role of this projection in intact animals have proven inconclusive. These studies have used various techniques to inactivate or stimulate the cortex while recording the visual responses of LGN cells. The inactivation methods employed include repetitive stimulation (Hull,1968); cooling (Kalil and Chase, 1970; Baker and Malpeli, 1977; Geisert et al., 1981); and ablation (Murphy and Sillito, 1987). Stimulation of the cortical feedback projection has been attempted electrically (Ahlsen et al., 1982), by iontophoresis of excitatory transmitters (Tsumoto et al., 1978), and with visual stimuli (Marrocco et al. 1982). The general conclusion from these studies was that the corticofugal projection to LGN can have either an inhibitory or excitatory influence; the conditions under which one or the other would prevail remains unknown.

Recent studies of the intrinsic properties of thalamic neurons have led to a reconsideration of the role of the thalamus in sensory processing. Recordings from isolated slices of guinea pig thalamus revealed that thalamic neurons, including those of the LGN, possess an ensemble of membrane conductances that profoundly change

the cells' patterns of spike output (Jahnsen and Llinas, 1984). These authors found that changes in standing membrane voltage can switch thalamic cells between a burst mode, in which cells fire action potentials at frequencies independent of external influences; and a tonic firing mode, where spike output appears to reflect the intensity of stimulation applied to the cell. Crick (1984) proposed that these modes could underlie different states of selective visual attention, and suggested that an extraretinal structure, the thalamic reticular nucleus, might be capable of causing cells to switch between these modes in vivo. For example, specific groups of cells could be switched to tonic firing modes when they were required for selective attention to parts of a visual scene.

The discovery of subclasses of excitatory amino acid receptors in the retinogeniculate projection has led to further refinement of hypotheses on the role of the LGN in gating of visual information. The N-methyl-D-aspartate (NMDA) type of excitatory amino acid receptor is present at postsynaptic sites on all cell classes found in the LGN (Kemp and Sillito, 1982; Heggelund and Harveit, 1990; Esguerra et al., 1990; Kwon et al., 1991). This receptor has the unusual property of allowing large currents to flow across the membrane only when the neurotransmitter binds and the membrane potential is depolarized to voltages more positive than -60 mV (Mayer and Westbrook, 1987). This feature is due to magnesium block of the channel pore, which is removed by depolarization (Ascher et al., 1988). The voltage-dependent magnesium block of the channel causes the appearance of a "negative slope conductance" region in the current-voltage characteristics of the

NMDA receptor gated current. Over the voltage ranges at which negative slope conductance is seen, membrane potential may be considered "unstable," since inward current would tend to depolarize the membrane and lead to further increases in inward current (Benson and Adams, 1987). Synaptic conductances that include such negative conductance regions should then be capable of amplifying small depolarizing changes in membrane voltage, given that the initial membrane potential is in the appropriate range.

It has been proposed that synaptic sites containing NMDA receptors operate as computational AND gates, that sense the conjunction of temporally close excitatory inputs and respond with a large current signal (Koch, 1987). Thus membrane depolarization of LGN cells, which would activate subsynaptic NMDA receptors concurrent with retinal input, should increase the probability and/or frequency of retinally evoked action potentials. This gating mechanism does not require a radical shift in membrane potential, as would be required to switch cells between burst and tonic modes; rather a change of a few millivolts, on the order of those produced by single synaptic inputs, would be sufficient to activate this mechanism. Activation of this amplification mechanism in specific portions of the visual representation would have important implications for selection of certain inputs over others, since these sites would be sending stronger signals to the visual cortex.

In order to support this hypothesis for the LGN, the following assumptions must be tested: 1) The action potential output of LGN cells must be sensitive to membrane voltage; 2) Sites of retinal input contain NMDA receptors which, upon

activation by depolarization, increase the current flow across the synapse to cause larger voltage changes in response to retinal activity; 3) Extraretinal projections exist that can depolarize the membrane at sites of retinogeniculate input; 4) The depolarization caused by activity in this pathway is sufficient to activate the NMDA receptors at sites of retinogeniculate input. The aim of this thesis is to test each of these assumptions by studying the synaptic responses of cells in the lateral geniculate nucleus of the ferret. Each of these issues is considered in order, in each of the succeeding chapters.

Specific Aims

The aim of this study was to determine whether a specific extraretinal input to LGN cells, the corticogeniculate projection, can alter the efficacy of retinogeniculate transmission by modulating membrane potential. This question was addressed by investigating the four issues outlined below.

1. The first goal was to describe how the ensemble of intrinsic, voltage sensitive membrane conductances in the ferret LGN modulates patterns of spike output produced by synaptic activation or direct current injection. This description would be used to predict the effects of voltage changes induced by stimulation of extraretinal afferents.

2. The second goal was the description of the excitatory postsynaptic potential (EPSP) evoked by activation of retinogeniculate synapses, in particular the effects of

membrane voltage changes on synaptic components mediated by NMDA receptors. I tested the specific prediction that these receptors enhance the efficacy of retinogeniculate transmission when they are activated during membrane depolarization.

3. The third goal was to describe LGN cell responses to corticogeniculate afferent stimulation. I investigated the time course and amplitude of responses to cortical afferent stimulation and its effects on the membrane potential recorded at the soma.

4. The fourth goal was to investigate the interaction between voltage changes induced by cortical afferent activation, and their effect on the retinogeniculate EPSP. Specifically, if corticogeniculate projection leads to depolarization of the membrane, is it sufficient to activate NMDA receptors at sites of retinogeniculate input? This result would support the hypothesis that a function of the corticofugal feedback projection is to gate the flow of visual information between the retina and visual cortex by altering the probability of action potential output at the lateral geniculate nucleus.

REFERENCES

Ahlsen, G., Grant, K., and Lindstrom, S. (1982). Monosynaptic excitation of principal cells in the lateral geniculate nucleus by corticofugal fibers. Brain Res. 234, 454-458.

Ascher, P., Bregestovski, P., and Nowak, L. (1988). N-methyl-D-aspartate-activated channels of mouse central neurones in magnesium-free solutions. J. Physiol. 399, 207-226.

Baker, F.H., and Malpeli, J.G. (1977). Effects of cryogenic blockade of visual cortex on the responses of lateral geniculate neurons in the monkey. Exp. Brain Res. 29, 433-444.

Benson, J. A., and Adams, W. B. (1987). The control of rhythmic neuronal firing. In Kaczmarek, L. K., and Levitan, I. B. eds. Neuromodulation. Oxford: Oxford University Press.

Crick, F.H.C. (1984). Function of the thalamic reticular complex: the search light hypothesis. Proc. Natl. Acad. Sci USA 81, 4586-4590.

Enroth-Cugell, C., and Robson, J. G. (1966). The contrast sensitivity of retinal

ganglion cells in the cat. J. Physiol. 187, 517-552.

Esguerra, M., and Sur, M. (1990). Corticogeniculate feedback gates retinogeniculate transmission by activating NMDA receptors. Soc. Neurosci. Abstr. 16, 159.

Geisert, E.E., Langsetmo, A., and Spear, P.D. (1981). Influence of the cortico-geniculate pathway on response properties of cat lateral geniculate neurons. Brain Res. 208, 409-415.

Heggelund, P., and Hartveit, E. (1990). Neurotransmitter receptors mediating excitatory input to cells in the the cat lateral geniculate nucleus. I. Lagged cells. J. Neurophysiol. 63, 1347-1360.

Hubel, D. H., and Wiesel, T. N. (1961). Integrative action in the cat's lateral geniculate body. J. Physiol. 155, 385-398.

Hubel, D. H., and Wiesel, T. N. (1977). Functional architecture of macaque monkey visual cortex (Ferrier lecture). Proc. Roy. Soc. Lond B 198, 1-59.

Hull, E. (1968). Corticofugal influence in the macaque lateral geniculate nucleus. Vision Res. 8, 1285-1298.

Jahnsen, H., and Llinas, R. (1984). Electrophysiological properties of guinea- pig thalamic neurones: an in vitro study. J. Physiol. 349, 205-226.

Kalil, R. E., and Chase, R. (1970). Corticofugal influence on activity of lateral geniculate neurons in the cat. J. Neurophysiol. 33, 459- 474.

Kemp, J. A., and Sillito, A. M. (1982). The nature of the excitatory transmitter mediating X and Y cell inputs to the cat dorsal lateral geniculate nucleus. J. Physiol. 323, 377-391.

Koch, C. (1987). The action of the corticofugal pathway on sensory thalamic nuclei: a hypothesis. Neuroscience 23, 399-406.

Kwon, Y. H., Esguerra, M., and Sur, M. (1991). NMDA and non-NMDA receptors mediate visual responses of neurons in the cat's lateral geniculate nucleus. J. Neurophysiol., in press.

Marr, D. (1982). Vision: a computational investigation into the human representation and processing of visual information. New York: WH Freeman.

Marrocco, R. T., McClurkin, J. W., and Young, R. A. (1982). Modulation of lateral geniculate nucleus cell responsiveness by visual activation of the corticogeniculate

pathway. J. Neurosci. 2, 256-263.

Mastronarde, D.N. (1987). Two classes of single-input X cells in the cat lateral geniculate nucleus. I. Receptive field properties and classification of cells. J. Neurophysiol. 57, 357-380.

Mayer, M. L., and Westbrook, G. L. (1987). The physiology of excitatory amino acids in the vertebrate central nervous system. Prog. Neurobiol. 28, 197-276.

Murphy, P.C., and Sillito, A.M. (1987). Corticofugal feedback influences the generation of length tuning in the visual pathway. Nature 329, 727-729.

Sherman, S. M., and Spear, P. D. (1982). Organization of visual pathways in normal and visually deprived cats. Physiol. Rev. 62, 738-855.

Steriade, M., and Deschenes, M. (1984). The thalamus as a neuronal oscillator. Brain Res. Rev. 8, 1-63.

GENERAL METHODS

Choice of preparation

Choice of species I chose to use ferrets for these experiments primarily because their visual systems are anatomically and physiologically very similar to those of the well-studied cat (Jackson and Hickey, 1985). The ferret's visual pathway contains the parallel X/Y and ON/OFF channels (Roe et al., 1988) whose physiological characteristics have been described in great detail in the past 20 years (Sherman and Spear, 1982; Sherman, 1985). Furthermore, the morphological cell types described for cat LGN (Friedlander et al, 1981) are present in the ferret, suggesting that estimates of the passive cable properties of ferret LGN cells may be obtained from the values derived for cat LGN cells (Bloomfield et al., 1987; Esguerra et al., 1987).

Ferrets have recently become a useful model for studies of visual development. Since ferrets are born after a gestation period 23 days shorter than the cat's (Linden et al., 1981), it is possible with newborn ferrets to investigate developmental phenomena which would have required prenatal interventions in the cat (e.g. Roe, 1991). The present studies were undertaken in part with the aim of describing the physiological properties of adult LGN cells for comparison with the developing LGN.

Choice of an <u>in vitro</u> preparation These experiments were carried out using intracellular recording in slices of the ferret lateral geniculate nucleus maintained <u>in</u>

vitro. I chose a slice preparation for the following reasons.

1) Intracellular recording is necessary for investigating voltage changes due to synaptic events. Such subthreshold events cannot be observed at the single-cell level with extracellular recordings.

2) Mechanical stability. In an intact animal, maintaining intracellular recordings is extremely difficult because of the instabilities introduced by breathing and heartbeat. These movements invariably cause the electrode to damage the cell membrane, leading to leaks which compromise the cell's physiological properties. Isolation of the nucleus removes it from the influences of respiration and pulse, allowing long-term stable impalements.

3) Visibility. In the isolated preparation, the lateral geniculate nucleus is readily identifiable under visual inspection. Slices can thus be cut and oriented to allow stimulation of specific afferent pathways and recording from specific locations within a nucleus. In the ferret lateral geniculate nucleus, the optic radiations (anterior to LGN) and optic tract (posterior and ventral to LGN), and the laminar divisions were clearly visible, allowing me to place stimulating and recording electrodes in specific locations.

4) Access to the extracellular environment. The in vitro preparation allows presentation of drugs in precise concentrations, and manipulation of ionic

composition of the extracellular fluid. These techniques are essential to understanding the role of neurotransmitters and ionic conductances in modulating the activity of a neuron.

5) Isolation from activity of ascending and descending modulatory influences. In the intact preparation, the lateral geniculate nucleus is subject to a continuous barrage of modulatory influences arising from spontaneous and evoked activity in the retina, cortex, and brainstem. The slice preparation removes the activity of these sensory modulatory influences and allows instead specific and controlled stimulation of the various pathways. The isolated lateral geniculate nucleus preparation is particularly attractive in this respect because the retinal projection, which enters through the optic tract at the posterior edge of the nucleus, is well separated from the corticofugal input, which enters through the anterior optic radiations. This geometry, combined with the option of pharmacological blockade of inhibition, allows intracellular recording from cells devoid of all input except 2 distinct excitatory afferent sources. Thus the LGN preparation is ideal for studies of summation of postsynaptic responses in single neurons.

LGN slice preparation and recording

In the following I shall describe the slice preparation, maintenance, and recording techniques that were common to the experiments described in this thesis. Techniques

specific to any given study are described in more detail in the Methods section of each chapter.

Preparation of LGN slices

Forty-nine ferrets at least 8 weeks of age obtained from Marshall Farms (North Rose, NY) and maintained under normal housing conditions were used for these experiments. Animals were anesthetized deeply with the combination of methoxyflurane (open drop inhalation) and pentobarbital (35 mg/kg i.p.), or with a mixture of ketamine (40 mg/kg i.m.) and xylazine (4 mg/kg i.m.), and were placed in a stereotaxic apparatus to immobilize the head during surgery. Large craniotomies were made to expose the surfaces of both cerebral hemispheres from the occipital pole to the level of the ansate sulcus. The animal then received a lethal dose of anesthetic, and was killed by decapitation. The brain was rapidly removed and placed in a beaker of artificial cerebrospinal fluid (ACSF; see below for composition) at 5°-8° C. The excised brain was immediately bisected sagittally and one half returned to cold ACSF while the other was prepared for slicing. The thalamus was exposed by dissecting away the cortex and hippocampus with forceps and a #11 scalpel blade. The medial face of the exposed hemithalamus was glued to a Petri dish held in the chuck of a Vibratome (Technical Products, St. Louis, MO) with the LGN oriented so that the blade entered the nucleus from the dorsolateral direction. Agar blocks were glued in place to support the tissue, which was then submerged in cold ACSF for slicing.

Parasagittal slices 400 μm thick were cut from each LGN and removed to cold ACSF. Slices cut from the first half of the brain were immediately placed in the recording chamber; slices from the other hemisphere were maintained for later use in continuously oxygenated ACSF at room temperature. I found no consistent physiological differences between slices used immediately after cutting and those maintained in the holding chamber for several hours before use.

Slice chamber and physiological recording

Early recordings in this series of experiments were made in a submersion chamber modified from an interface design (Medical Systems, Greenvale, NY) in which slices were submerged under 2 mm of continuously flowing oxygenated ACSF. In later experiments, recordings were made in an interface chamber (Fine Science Tools Inc., Belmont, CA) in which slices rested on nylon mesh at the interface between oxygenated ACSF and a humidified atmosphere of 95% O_2 / 5% CO_2. This chamber afforded greater visibility and mechanical stability than did the submersion chamber, as well as finer control over agonist presentation (see below). In both chambers, slice temperature was maintained at 35° C and the ACSF flow rate was 1.0-1.5 ml/minute.

The ACSF used in these experiments contained the following (in mM): NaCl, 126; KCl, 3; NaH_2PO_4, 1.25; dextrose, 10; $NaHCO_3$, 20; $MgSO_4$, 1.2; and $CaCl_2$, 2.5; pH 7.4 when saturated with 95% O_2/ 5% CO_2. This mixture closely approximates the composition of cerebrospinal fluid in vivo (Kerkut and Wheal,

1981); therefore the reversal potentials and driving forces on ionic currents observed in the slice preparation were expected to be similar to those seen in vivo.

Optic tract stimulation

Bipolar stimulating electrodes were placed on the optic tract at the outer edge of the slice, or in the optic radiations 100 μm from the anterior edge of lamina A (Figure 1). The stimulating electrodes were constructed by twisting together a pair of teflon-insulated platinum-iridium wires (diameter, 0.002") and cutting their tips flush. This assembly was glued inside a glass capillary tube held in a micromanipulator. The cut ends of the wires protruded from the end of the tube and provided an area of uninsulated metal sufficient for passage of up to 1.0 mA stimulating current. A constant current source (Grass Instruments, Quincy MA) delivered single-shock electrical stimuli at currents of 0.1-0.8 mA, 0.05-0.08 ms duration at 0.5 Hz. These currents corresponded to stimulation voltages between 2 and 20 V when measured with a high impedance AC probe placed across the isolation unit output. In the early experiments, this probe was used to monitor continuously the stimulation electrode voltage, to ensure that the current passing characteristics of this design did not change during repetitive stimulation at 0.5 Hz.

One hour after placement in the chamber, the quality of the tissue was assessed by passing a tungsten recording electrode through the slices and observing extracellular action potentials. I made intracellular recordings only from sites that showed vigorous multi-unit activity with large-amplitude, narrow spikes and no sign

of spreading depression. In healthy slices, the optic tract, optic radiations, and eye-specific laminae were clearly visible under either transillumination or epi-illumination, and electrodes were easily placed in any of these regions. To increase the probability of recording postsynaptic responses to afferent stimulation, recordings were made in the A-laminae close to presumed lines of projection, i.e., along lines emanating from the stimulating electrodes perpendicular to laminar borders and the edge of the optic tract.

Intracellular recording

Intracellular recordings were made with unbeveled micropipettes formed from thin wall capillary tubing (WPI, Sarasota, FL) on a Flaming-Brown puller (Sutter, San Rafael, CA). Electrode impedances (d.c.) were between 30-60 MΩ after filling with 4M potassium acetate or 4M cesium acetate. Intracellular signals were recorded through an Axoclamp 2A amplifier operating in bridge mode (Axon Instruments, Foster City, CA). Neurons were impaled by brief capacity overcompensation.

Digitized responses were collected online using the Labmaster DMA data acquisition board and pClamp program suite (Axon Instruments) running on an 80286 based microcomputer. Data were also continuously digitized through a video interface (Neurodata Instruments, New York, NY) and saved on videotape for offline analysis.

Sampling criteria

Successful impalements of LGN cells were signaled by a sudden voltage drop of about 20 mV, a large increase in resistance and time constant, and a barrage of injury spikes which simultaneously increased in amplitude and subsided in frequency. Membrane potential continued to improve over the next 2-5 minutes, either spontaneously or in response to hyperpolarizing current injection and/or small adjustments of electrode position. A recording was judged stable when I observed a resting potential of at least 50 mV, input resistance of at least 10 MΩ without fluctuation, and no spontaneous action potentials.

Drug presentation

The NMDA receptor antagonist d-2-amino-5-phosphonovaleric acid (d-APV, 10-40 μM; Cambridge Research Biochemicals, Valley Stream, NY) was introduced via the bathing solution by switching to a second ACSF reservoir to which the drug had been added in known concentrations. In some experiments I also applied to the bath the non-NMDA receptor antagonist 6-cyano-7-nitroquinoxaline-2,3-dione (CNQX, 5-10 μM; Cambridge Research Biochemicals) or the $GABA_A$ receptor antagonist bicuculline methiodide (BIC, 10 μM; Sigma, St. Louis, MO).

Agonists were presented by different means, in order to allow rapid presentation and washout of the drugs. In the submersion chamber, a hand-held micropipettor was used to inject microliter amounts of stock agonist solution directly into the recording well (well volume, 2 ml). In the interface chamber, agonists dissolved in ACSF were presented in hanging drops produced by pulses of pressure through a

broken micropipette connected to a Picospritzer (General Valve) operating at 20-40 psi nitrogen pressure. The pipette tip was lowered onto the tissue within 100 μm of the recording site and the drop allowed to spread out over the slice.

When magnesium was removed from the medium, it was replaced with equimolar sodium to preserve osmotic balance and pH.

Measures of synaptic responses

The pClamp software was used to measure amplitudes and time courses of retinogeniculate EPSPs. Peak EPSP amplitudes were measured relative to the baseline voltage immediately prior to optic tract stimulation. The program estimated exponential decay constants for falling phases of EPSPs by least square fits to curves described by

$$y(t) = A_0 + A_1 e^{(-t/\tau)}$$

where y = voltage, A = amplitude, t = time in ms, and τ = decay constant.

Interpretation of data from LGN slices

Several factors must be considered when interpreting intracellular recordings from this preparation.

Damage due to slicing While the slicing procedure would appear to be highly traumatic, slices of lateral geniculate nucleus usually recovered well from the procedure. In the chamber, the cells maintained deep resting potentials and large

input resistance, and continued to fire large spikes for up to 12 hours. It seems unlikely that a highly damaged cell would be capable of remaining viable for this length of time. Furthermore, my sampling_criteria are designed to eliminate cells that have sustained extensive damage, for example those at the surface of the slice, whose physiological properties have been compromised by tearing of their somatic and dendritic membranes.

Limitations of intracellular current injection It is important to note that these recordings were made with the amplifier operating in bridge mode rather than in discontinuous current clamp mode. Bridge mode offers the advantage of allowing continuous ejection of constant current with simultaneous monitoring of intracellular voltage. A disadvantage of bridge recordings is that large inaccuracies in observed voltages can result from small changes in electrode tip resistance. While this problem would be eliminated with discontinuous current clamp recordings, my electrode configuration would have limited the sampling rate to 3-5 kHz. This low rate would severely attenuate fast events such as EPSP rise times. Thus, I recorded in bridge mode and continuously monitored the balance circuit to ensure that voltage drops across the electrode resistance were always cancelled and did not contribute to observed voltages. In any event, recalibration of the bridge setting was rarely necessary once a cell was impaled, even after passage of many current pulses. I attribute this stability to my use of low-impedance (30-60 MΩ) thin-wall microelectrodes, which are less prone to tip blockage once intracellular.

A more serious limitation of the intracellular method is that the space clamp

achieved with sharp electrodes is typically quite poor in multipolar cells (Johnston and Brown, 1983). This means that I was able to affect voltage-sensitive conductances only in membrane regions close to the recording electrode, i.e. in the soma and primary dendrites. Filling of the recording pipette with a cesium solution alleviated this problem somewhat by increasing input resistance via block of outward potassium currents; however, conductances on distal processes were probably still beyond the influence of these electrodes. Hence, the results reported here must be interpreted as reflecting the modulation of somatic and proximal dendritic conductances.

Electrical stimulation vs. sensory input The stimulation paradigm used here simultaneously excites many afferent fibers in the optic tract and optic radiations. Thus, when a cell under study is stimulated, all the surrounding cells are likely to be active as well. Such monolithic stimuli are probably rarely experienced by the LGN under normal conditions. However, the functional consequences of sychronous stimulation are likely to be minimal in the LGN. There is no evidence for excitatory or recurrent connections between cells of the LGN (Friedlander et al., 1981); therefore epilepsy-like seizures would not be induced in this nucleus as they might be in a slice cortex. Synchronous stimulation might also be expected to cause simultaneous release of large amounts of excitatory amino acid transmitters into the slice. However, since the neurons in this preparation remain electrophysiologically viable for many hours, it is likely that high affinity glutamate reuptake in neurons and especially glia (Fonnum, 1984) continues to function normally as well.

REFERENCES

Bloomfield, S. A., Hamos, J.E., and Sherman, S.M. (1987) Passive cable properties and morphological correlates of neurones in the lateral geniculate nucleus of the cat. J. Physiol. 383, 653-692.

Esguerra, M., Roe, A.W., and Sur, M. (1987). Morphology of identified ferret LGN neurons characterized in vivo and in vitro. Soc. Neurosci. Abstr. 13, 1434.

Fonnum, F. (1984). Glutamate: a neurotransmitter in mammalian brain. J. Neurochem. 42, 1-11.

Friedlander, M. J., Lin, C.-S., Stanford, L.R., and Sherman, S.M. (1981). Morphology of functionally identified neurons in lateral geniculate nucleus of the cat. J. Neurophysiol. 46, 80-129.

Jackson, C. A., and Hickey, T. L. (1985) Use of ferrets in studies of the visual system. Lab. Animal Sci. 35, 211-215.

Johnston, D., and Brown, T.H. (1983). Interpretation of voltage-clamp measurements in hippocampal neurons. J. Neurophysiol. 50, 464-486.

Kerkut, G.A., and Wheal, H. V. (1981). Electrophysiology of isolated mammalian CNS preparations. New York: Academic Press.

Linden, D. C., Guillery, R.W., Cucchiaro, J. (1981). The dorsal lateral geniculate nucleus of the normal ferret and its postnatal development. J. Comp. Neurol. 203, 189-211.

Roe, A.W., Garraghty, P.E., and Sur, M. (1989). Terminal arbors of single ON-center and OFF center X and Y retinal ganglion cell axons within the ferret's lateral geniculate nucleus. J. Comp. Neurol. 288, 208-242.

Roe, A.W. (1991). Functional transformations of visual input by auditory thalamus and cortex: an experimentally induced visual pathway in ferrets. Ph.D. dissertation, MIT.

Sherman, S.M. (1985). Functional organization of the W-, X-, and Y-cell pathways in the cat: a review and hypothesis. Prog. Psychobiol. Physiol. Psych. 2, 233-314.

FIGURE LEGENDS

Figure 1. Schematic representation of LGN slice prepared for dual optic tract and optic radiation stimulation. Bipolar stimulating electrodes were placed on the optic tract (OT) just outside the C laminae and in the optic radiations (OR) about 100 μm from the inner border of lamina A. Recordings were made from cells in line with the two electrodes.

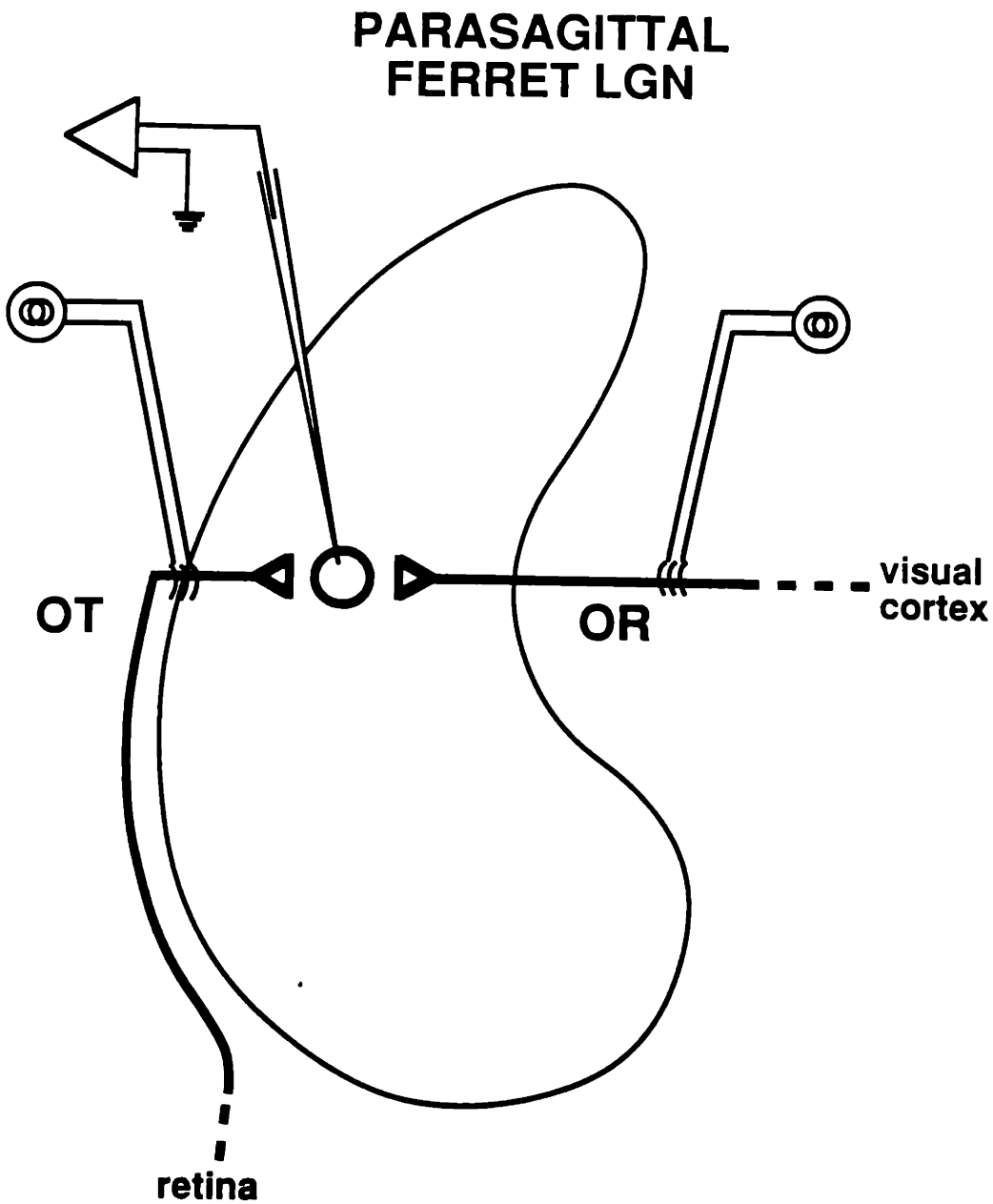
PARASAGITTAL
FERRET LGN
OT
OR
visual
cortex
retina

Chapter 2

Electrophysiological properties and signaling modes of neurons in the ferret lateral geniculate nucleus

ABSTRACT

I used intracellular recordings to examine the action potential firing modes of cells in the ferret lateral geniculate nucleus (LGN) in vitro. I compared the effects of altering membrane voltage on the patterns of action potentials evoked by stimulation with direct current injection and by afferent (synaptic) stimulation. My results confirm that LGN cells in the ferret can fire action potentials in the "burst" and "tonic" modes that have been described previously for other species. At depolarized membrane potentials, LGN neurons respond to sustained depolarization with short-latency trains of action potentials whose frequency is directly proportional to the amount of current injected. At hyperpolarized membrane potentials, LGN cells enter burst mode, in which the input is differentiated into brief high-frequency discharges whose latency varies with membrane potential. I also observed a "mixed" mode in which LGN cell responses, over a narrow range of membrane potentials, reflect aspects of both burst and tonic firing simultaneously. Thus a striking consequence of the interplay among thalamic membrane conductances is wide variability in length, duration, and latency of spike discharges elicited by identical stimuli. My results suggest that the concept that LGN cells display only 2 active response modes must be qualified to include varying amounts of delay and the possibility of mixed discharges.

INTRODUCTION

Neurons of the mammalian lateral geniculate nucleus (LGN) receive converging synaptic inputs from numerous sources, including retinal afferents, intrathalamic connections, feedback projections from target structures, and ascending projections from the brainstem and basal forebrain (Sherman and Koch, 1986; Steriade and Llinas, 1988). The synaptic conductances that these pathways activate lead to immediate and profound changes in the membrane potential of LGN cells. The membrane of thalamic neurons also contains many intrinsic voltage-sensitive conductances whose activation can either counter or enhance these changes in membrane potential. Thus thalamic cells are subject to powerful regulation of their spike output when these rapid hyperpolarizing and depolarizing conductances interact with synaptic responses to retinal afferent activity. Extraretinal brain structures may thus act in concert to modulate the strength and timing of spike trains carrying visual information through the LGN to the cortex. This chapter describes the patterns of action potentials elicited by synaptic and direct current stimulation in cells of the ferret LGN held at varying membrane potentials.

I shall briefly summarize here the major classes of intrinsic membrane conductances found in thalamic neurons; a more detailed treatment can be found in the review of Steriade and Llinas (1988). The conventional voltage-gated sodium and potassium dependent conductances underlie somatic and axonal action potentials

in LGN cells, giving rise to narrow overshooting spikes. The other major currents in the cell body and dendrites are carried primarily by calcium, potassium, and sodium ions. Calcium ions underlie a conductance known as I_T or low-threshold calcium current, which is responsible for rhythmic bursting activity at hyperpolarized membrane potentials. This conductance is largely inactivated at membrane potentials positive to about -65 mV. Negative to -65 mV, I_T can be activated by small depolarizing voltage steps to give rise to a slowly inactivating low threshold "spike" capped by bursts of fast action potentials (Jahnsen and Llinas, 1984; McCormick and Feeser, 1990; Coulter et al., 1989). Calcium ions also mediate a high-threshhold current activated near -55 mV, that may contribute to active dendritic spiking (Crunelli et al., 1989; Hernandez-Cruz and Pape, 1989).

The membrane of thalamic cells contains an abundance of voltage dependent potassium currents (Rudy, 1988). These include several species of "A" currents (I_A), which are activated near action potential threshold. These currents are believed to regulate the frequency of tonic action potential trains and underlie delayed- onset spiking (McCormick, 1990). Other cation currents that are activated by hyperpolarization tend to force membrane potential back toward resting levels. These include the potassium mediated inward rectifier, which activates at membrane potentials negative to E_K; and the mixed cation current I_H, which activates between -60 and -95 mV (McCormick and Pape, 1990). An important current carried primarily by sodium ions is the non-inactivating or "persistent" sodium conductance activated near spike threshold, which ramps the membrane potential slowly in the

depolarizing direction to modulate the onset of spiking and to maintain prolonged spike discharges. The integration of these membrane and synaptic currents allows complex modulation of membrane voltage, especially in the ranges just subthreshold for action potential generation.

This chapter will describe the effects of membrane potential on the final spike output of neurons in the ferret lateral geniculate nucleus in vitro. It is not intended to be an exhaustive account of the ensemble of membrane currents present in ferret LGN cells, but rather examines how membrane voltage, acting through these currents, influences the spike pattern that is finally relayed to the cortex. My results confirm that cells in the isolated ferret LGN fire action potentials in several modes, dependent on the standing membrane potential at the time of stimulation.

METHODS

Preparation of LGN slices

Slices of adult ferret LGN were prepared for recording and stimulation as described previously in the chapter on General Methods.

Current injection procedure

The recording electrodes used in this study contained either 4 M potassium acetate or 4 M cesium acetate in distilled water. Membrane potential was adjusted by injection of current through the recording electrode. Between 9 and 16 current steps were presented serially, either manually or under computer control, usually beginning with the largest hyperpolarizing step and progressing in the depolarizing direction in 0.1 nA steps.

RESULTS

Thirty-three neurons that met the criteria for stable intracellular recording were used for analysis of physiological properties. Since complete sets of analyses were not obtained from all cells, subsets of this sample were used for each of the studies described below.

Passive electrical characteristics

The resting potential measured after stabilization of recording and confirmed

upon rapid retraction of the electrode from the cell was -61.8 ± 6.1 mV (mean ± S.D., n= 33). In the absence of stimulation, resting membrane potentials showed no signs of spontaneous fluctuation or oscillations. I only rarely observed spontaneous EPSP or IPSP activation in this preparation. Input resistances were estimated by measuring the voltage change induced at the end of a hyperpolarizing current pulse > 100 ms in duration. In order to minimize contamination by active conductances or other nonlinearities, I measured input resistances only from traces where the voltage drop was less than 15 mV. The apparent input resistance of LGN cells was 38.9 ± 28.5 MΩ, ranging between 11.3 and 124.5 MΩ (n=27). Input resistances were not well correlated with resting membrane potentials ($r < .20$), suggesting that leakage of current around the recording electrode, which would tend to lower apparent input resistance, did not significantly affect membrane potential (Adams and Brown, 1975).

The passive membrane time constant was estimated by least-squares fitting of the voltage decay at the end of the current step to a single-term exponential of the form

$$y(t) = A_0 + A_1 e^{(-t/\tau_m)}$$

where y = voltage, A = amplitude, t = time in ms, and τ_m = time constant. The membrane time constant of LGN cells was 14.5 ± 11.8 ms (n = 25), as measured from fits where $r > 0.98$. If we assume a specific membrane capacitance C_m of 1

$\mu F / cm^2$ (Hille, 1984), then from

$$\tau_m = R_m C_m ,$$

where R_m = specific resistivity, my estimate for the specific membrane resistivity of ferret LGN cells is approximately 14500 Ω cm^2. Table 1 summarizes the passive electrophysiological characteristics of 17 ferret LGN cells recorded over 11 experiments. My values for the passive properties of ferret LGN cells are slightly lower than the same measures from LGN cells of other species, but are otherwise in general agreement (Table 2). The spike heights may have been attenuated slightly by the sampling rate used to digitalize my data (10 kHz).

Current-voltage relationships

I investigated in detail the current-voltage relationships of 17 representative LGN cells. Square current pulses >100 duration and varying in amplitude between -1.0 nA (hyperpolarizing) and +1.0 nA (depolarizing) were injected through the recording electrode and the resulting voltage deflections were measured. The cells were tested at starting membrane potentials between -75 and -44 mV. The voltage changes often included active components that either inactivated or reached a steady state by the end of the current pulse. Therefore I measured voltage deflections at 2 points, one 40 ms after the onset of current, and the other in the steady-state region just before the end of the current pulse (see inset in Figure 1). The current-voltage plots for most of the neurons tested (13 of 17) showed 2 distinct types of nonlinearity. The

first was a conductance increase toward the hyperpolarizing direction in response to depolarizing current pulses (Figure 1, open circles). The second type of current-voltage nonlinearity was a depolarizing conductance increase at deeply hyperpolarized membrane potentials (n=12). The triangles in Figure 1 indicate voltages attained 40 ms after the start of current injection; comparison with the steady-state values (circles) suggests that membrane conductance is higher at the end of the pulse for hyperpolarizing currents. This component of the response suggests that deep hyperpolarization activates an inward membrane conductance that drives the membrane voltage back toward resting values; this rectification may be necessary for regulating the frequency of spontaneous oscillations that are sometimes observed in LGN cells (see below, under **Burst firing mode**).

Firing modes of ferret LGN cells

When held at varying membrane potentials, cells in the isolated LGN fired action potentials in several patterns upon stimulation with depolarizing current pulses. The expression of these patterns was exquisitely sensitive to small changes in the pre-stimulation membrane voltage. Figure 2 shows traces from a representative LGN cell exemplifying these firing modes; all responses were elicited by a depolarizing step of the same amplitude and duration. At membrane potentials depolarized from rest (-54 mV in Figure 1), the cell fired short-latency trains of spikes that lasted over the duration of the current injection with little or no spike frequency adaptation. At membrane potentials hyperpolarized from rest (-73 mV),

this cell did not fire action potentials, but responded with partial activation of a slow depolarizing potential (open arrow) that developed at more hyperpolarized levels into large, long-duration potentials. These low-threshold potentials (shown at -78 and -89 mV) often were capped by brief bursts of action potentials whose latency increased with deeper hyperpolarization. I examined synaptic responses and responses to current injection in greater detail throughout this range of membrane potentials.

Depolarized membrane potentials: tonic firing mode

At membrane potentials between rest and -53 mV, depolarization by current injection elicited sustained firing of action potentials. Figure 3A shows responses of an LGN cell to injection of 0.3 to 0.8 nA depolarizing current pulses (120 ms duration) from a resting potential of -61 mV. As expected, increasing the amount of depolarization elicited action potential trains of increasing frequency, ranging from a train with a mean frequency of 100 Hz with application of 0.8 nA, to a single spike response at 0.4 nA. In all 17 cells tested, the increase in spike frequency was directly proportional to the amount of injected current as shown here (Figure 3c). The frequency of these tonically activated spikes rarely exceeded 150 Hz.

At some stimulus intensities, action potential frequency appeared to slow slightly at the end of long duration pulses. The amount of spike frequency adaptation appeared to be inversely related to the amount of injected current and mean spike frequency (Figure 3b). At the highest stimulation intensity, the interspike intervals

remained relatively constant over the duration of the spike train; however, with less current injection interspike intervals increased for each successive action potential during the train.

When initiated from voltages between -61 mV (near rest) and threshold, the onset latency of spike trains in response to depolarizing steps was always less than 5 ms (n=17). In some cells, small hyperpolarizations caused spike trains to display distinctly nonlinear behaviors. In these cells, hyperpolarizations to holding voltages about 4 mV negative to resting potential substantially altered the latency of the first spike of the action potential train (n=4). Figure 4 shows responses of such a cell to identical depolarizing current steps activated from slightly different starting potentials. At rest (-61 mV) the cell responded to 0.1 nA depolarizing current with a short latency train of spikes. When the cell was hyperpolarized slightly from rest to -65 mV, the same stimulus elicited a train of action potentials that began after a 13 ms delay (fig 4, center). Adjustment to a slightly more negative potential (-66 mV) further increased the first-spike latency to 24 ms. A similar delay has been described for thalamic cells in the cat, where it appears to depend on simultaneous activation of a noninactivating persistent sodium current ($gNa_{noninact}$; Steriade and Llinas, 1988) and outward potassium currents (I_{As} and I_{Af}; McCormick, 1990).

Hyperpolarized membrane potentials: burst firing mode

In most of the cells studied (n = 32), deep hyperpolarization from resting levels, followed by depolarizing steps, activated a large, slow depolarizing potential that

closely resembled the low threshold spike (LTS) that has been previously described for thalamic cells from the rat, cat, and guinea pig (Jahnsen and Llinas, 1984; Crunelli et al., 1989; Coulter et al., 1989a; Hernandez-Cruz and Pape, 1989; McCormick and Feeser, 1990; Scharfman et al., 1990). The depolarizing conductance that I observed in ferret LGN was similar to the low threshold spike in the following respects. 1) The current de-inactivated at potentials negative to -65 mV as measured at the soma. 2) The low-threshold spike itself was not expressed until activated by depolarizing current steps. 3) The low-threshold spike was of slow duration (half-width > 20 ms). 4) The slow spike often was crowned by a burst of fast action potentials. 5) I observed a refractory period of > 100 ms between successive low-threshold spikes (tested for 3 cells, data not shown). These qualitative and quantitative characteristics correspond closely with those of the previously described low-threshold calcium spike, and I shall refer to it as such in this chapter.

In slices of ferret LGN, the low-threshold calcium spike was evoked by either inhibitory potentials (IPSPs; n=3) or by injection of hyperpolarizing current (n= 32). Figure 5a shows a low threshold spike occurring after an IPSP elicited by optic tract stimulation, with the membrane potential held at -74 mV. After the IPSP had decayed to baseline, the membrane continued to depolarize until it gave rise to a fully-developed calcium spike. An identical low-threshold spike was evoked in the same cell upon return from a hyperpolarization induced by current injection (Figure 5b). In this case the low threshold spike appears with a shorter latency, presumably

because the slope of recovery from the square hyperpolarizing step (1.4 V/s) is more rapid than the decay of the IPSP (0.2 V/s). This is in agreement with the previously reported dependence of low-threshold spike activation on the rate of change of membrane potential, $\delta V/\delta T$ (Crunelli et al., 1989).

The low-threshold current activated fast action potentials if its peak crossed spike threshold (about -55 mV). The probability of action potential activation depended on many factors that affected the low-threshold spike amplitude, including degree of hyperpolarization, size of the underlying depolarization, and in the case of the optic-tract evoked low-threshold spike, the rate of rise of the depolarization (See Figure 6B, Chapter 3). Within these bursts, spikes occurred at high frequencies, typically between 200 and 400 Hz. Bursts contained between 1 and 5 spikes; the total burst duration was always less than 25 ms. The number of spikes also increased up to 5/burst with increasing amplitude of the underlying low-threshold spike (Figs. 5, 6, 7).

When cells were held at deeply hyperpolarized potentials, EPSPs or small injections of depolarizing current could also elicit low threshold spikes and action potential bursts (n= 31). Under these conditions, it was evident that the latency to the low threshold spike peak or to firing of the first action potential was dependent on the initial membrane potential. The low-threshold spike latencies were shortest when they were evoked from membrane potentials about -70 mV, i.e. near the start of the activating range. Low-threshold spike latency increased with increasing hyperpolarization, until the low-threshold spike could no longer be activated at about

-95 mV. The voltage dependence of the low-threshold spike latency was seen for both optic tract-evoked and current injection-evoked low-threshold spikes (Figure 6). Thus, at these hyperpolarized membrane potentials, LGN cells are clearly capable of highly nonlinear transformations of inputs, both in numbers of spikes and in latency of spikes.

Figure 7 shows the systematic variation in the latency of action potentials evoked by low-threshold spikes depending on the initial membrane voltage. As low threshold spikes were elicited from progressively hyperpolarized levels, the first-spike latency increased until the low-threshold spike again was completely inactivated at the most negative voltages. Responses of an LGN cell to small depolarizing currents elicited at deeply hyperpolarized membrane potentials are shown in Figure 7. At initial voltages between -70 and -90 mV, this stimulus led to a low-threshold spike capped by several high-frequency action potentials (Figure 7a). The latency of this burst (~8-10 ms after start of pulse) remained relatively constant between -71 and -81 mV (Figure 7b). At more hyperpolarized potentials, the latency of the burst increased toward a maximum of 50 ms at -91 mV; at even more negative potentials the low-threshold spike inactivated. A cell receiving sensory input in this mode would respond with bursts of spikes that were out of phase with the stimulus onset by as much as 50 ms. Such large and variable delays, combined with the low numbers of spikes elicited, would seem to preclude faithful transmission of visual information to the cortex by cells in burst mode.

In some cells (n=4), a large and rapid hyperpolarizing step from rest led to

spontaneous oscillations of membrane potential characterized by repetitive activation of low-threshold spikes (Figure 8a). The spontaneous bursts typically repeated at frequencies between 2 Hz and 10 Hz, and could persist for up to 1 minute with continuous hyperpolarization. Spontaneous bursting was not seen after afferent stimulation. Indeed, when cells were in this mode, optic tract stimulation during the period of oscillations appeared to have no effect on membrane voltage (arrowheads in Figure 8a). This bursting appears to result in part from a rectifying conductance that is activated by hyperpolarization and drives membrane potential back toward rest (McCormick and Pape, 1990). Figure 8b shows the response of the same cell to a 100 ms pulse of hyperpolarizing current. The response shows a depolarizing "sag" that moves membrane voltage back toward resting levels. If rapid enough, these depolarizing sags sometimes activated the low-threshold spike (not shown here). The voltage characteristics of this current match those of the cation current I_H, which is active at these membrane potentials, and has been shown to play a role in maintenance of LGN cell oscillations (McCormick and Pape, 1990).

Intermediate membrane potentials: mixed burst/tonic modes

Within a narrow range of membrane potentials, both current injection and synaptic stimulation led to partial activation of the low-threshold conductance. Figure 2 contains a partially activated low-threshold spike that did not lead to action potentials, but rather appeared as an early bump on the otherwise ohmic response of the membrane (open arrow on trace at -73 mV). In some cells (n=4), I observed

action potentials whose frequency appeared to be determined by the sequential activation of a low-threshold burst followed by tonic firing. Figure 9a shows an LGN cell's responses to depolarizing current steps at three membrane potentials. At a depolarized membrane potential (-56 mV) the cell responded with a continuous train of spikes at constant frequency. At a deeply hyperpolarized potential (-75 mV), the cell responded with a typical burst of 2 action potentials astride a low-threshold spike. At an intermediate potential (-61 mV), the cell's response appeared to comprise a mixture of burst and tonic firing. Action potentials fired initially at a high frequency which rapidly subsided toward the usual tonic levels. Figure 9b shows that this accommodation to tonic levels took place after the first 4 spikes. The figure also shows that for the 8 overlapping responses shown, the variability in timing between spikes is extremely low for the first two spikes, and increases for later spikes in each train. Further support for the hypothesis that this mode of firing constitutes a mixture of initial activation of low threshold current followed by tonic mode firing comes from qualitative observation of the shapes of the interspike intervals in each of these modes considered in isolation. In between action potentials elicited in burst mode, the depolarizing deflection immediately preceding a spike has a time course that decelerates, i.e. it appears convex upward (open circle, center trace in Figure 9A. See also Figure 2, trace at -89 mV). This shape is presumably the result of repetitive activation of the low-threshold current I_T. In tonic mode firing, the interspike voltage tends to accelerate, giving the interspike interval a concave-upward course (closed circle, Figure 9A; compare to Figure 2, trace at -54

mV). These data together suggest that the initial response and the later response at intermediate membrane potentials comprise different firing modes for the cell.

LGN cells also responded to synaptic stimulation with mixed burst/tonic trains. Figure 10 shows the synaptic responses of another cell that showed mixed-mode current injection responses when depolarized from -57 mV (current injection data not shown). Optic tract stimulation during a train of sustained action potentials at -53 mV transiently increased the mean frequency of firing from 125 Hz before synaptic stimulation, to 313 Hz for the duration of the EPSP (Figure 10, left-hand trace). At more deeply hyperpolarized membrane voltages (-70 mV), optic tract stimulation activated a low-threshold spike capped by an action potential burst (right-hand trace). Optic tract stimulation at intermediate membrane potentials (between -61 mV and rest) led to spike responses qualitatively similar to the mixed firing mode seen during current injection. As shown in the center trace of Figure 10, optic tract stimulation at -55 mV evoked 2 action potentials 3.4 ms apart (292 Hz), followed by a third spike after a 22 ms delay (cf. Figure 9a, middle trace).

DISCUSSION

The results of this study may be summarized as follows:

1. Changes in membrane voltage modulate in similar fashion the spike responses produced by synaptic or direct current stimulation in ferret LGN cells in vitro.

2. Ferret LGN cells respond to current injection or synaptic stimulation by firing action potentials in the patterns described previously for thalamic cells recorded both in vivo and in vitro. At depolarized membrane potentials cell enter a tonic firing mode where constant current injection produces non-adapting trains of fast action potentials whose frequency is proportional to the amount of injected current. At hyperpolarized voltages, LGN cells enter burst mode, where the spike output is differentiated into brief bursts by the activation of a low-threshold calcium mediated slow spike.

3. Within each of these modes, small changes in membrane voltage lead to modulation of spike numbers and spike latency. In particular, latency to the first spike may vary between 1 and 50 ms.

4. In a range of membrane potentials intermediate between those leading to tonic or burst firing, LGN cells express a "mixed" firing mode characterized by an initial transient of high frequency action potentials followed by steady lower frequency firing. This dual expression of firing modes appears to be due to initial activation of the low-threshold calcium current followed by continued firing in tonic mode.

Membrane voltage changes and sites of synaptic input on LGN neurons

Despite the shorter and more dynamic voltage changes induced by synaptic

currents, action potential trains and burst evoked by optic tract stimulation showed voltage-dependent modulations similar to spikes elicited by constant current injection. The voltage ranges over which these modulations occurred were similar for synaptic and direct current stimulation. This result suggests that the regions containing voltage-sensitive membrane conductances as well as the site of action potential generation in LGN cells are electrically close to the site of current injection. Johnston and Brown (1983) have estimated that with sharp electrodes, space clamp in multipolar neurons is effective only over about 0.1 electrotonic lengths. In cat LGN neurons this corresponds to an anatomical distance of roughly 30 μm (Friedlander et al., 1981; Bloomfield et al., 1987), which would encompass the cell body and proximal primary dendrites. These previous results, together with the observations reported here, suggest that much of the voltage-dependent modulation of action potentials evoked by synaptic inputs is due to activation of membrane conductances at sites close to the cell body of LGN neurons.

Inputs that modulate membrane voltage

In this study I have used constant current injection to set the membrane potential of the neuron at the various hyperpolarized and depolarized levels. In addition to retinal afferents, cells in the LGN receive several types of non-retinal inputs whose activity can lead to slow depolarizations and hyperpolarizations of the membrane, including cholinergic inputs from the basal forebrain and midbrain reticular formation, noradrenergic fibers from the locus coeruleus, histaminergic input from the hypothalamus, and serotoninergic inputs from the brainstem raphe formation

(McCormick, 1989). For example, activation of the ascending cholinergic systems depolarizes LGN relay cells. Under appropriate conditions, this pathway is capable of bringing thalamic cells into the voltage range corresponding to tonic firing and linear processing of retinal inputs (McCormick and Prince, 1987). While this mechanism has been postulated to play a role in arousal from sleep (Steriade and Deschenes, 1984), some studies have suggested that cholinergic inputs to LGN modulate the gain of visual transmission as well (Singer, 1977; Sillito, Kemp, and Berardi,1983; Uhlrich et al, 1989). Long-lasting hyperpolarizations of membrane potential are largely the result of potassium conductance activation by various mechanisms, including muscarinic M_2 receptors on inhibitory interneurons, serotonergic inputs, and synaptic activation of $GABA_B$ receptors (Rogawski and Aghajanian, 1980; McCormick and Pape, 1987; Crunelli and Leresche, 1991). Activation of these inputs may be necessary to move LGN cells into burst mode, in which transmission of sensory information to cortex appears to be suppressed. The latter hypothesis is supported by the observation that burst mode firing occurs primarily during periods of sleep or inattentiveness (Steriade and Llinas, 1988), as well as in petit mal "absence" seizures (Coulter et al., 1989b); i.e., conditions in which the tranmission of visual information is reduced drastically or is nonfunctional. Exploration of the role of low-threshold spikes in normal visual function has begun only recently (Lo et al., 1991).

Functional consequences of LGN firing modes

The action potential patterns observed at various membrane voltages were

evoked by both direct injection and synaptic stimulation (Figures 2 and 10). The subthreshold EPSP's evoked at these voltages reflect the differential activation of the membrane conductances described here. In the following Chapters of this thesis, I describe in detail the subthreshold responses of ferret LGN cells to optic tract stimulation. At depolarized membrane potentials, stimulation leads to unimodal EPSP's that decay with a smooth time course (Figures 3,4,6,7 in Chapter 4); these responses would evoke tonic firing if allowed to pass threshold. At hyperpolarized membrane potentials, EPSPs can trigger low threshold spikes (Figure 10, this paper; Figure 6B, Chapter 4). At these potentials, optic tract stimulation evokes EPSP's that can lead to either fully developed or partially activated low-threshold spikes (Figure 6B, Chapter 4). This is distinct from the mixed mode response described in this paper, which is observed at intermediate membrane potentials and which is characterized by an initial spike response typical of the burst mode, followed by a later response typical of tonic mode firing. This latter (mixed) response is likely due to an initial component that leads to activation of the low-threshold spike, but also inactivates the low-threshold conductance; a further consequence of this depolarization is tonic mode firing. The former response is due to the optic tract EPSP triggering a partial or fully developed low threshold spike, but recovering rapidly enough that membrane voltage remains in the range where low-threshold currents are de-inactivated. A similar response is shown by Jahnsen and Llinas (1984) in their recordings from guinea pig thalamic cells; however, these authors do not attribute this firing pattern to successive activation of burst and tonic mode

mechanisms.

The profusion of intrinsic membrane currents suggests that LGN cells are potentially able to regulate their membrane voltage within rigid limits through the integration of voltage-gated depolarizing and hyperpolarizing currents. Such tight control may be necessary during normal function to maintain the cell in the firing modes described here. For example, tonic mode firing must faithfully carry information about changes in luminance during visual stimulation. In this mode, changes as small as 5 mV of membrane potential can add several milliseconds to the latency of a spike train. For a cell in burst mode, the latency of the first spikes in response to a rapid depolarizing input could vary by as much as 50 ms. Similarly, the maintenance and regularity of thalamic oscillations observed during sleep must depend on precise control of membrane voltage (Steriade and Deschenes, 1984).

An important functional implication of these results is that the same stimulus can evoke radically different responses from an LGN cell depending on the cell's membrane potential at the time of stimulation. Terminals of thalamic cells in visual cortex will thus transmit spike patterns of variable length, frequency, and latency that reflect the integration of the many inputs and intrinsic membrane conductances at the cell's dendrites and cell body. An specific proposal is that the visual cortex can help to regulate its own input through the action of the corticofugal feedback projection on the membrane potential of LGN neurons (Esguerra and Sur, 1990). This last issue is addressed in Chapter 5.

REFERENCES

Adams, P.R., and Brown, D.A. (1975). Actions of Γ-aminobutyric acid on sympathetic ganglion cells. J. Physiol. 250, 85-120.

Bloomfield, S. A, Hamos, J. E., and Sherman, S. M. (1987). Passive cable properties and morphological correlates of neurones in the lateral geniculate nucleus of the cat. J. Physiol. 383, 653-692.

Coulter, D.A., Huguenard, J.R., and Prince, D.A. (1989a). Characterization of ethosuximide reduction of low-threshold calcium current in thalamic neurons. Ann. Neurol. 25, 582-593.

Coulter, D.A., Huguenard, J.R., and Prince, D.A. (1989b). Specific petit mal anticonvulsant reduce calcium currents in thalamic neurons. Neurosci. Lett. 98, 74-78.

Crunelli, V., Lightowler, S., and Pollard, C. E. (1989). A T-type Ca2+ current underlies low-threshold Ca2+ potentials in cells of the cat and rat lateral geniculate nucleus. J. Physiol. 413, 543-561.

Crunelli, V., and Leresche, N. (1991). A role for $GABA_B$ receptors in excitation and

inhibition of thalamocortical cells. TINS 14, 16-21.

Esguerra, M., and Sur, M. (1990). Corticogeniculate feedback gates retinogeniculate transmission by activating NMDA receptors. Soc. Neurosci. Abstr. 16, 159.

Friedlander, M. J., Lin, C.-S., Stanford, L. R., and Sherman, S. M. (1981). Morphology of functionally identified neurons in lateral geniculate nucleus of the cat. J. Neurophysiol. 46, 80-129.

Hernandez-Cruz, A., and Pape, H.-C. (1989). Identification of two calcium currents in acutely dissociated neurons from the rat lateral geniculate nucleus. J. Neurophysiol. 6, 1270-1283.

Hille, B. (1984). Ionic channels of excitable membranes. Sinauer Associates, Sunderland, MA.

Jahnsen, H., and Llinas, R. (1984). Electrophysiological properties of guinea-pig thalamic neurones: an in vitro study. J. Physiol. 349, 205-226.

Johnston, D., and Brown, T. H. (1983). Interpretation of voltage-clamp measurements in hippocampal neurons. J. Neurophysiol. 50, 464-486.

Lo, F.-S., Lu, S.-M., and Sherman, S.M. (1991). Intracellular and extracellular in vivo recording of different response modes for relay cells of the cat's lateral geniculate nucleus. Exp. Brain Res. 83, 317-328.

McCormick, D.A. (1989). Cholinergic and noradreneregic modulation of thalamocortical processing. TINS 12, 215-221.

McCormick, D.A. (1990). Possible ionic basis for lagged visual responses in cat LGNd relay neurons. Soc. Neurosci. Abstr. 16, 159.

McCormick, D.A., and Prince, D.A. (1987). Actions of acetylcholine in the guinea-pig and cat medial and lateral geniculate nuclei, in vitro. J. Physiol. 392, 147-165.

McCormick, D.A., and Feeser, H. R. (1990). Functional implications of burst firing and single spike activity in lateral geniculate nucleus neurons. Neuroscience 39, 103-113.

McCormick, D.A., and Pape, H.-C. (1990). Properties of a hyperpolarization activated cation current and its role in rhythmic oscillation in thalamic relay neurones. J. Physiol. 431, 291-318.

Rogawski, M. A., and Aghajanian, G.K. (1980). Norepinephrine and serotonin: opposite effects on the activity of lateral geniculate neurons evoked by optic pathway stimulation. Exp. Neurol. 69, 678-694.

Rudy, B. (1988). Diversity and ubiquity of potassium channels. Neuroscience 25, 729-749.

Sherman, S.M., and Koch, C. (1986). The control of retinogeniculate transmission in the mammalian lateral geniculate nucleus. Exp. Brain Res. 63, 1-20.

Sillito, A. M., Kemp, J. A., and Berardi, N. (1983). The cholinergic influence on the function of the cat dorsal lateral geniculate nucleus (dLGN). Brain Res. 280, 299-307.

Steriade, M., and Deschenes, M.(1984). The thalamus as a neuronal oscillator. Brain Res. Rev. 8, 1-63.

Steriade, M., and Llinas, R. (1988) The functional states of the thalamus and the associated neuronal interplay. Physiol. Rev. 68, 649-742.

TABLE 1. Electrophysiological properties of LGN cells

Cell	Rn (MΩ)	Time constant (ms)	Vm (mV)	Spike amplitude (mV)	Spike width (ms)	Spike threshold (mV)
1	11.3	6	-58	†	†	†
2	11.8	7.7	-62	†	†	†
3	25.0	11.3	-64	65	1.1	-54
4	52.5	22.8	-65	71	0.9	-51
5	57.5	31.1	-68	68	1	-55
6	124.5	53.6	-56	67	1	-49
7	12.8	6.2	-65	85	0.8	-52
8	46.5	10.5	-53	53	0.8	-44
9	99.0	39.3	-55	85	0.75	-38
10	27.0	11.1	-59	54	1	-58
11	71.0	16	-65	40	0.72	-61
12	36.0	3.3	-54	34	1.2	-57
13	19.7	7.7	-65	68	1.4	-55
14	83.0	16.7	-63	66	1.6	-57
15	46.5	15	-66	58	0.6	-55
16	28.9	11.1	-63	59	0.6	-56
17	25.9	9	-72	76	0.6	-60
Mean	45.8	16.4	-61.9	63.3	0.9	-53.5
± S.D.	32.3	13.6	5.4	14.9	0.3	6.3

Rn, input resistance; Vm, resting membrane potential. Spike amplitude was measured from Vm to peak; spike widths were measured at base. Spikes were elicited with square current pulses > 100 ms in duration.

† For these 2 cells, episodes containing action potentials were not saved on tape for offline analysis

TABLE 2. Comparison of electrophysiological properties of cells in the ferret LGN with thalamic cells from other species

Species	Rn (MΩ)	Time constant (ms)	Vm (mV)	Spike amplitude (mV)	Reference
Cat: X cells†	22.6 ± 3.2 (X)	10.28 ± 1.30	-60.0 ± 5.5	---	Bloomfield et al., 1987
Y cells†	16.0 ± 3.6 (Y)	8.15 ± 0.81	-61.6 ± 6.5	---	
Guinea Pig	51 ± 19	---	-65 ± 7	79 ± 7	McCormick and Prince, 1987
Guinea Pig	42 ± 18	14 ± 6	-64 ± 5	80 ± 7	Jahnsen and Llinas, 1984
Guinea Pig / Cat	46 ± 12	---	-66 ± 3	91 ± 6	McCormick and Pape, 1990
Cat / Rat	69 ± 5	21 ± 3	-62 ± 2	---	Crunelli et al, 1988
Ferret	38.9 ± 28.5	14.5 ± 11.8	-61.8 ± 6.1	63.3 ± 14.3	present study

All values expressed as mean ± SD

† In vivo recordings

FIGURE LEGENDS

Figure 1. Current-voltage relationship of a ferret LGN cell. Plot was constructed by injection of 120 ms hyperpolarizing and depolarizing current pulses in 0.1 nA increments and measuring voltage deflections 40 ms (triangles) and 110 ms (circles) after the start of current injection. Note decrease in slope of both the 40 ms and 110 ms components with depolarization, and decrease of slope of 110 ms component at hyperpolarizing potentials. Inset: examples of traces used to construct the plot. The measurements were taken with the cell at its resting potential of -61 mV.

Figure 2. Responses of a ferret LGN cell to injection of 0.1 nA depolarizing current at different membrane potentials, in the absence of optic tract stimulation. Stimulation at depolarized levels (-54 mV) elicits a train of action potentials at a frequency of 50 Hz. Hyperpolarization de-inactivates a low threshold current which is partially activated by depolarization at -73 mV (arrow), and which develops into a low-threshold spike capped by action potentials at more hyperpolarized voltages (-78 and -89 mV). Note increase in spike latency with progressive hyperpolarization. Resting potential, -62 mV. Duration of current injection, 120 ms. Capacitive transients at the start and end of current injection response have been shortened for clarity.

Figure 3. Tonic response of a ferret LGN cell to different amounts of depolarizing

current at a fixed membrane potential. A: Action potential trains elicited by injection of the indicated amounts of depolarizing current. The membrane potential was held at rest (-61 mV) during successive presentation of stimuli. B: Loss of spike train frequency accommodation with increasing current. The plot was constructed by measuring the separation between successive action potential peaks in trains elicited from the cell in A. The plot includes only responses where 2 or more spikes were elicited. C: Linear relationship of spike frequency to amount of injected current in tonic mode. Interspike intervals were measured as in B and averaged; error bars show standard deviation for each set of measurements. The mean frequency of each spike train was derived from the reciprocal of each interspike interval.

Figure 4. Variable latency firing of an LGN cell in tonic mode. A: Spike trains elicited by 0.1 nA depolarizing current with cell held at resting potential (-61 mV) and slightly hyperpolarized from rest (-65 and -66 mV). Arrow indicates ramping potential, suggesting presence of the non-inactivating (persistent) sodium current during spike delay. B. Plot of latency to peak of first spike for trains elicited from cell in A, at varying membrane potentials. The latency increases with hyperpolarization over a 6 mV range between -62 and -68 mV.

Figure 5. Low-threshold spikes initiated by hyperpolarizing inputs. A: Synaptic input. Electrical stimulation of the optic tract (at time indicated by the arrowhead) elicited an IPSP. After recovery from the IPSP, the cell's membrane potential

continued to depolarize and accelerate toward activation of the low-threshold spike. Dashed line indicates initial membrane potential. B. Current injection. Injection of 0.2 nA hyperpolarizing current (120 ms duration) elicited a low threshold spike upon rebound from the passive voltage drop. Note the close similarity of this low-threshold spike with the one shown in A.

Figure 6. Low threshold spikes elicited by depolarizing synaptic inputs and depolarizing current pulses. Left, optic tract stimulation; right, injection of depolarizing current. Stimulation by either means with the cell held at -76 or -78 mV evoked a low-threshold spike and action potential burst at a short latency (synaptic stimulation: 8 ms; current injection: 21 ms). Stimulation at -82/-83 mV evoked low threshold spikes at longer latencies (60 ms and 40 ms for optic tract and current injection stimulation respectively). Dashed lines indicate -55 mV, the voltage at which latency measurements were made.

Figure 7. Increase in low threshold spike latency and inactivation with progressive hyperpolarization. A: Depolarization elicited low threshold spikes and bursts whose latency increased progressively with hyperpolarization. The same stimulus (0.2 nA) was used at all indicated membrane voltages. B: Burst latency was plotted for the cell shown in A at 16 membrane potentials. Latency to first action potential was measured at -55 mV. Open circles at deeply hyperpolarized voltages indicate

responses that evoked neither low threshold spikes nor action potentials. Action potentials in A have been arbitrarily clipped to save space.

Figure 8. Spontaneous oscillation and repetitive bursting of a ferret LGN cell. A: Response to a continuous 0.5 nA hyperpolarizing step. The response consists of rapid depolarizations toward rest that activate low-threshold spikes capped by action potentials. The process repeats 6 times, then inactivates due to progressive sag of the baseline toward rest (dots). Arrowheads indicate times of optic tract stimulation during oscillation; note the lack of effect of afferent stimulation on oscillation frequency and amplitude. The action potential amplitudes appear to vary due to aliasing at low data sampling rate (0.5 kHz). B: Response of the same cell to a single 0.5 nA hyperpolarizing current pulse, shown at a fast sweep speed. This stimulus evokes a passive hyperpolarization that is subsequently reduced by a depolarizing sag toward baseline (arrows). The rebound from hyperpolarization elicits a low threshold spike and burst. The optic tract was not stimulated during collection of this trace.

Figure 9. Characterization of action potential trains comprising both burst and tonic mode firing. A: Identical depolarizing current injections (0.2 nA) lead to tonic firing when initiated at -56 mV; a long-latency low threshold spike at -75 mV; and mixed burst/tonic firing at -61 mV (rest). Note initial high-frequency burst response followed by lower frequency tonic firing at -61 mV. During the interspike intervals

at -61 mV, membrane voltage decelerates (convex upward) between the first 3 spikes (open dot); all subsequent intervals are concave upward (closed dot), indicating acceleration of membrane voltage toward threshold. See also Figure 2, where spikes are interspersed with accelerating voltages in tonic mode (-54 mV), while decelerating voltage changes occur between spikes in burst mode (-89 mV). B: Eight identical depolarizing pulses were applied to the cell shown in A, with starting membrane voltage held at -61 mV. Upper traces: Eight mixed-mode action potential trains elicited from this cell by eight successive current steps of 0.2 nA each are shown overlapped. Lower plot: Mean interspike intervals increase progressively over the duration of the train (closed circles). The variability, shown as error bars representing standard deviation, also increases over the duration of the train. Spike frequency was calculated from the reciprocal of each interval (open circles). Means were derived by measuring successive intervals from each of the 8 spike trains and averaging measurements corresponding to the same interval across trains.

Figure 10. Synaptic responses leading to action potentials in tonic, burst, and mixed burst/tonic modes in a ferret LGN cell. Identical stimuli (80 uV x 8 mA) were delivered to the optic tract at times indicated by the arrowheads, at the indicated membrane voltages. The cell was depolarized to -53 mV by a current step that induced firing of a 125 Hz tonic action potential train typical of tonic mode firing. Stimulation of the optic tract briefly accelerated the action potential frequency to a

mean of 313 Hz, after which the cell resumed the original spike frequency. Optic tract stimulation at -70 mV led to a low-threshold spike capped by a group of action potentials typical of the burst firing mode. At -55 mV, optic tract stimulation elicited 2 fast action potentials that were 3.4 ms apart, followed by a third action potential after another 22 ms. The first two spikes resemble firing in the burst mode, while the third spike is similar to spikes elicited in the tonic mode. Compare with Figure 9, and see text for details.

Figure 1

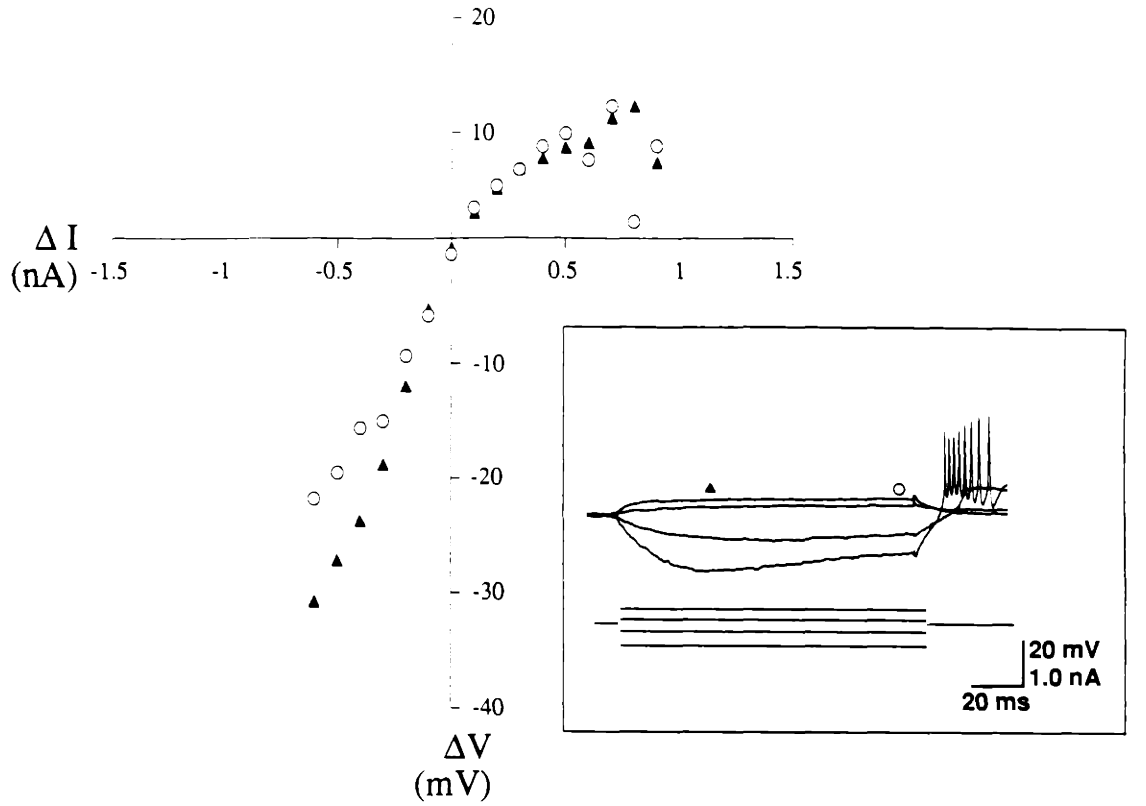

Figure 2

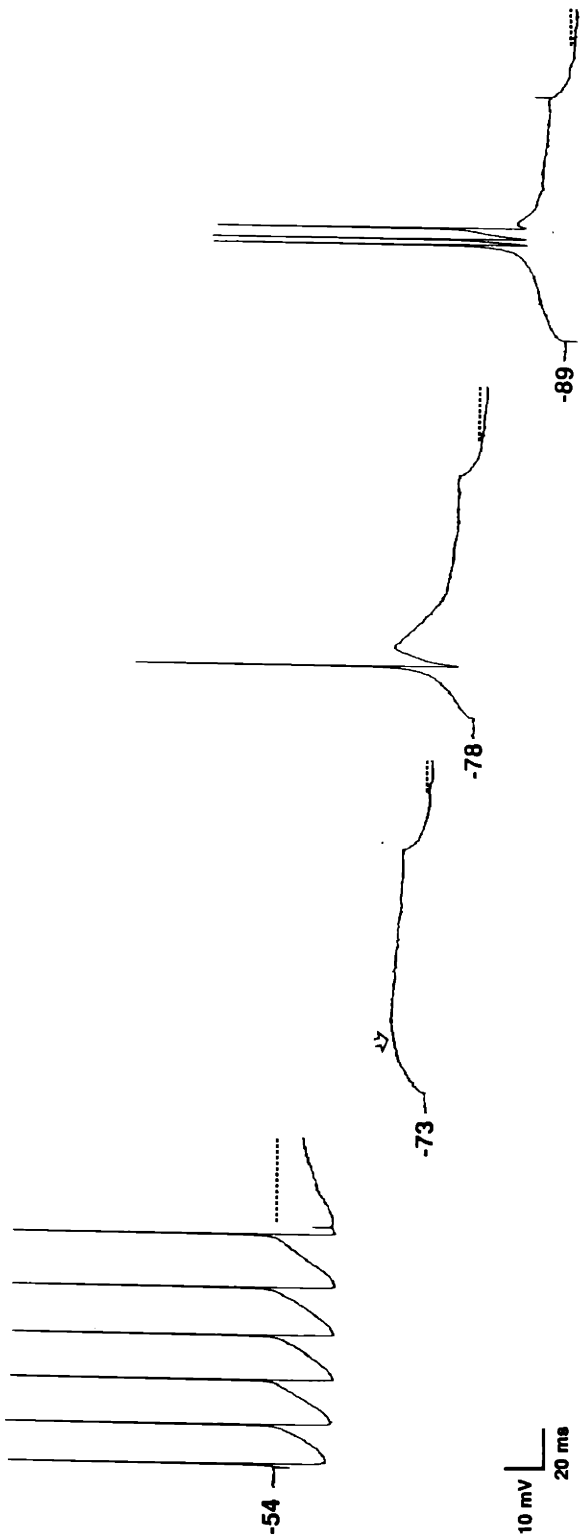

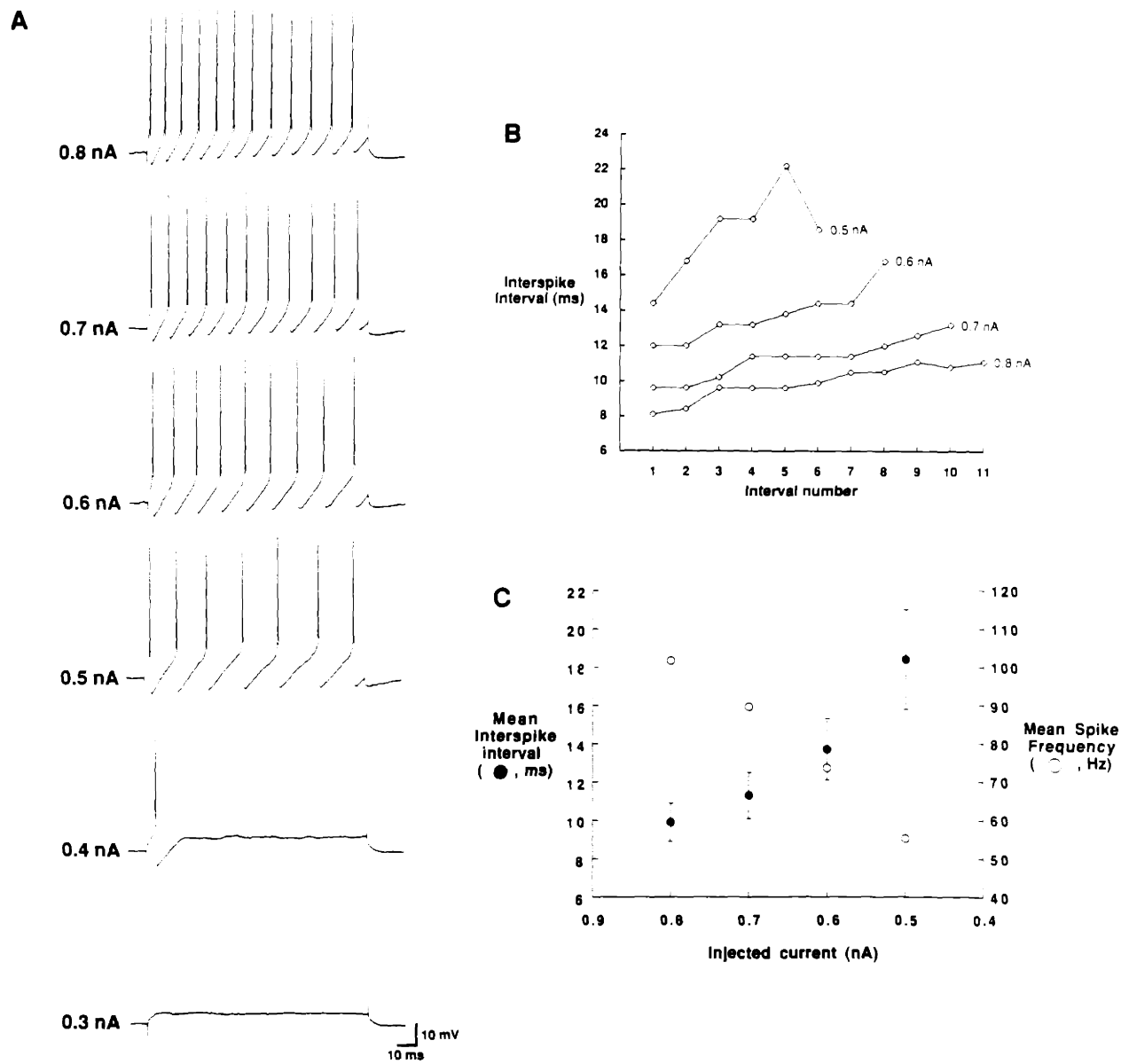
A
0.8 nA
0.7 nA
0.6 nA
0.5 nA
0.4 nA
0.3 nA
10 mV
10 ms
B
Interspike interval (ms)
0.5 nA
0.6 nA
0.7 nA
0.8 nA
Interval number
C
Mean Interspike interval (● , ms)
Mean Spike Frequency (○ , Hz)
Injected current (nA)

Figure 4

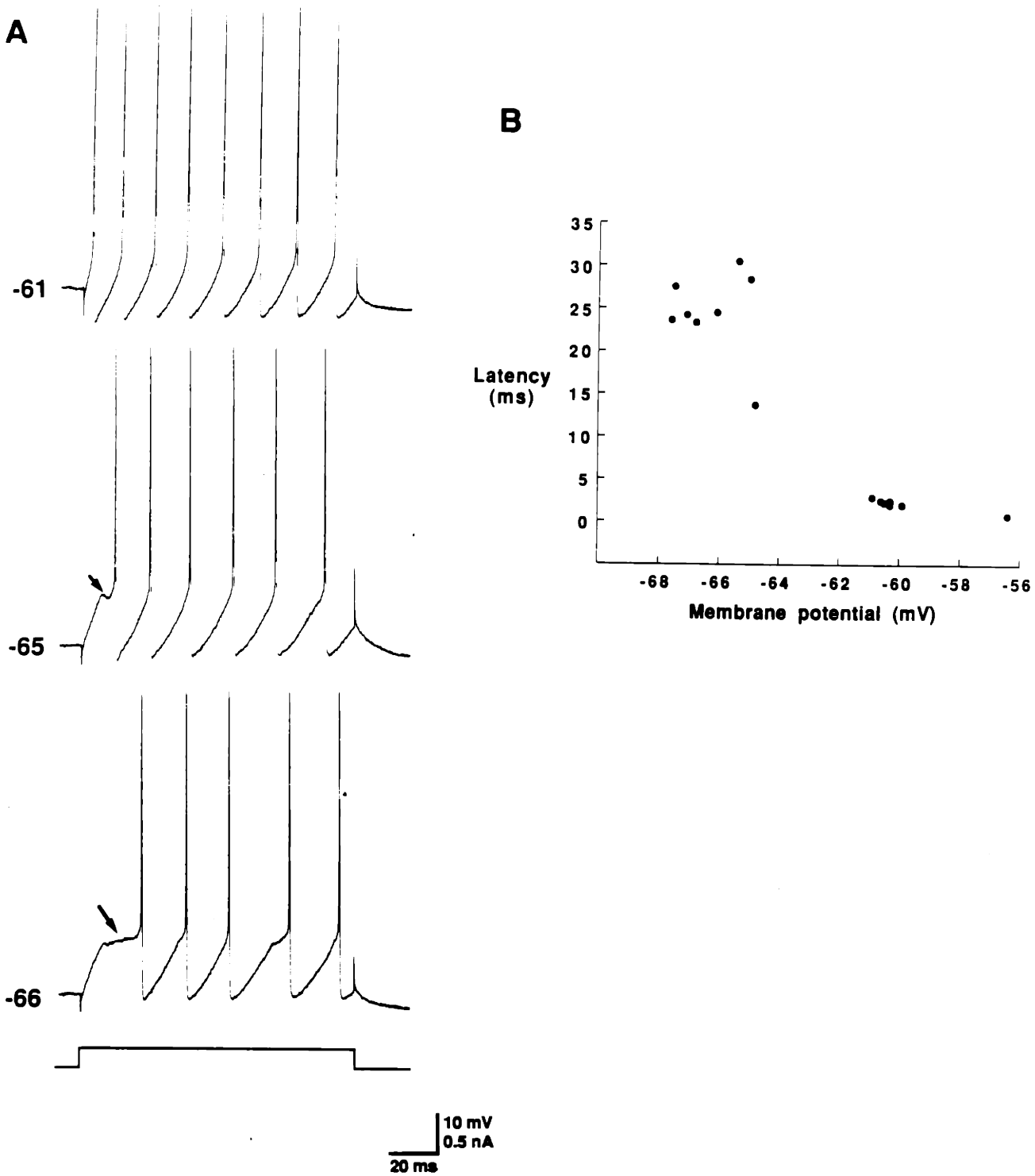
A
-61
-65
-66
10 mV
0.5 nA
20 ms
B
Latency (ms)
35
30
25
20
15
10
5
0
-68
-66
-64
-62
-60
-58
-56
Membrane potential (mV)

Figure 5

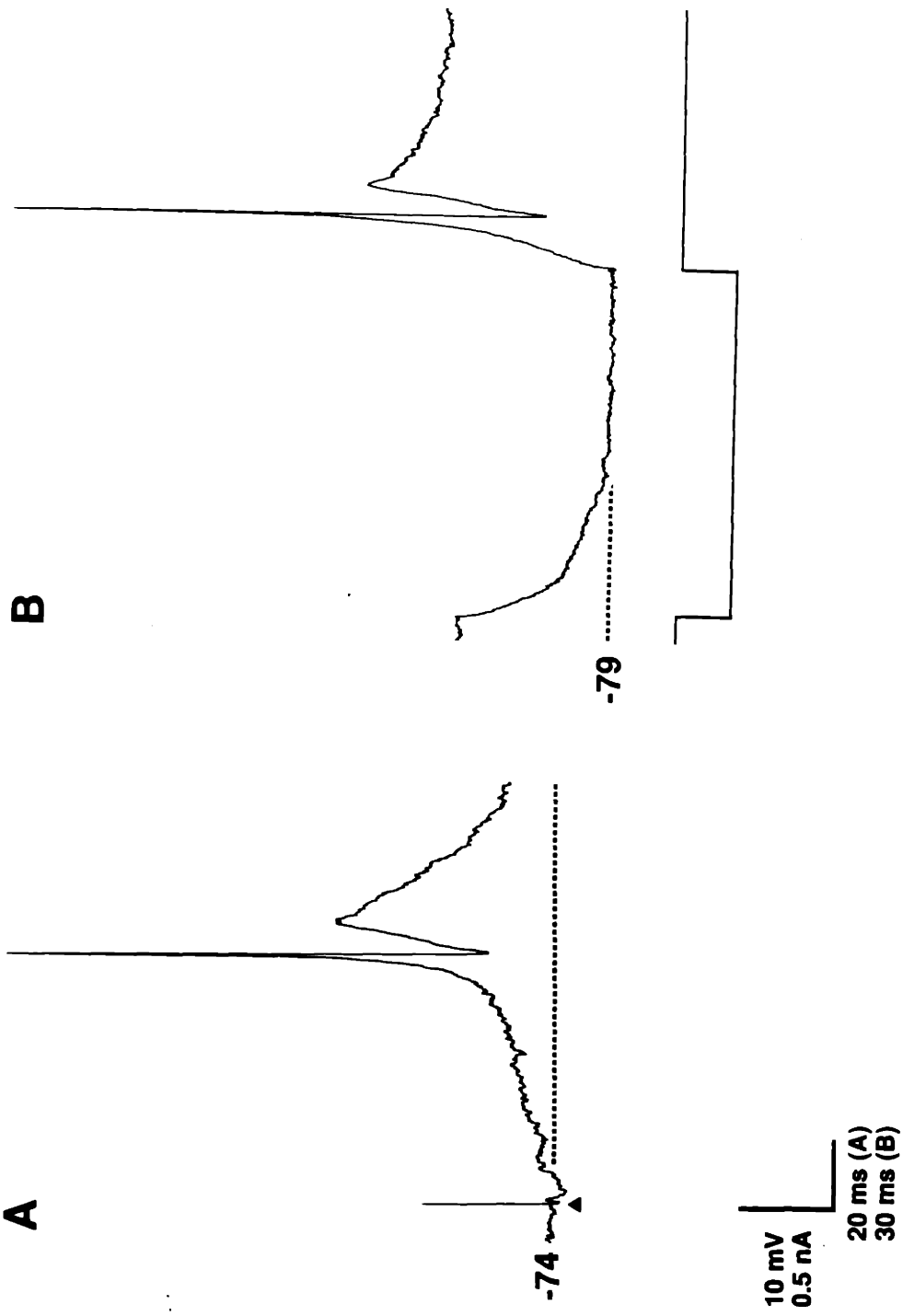

Figure 6

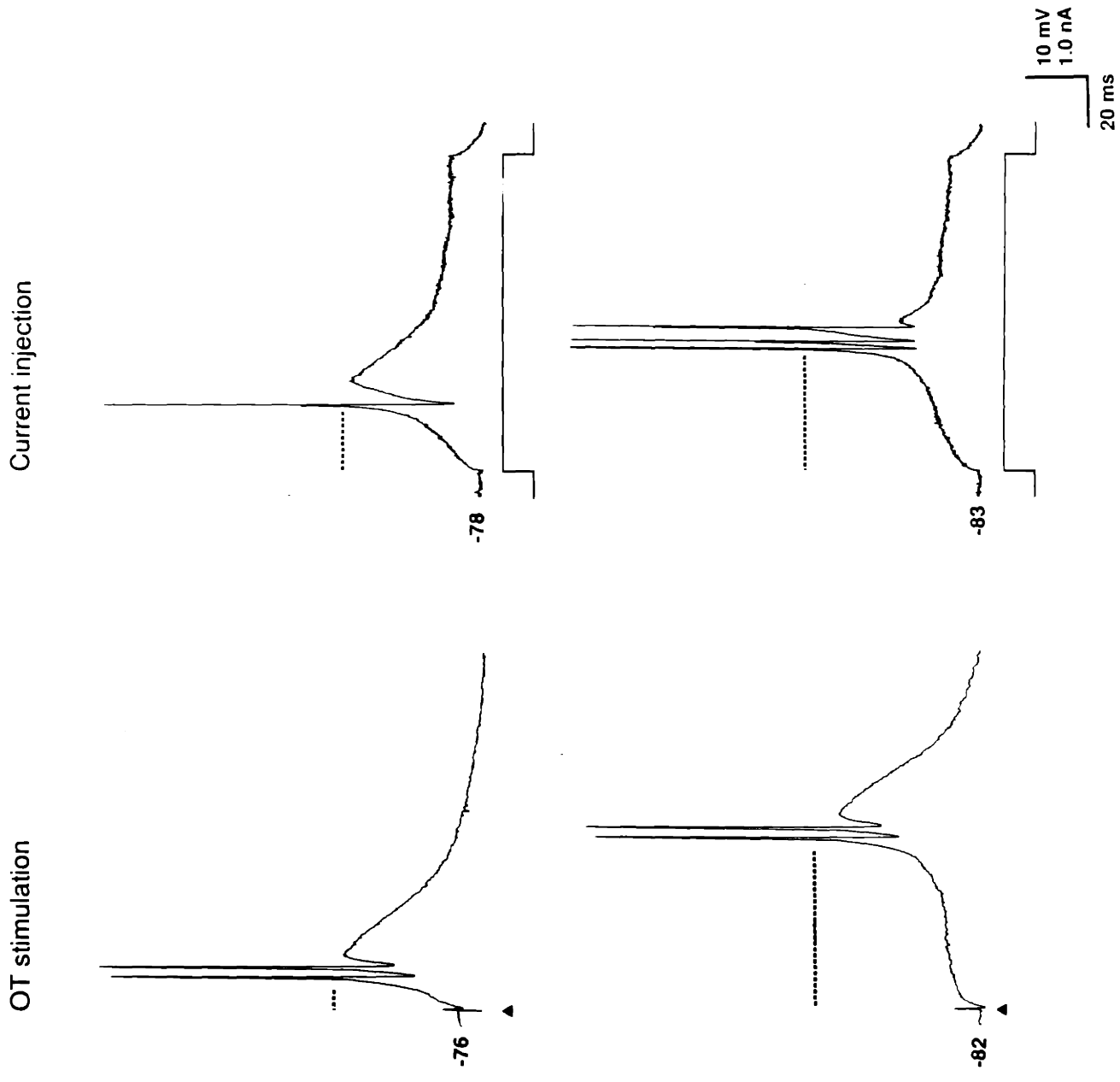

Figure 7

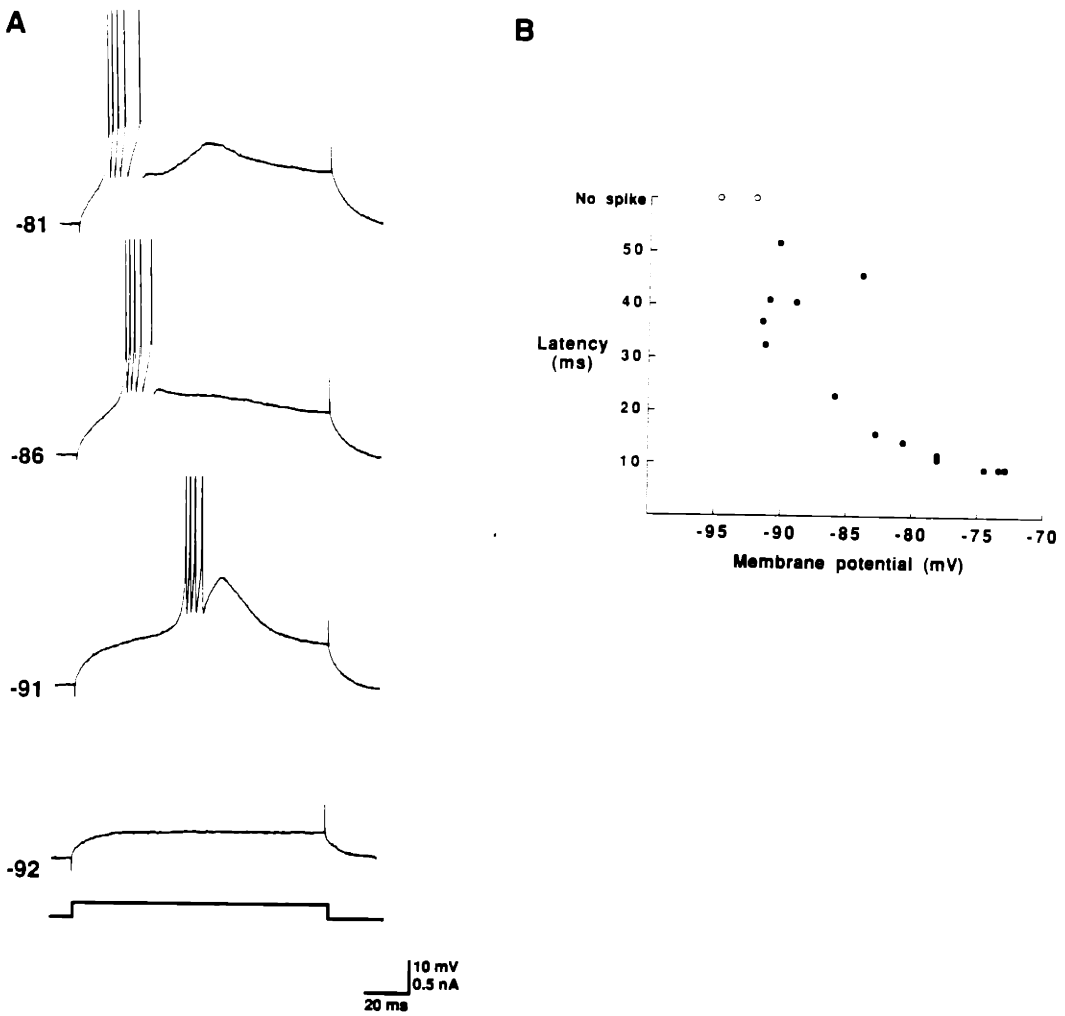
A
-81
-86
-91
-92
10 mV
0.5 nA
20 ms
B
No spike
50
40
Latency (ms)
30
20
10
-95
-90
-85
-80
-75
-70
Membrane potential (mV)

Figure 8

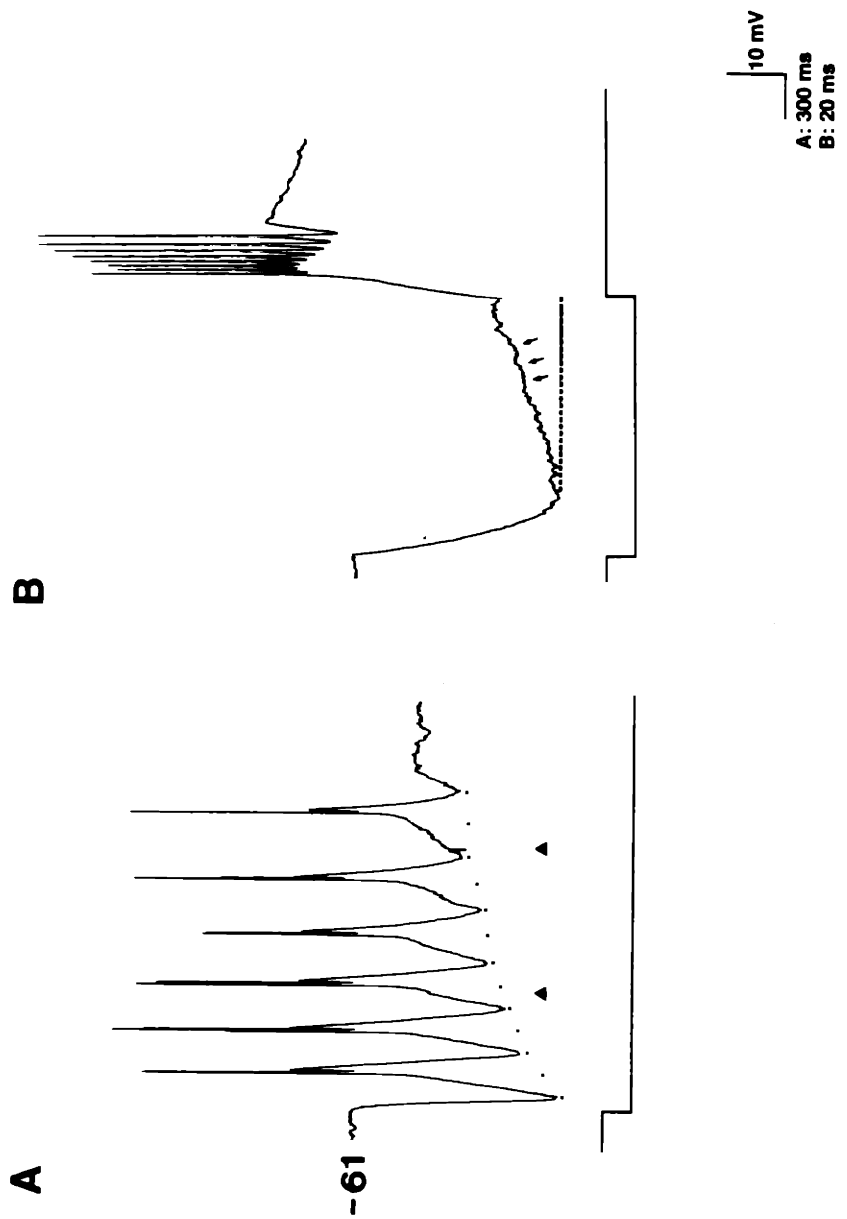

Figure 9

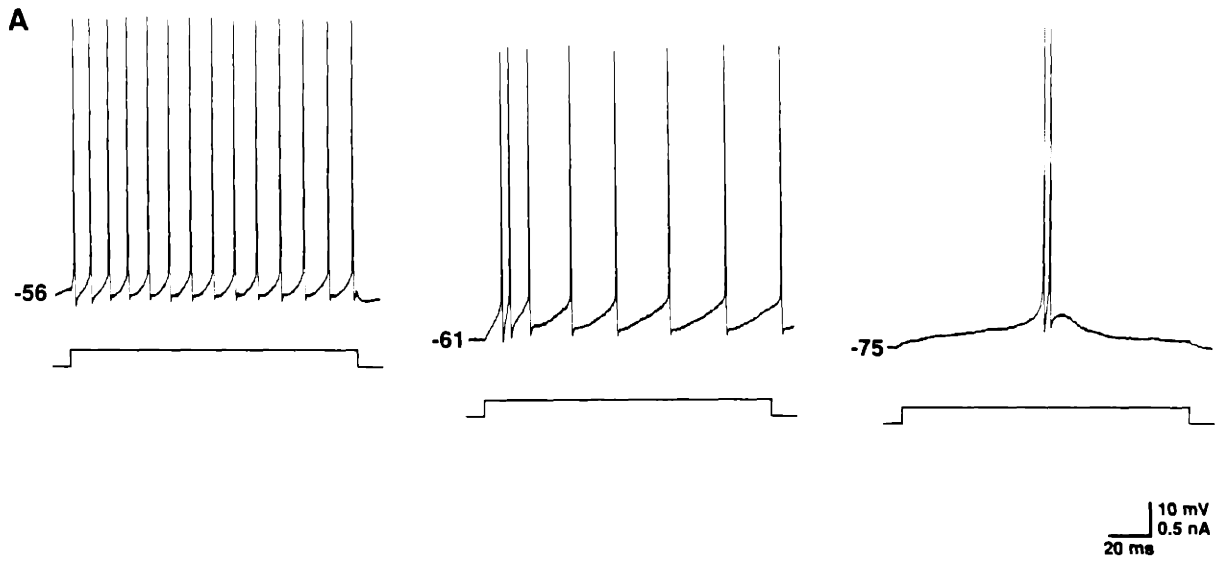
A
-56
-61
-75
10 mV
0.5 nA
20 ms

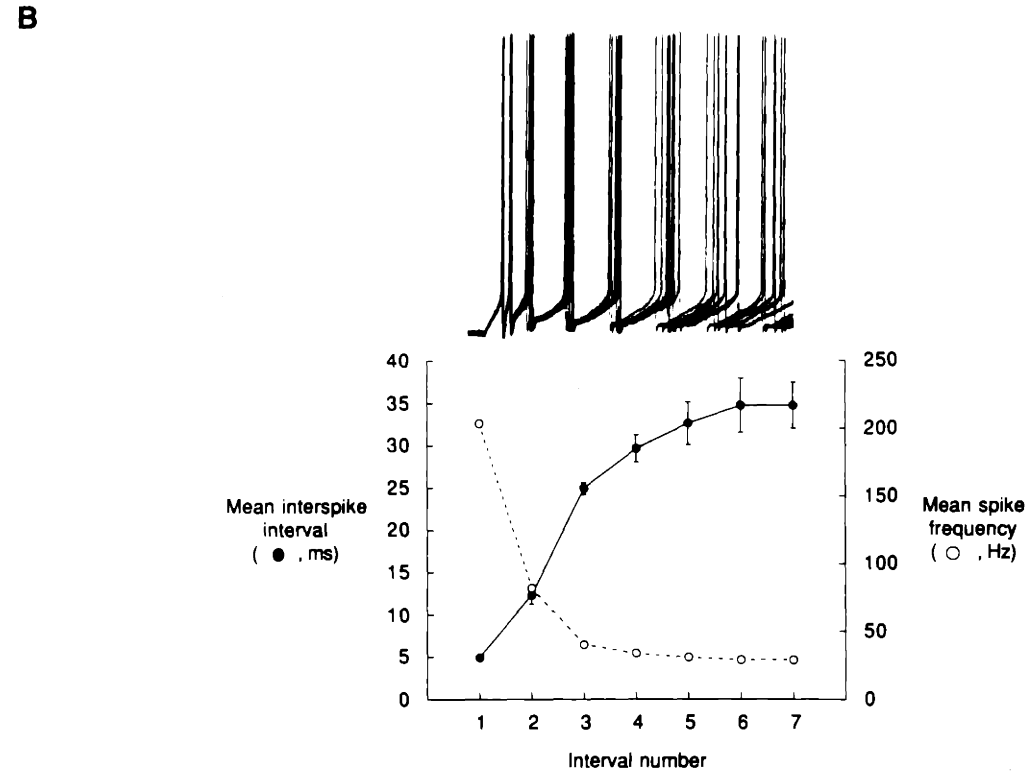
B
Mean interspike interval (● , ms)
Mean spike frequency (○ , Hz)
Interval number
0
5
10
15
20
25
30
35
40
50
100
150
200
250
1
2
3
4
5
6
7

Figure 10

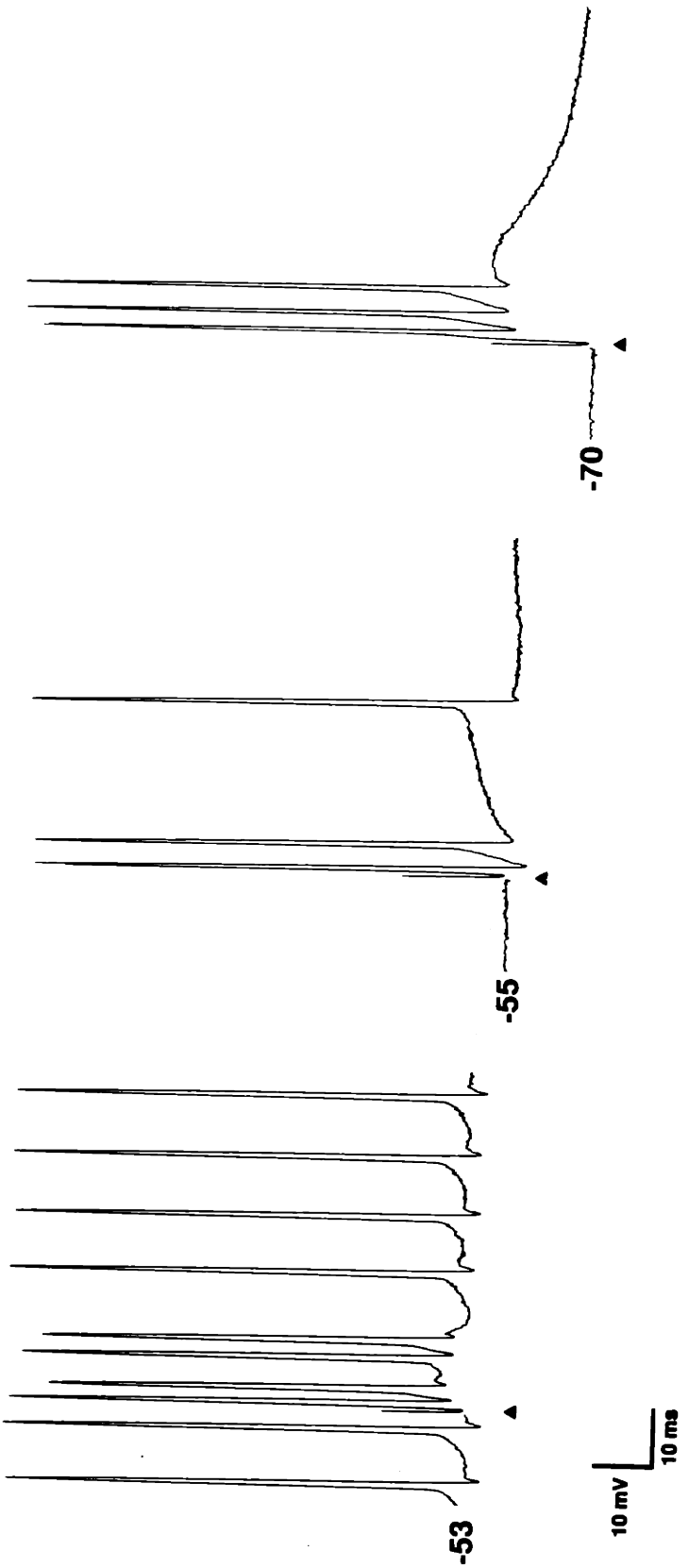

Chapter 3

Retinogeniculate EPSPs recorded intracellularly in the ferret lateral geniculate nucleus in vitro: role of NMDA receptors

[This chapter is a slightly revised version of a manuscript that has been submitted for review to the editors of Visual Neuroscience]

ABSTRACT

I used an in vitro preparation of the ferret lateral geniculate nucleus (LGN) to examine the role of the NMDA class of excitatory amino acid (EAA) receptors in retinogeniculate transmission. Intracellular recordings revealed that blockade of NMDA receptors both shortened the time course and reduced the amplitude of fast and slow components of excitatory postsynaptic potentials (EPSPs) evoked by optic tract stimulation. The amplitude and width of the EPSPs mediated by NMDA receptors increased as membrane potential was depolarized towards spike threshold. Individual LGN cells were influenced to varying extents by blockade of NMDA receptors; NMDA and non-NMDA receptor blockade together attenuated severely the entire retinogeniculate EPSP. The dependence of all components of retinogeniculate EPSPs (and action potentials) on NMDA receptor activation supports the hypothesis that the NMDA receptor participates in fast (<10ms) synaptic events underlying conventional retinogeniculate transmission. The voltage dependence of the NMDA receptor-gated conductance suggests strongly that the transmission of retinal information through the LGN is subject to modulation by extraretinal inputs that affect the membrane potential of LGN neurons.

INTRODUCTION

There is increasing physiological and pharmacological evidence that an excitatory amino acid (EAA) such as glutamate or one of its endogenous analogues is the major neurotransmitter released at the mammalian retinogeniculate synapse (Kemp and Sillito, 1982; Crunelli et al., 1987; Sillito et al., 1990a,1990b; Heggelund and Hartveit, 1990; Kwon et al., 1991). Excitatory amino acid receptors are generally classified into the N-methyl-d-aspartate (NMDA) and non-NMDA subtypes based on their agonists and ionic conductances (MacDermott and Dale, 1987). The NMDA receptor has attracted particular interest because its activation depends on both transmitter binding and membrane potential; a magnesium ion blockade of the NMDA receptor gated channel reduces ionic flow at transmembrane voltages more negative than about -50 mV (Mayer and Westbrook, 1987). The NMDA receptor therefore has been implicated in nonlinear stimulus-response transformations in visual cortex (Fox et al, 1990), in associative neural mechanisms for development and plasticity including long-term potentiation in hippocampus (e.g., Kauer et al., 1988) and visual cortex (Artola and Singer, 1987), and activity-dependent segregation of retinal afferent fibers in the optic tectum (Cline et al, 1987) and LGN (Hahm et al., 1990).

Both in vitro and in vivo physiological experiments indicate that the NMDA and non-NMDA receptor subtypes are present on cells of the adult mammalian lateral geniculate nucleus. In slices of rat LGN in vitro, postsynaptic responses evoked by

optic tract stimulation are attenuated by the EAA antagonist gamma-D-glutamylglycine (DGG; Crunelli et al., 1987). In slices of cat LGN, the NMDA receptor antagonist DL-2-amino-5-phosphonovaleric acid (DL-APV) attenuates the optic tract-evoked EPSP (Scharfman et al, 1990). In vivo iontophoresis of glutamate receptor antagonists reduces the overall visual responses of X and Y neurons in the cat LGN (Kemp and Sillito, 1982). More recent iontophoretic experiments with more specific EAA antagonists suggest that while the visual responses of all LGN cells are sensitive to both NMDA and non-NMDA receptor blockade (Sillito et al., 1990 a, 1990b), the lagged cell subclass is especially sensitive to NMDA receptor antagonists (Heggelund and Hartveit, 1990; Kwon et al., 1991).

In this study I investigated mechanisms by which NMDA receptors on LGN cells might modulate excitatory postsynaptic responses evoked by retinal inputs, using an in vitro slice preparation of the ferret LGN. I find that both fast and slow components of the optic tract EPSP are attenuated by NMDA receptor blockade over a wide range of membrane potentials. In addition, when outward potassium currents are reduced, I observe a voltage dependent subthreshold enhancement of EPSP amplitude and duration which is blocked by d-APV. Consistent with my results from in vivo recordings in the cat LGN (Kwon et al., 1991), the magnitude of the effect of d-APV varies among cells in the ferret LGN.

Portions of these results have been previously presented in abstract form (Esguerra et al. 1989, Esguerra and Sur 1990).

METHODS

Slices of adult ferret LGN were prepared for recording and stimulation as described previously in the General Methods section of Chapter 1. Bipolar stimulating electrodes were placed in the optic tract at the outer border of lamina C. I made intracellular recordings along a line emanating from the stimulation site and orthogonal to laminar borders.

RESULTS

A total of 59 cells met my criteria for stable intracellular recording. Of these, 27 showed clear postsynaptic responses to optic tract stimulation. The mean resting potential of the 27 cells was -61.6 ± 5.2 mV (s.d.); mean apparent input resistance was 45.8 ± 32.5 MΩ; mean membrane time constant was 16.4 ± 13.4 ms.

Neurons in the ferret LGN showed responses to intracellular current injection that were very similar to those described for thalamic cells from other species. In particular, nearly every cell (25 of 27) showed 2 distinct modes of firing in response to current steps, depending on the cell's membrane potential. Figure 1 shows a typical cell responding in these 2 modes. At membrane potentials more positive than about -70 mV (the actual value varied from -62 to -70 mV in different cells), a depolarizing current pulse gave rise to a sustained train of overshooting action potentials (Figure 1A). The spike frequencies usually lacked pronounced adaptation and varied between 10 and 150 Hz, depending on the amount of depolarization and the starting membrane potential. Such responses represent the "tonic" firing mode of thalamic neurons (Jahnsen and Llinas, 1982; McCormick and Feeser, 1990). At membrane potentials between -70 and about -100 mV, a depolarizing current pulse evoked a slow, large-amplitude depolarization on which were superimposed several fast action potentials. The depolarization resembles closely in time course, amplitude, and voltage-dependence the low-threshold "calcium spike" that underlies the "burst" mode of firing of thalamic neurons (Llinas

and Jahnsen, 1982; Steriade and Llinas, 1988; McCormick and Feeser, 1990).

Agonist application

Application of NMDA to intracellularly recorded LGN cells via the submersion bath (instantaneous concentration, 50-100 μM; n=2) or with hanging drops in the interface chamber (pipette concentration 10-20 μM; n=3) resulted in large depolarizations with time to peak amplitude ranging between 10 and 60 seconds (Figure 2) This depolarization was accompanied by a train of action potentials which quickly inactivated during the sustained depolarization (asterisk in Figure 2). During NMDA activation, the cells' input resistance decreased (average decrease, 54%), and sometimes increased temporarily during the earlier stages of recovery. Recovery to baseline sometimes required many minutes.

Synaptic responses to optic tract stimulation

Effects of d-APV on EPSPs. Intracellularly recorded responses to optic tract stimulation were identified as postsynaptic when the responses were graded with stimulus strength, had somewhat variable starting delays after optic tract stimulation, fired action potentials at threshold, and were sensitive to EAA receptor antagonists. I routinely measured, for EPSPs elicited at resting membrane potentials, peak height measured from baseline voltage at the time of optic tract stimulation, EPSP width at one-half peak amplitude, latency to peak, and decay constant. These values for the cells in my sample are shown in Table 1. Application of d-APV attenuated the peak

amplitude and duration of optic tract-evoked EPSPs (n=14; $p<.05$, Mann-Whitney U test, for each comparison between normal and d-APV EPSPs). The latency to peak increased slightly, and the decay constant was somewhat shortened by d-APV, although the differences from normal were not significant. Three cells were tested in the presence of 10 μM bicuculline; their sensitivity to d-APV did not differ from those tested with $GABA_A$ inhibition intact, and they were pooled with the other cells for the purposes of this report.

Figure 3 shows an example of an EPSP evoked in an LGN cell at rest following stimulation of the optic tract, and the effect of 20 μM d-APV at different times after bath application. At steady state (10 minutes), d-APV had reduced the EPSP amplitude by an average of 54% and half-width by 58%. The component of the EPSP that was sensitive to d-APV application, and that was hence mediated by NMDA receptors, was substantial even following a single shock to the optic tract. The shapes of EPSPs varied slightly at different times after d-APV application, but the overall contribution of the NMDA-mediated component remained very similar.

Voltage dependence of NMDA receptor-mediated EPSPs. We investigated the voltage-dependence of the EPSP in individual neurons by injecting current through the recording electrode in bridge mode, and observing the effects of the resulting changes in membrane potential on EPSP amplitude and time course. The amplitude and duration of optic tract-evoked EPSPs were markedly enhanced as membrane

potentials were varied from severely hyperpolarized levels to a level just subthreshold for spike generation; this enhancement was abolished by d-APV (n=4). I observed such voltage dependence only when responses were recorded with cesium-containing electrodes. With these electrodes, I was able to change membrane potential between -120 and 0 mV; in some cells, at membrane potentials more depolarized than about -60 mV, even small EPSPs or small amounts of current injection led to action potentials that obscured synaptic components. Figure 4 shows the effects of varying transmembrane potential on the EPSP recorded from an LGN cell with a cesium-containing electrode. At potentials negative to -70 mV, the EPSP was of relatively small amplitude and decayed with a rapid time course. At -71 mV, the EPSP began to lengthen until it reached its peak width and amplitude at -67 mV. At -63 mV, optic tract stimulation (of the same intensity as before) evoked a train of action potentials in this cell; the site of the inflection point between the rising EPSP and takeoff of the first action potential suggests that this EPSP in isolation would have been even larger than that recorded at -67 mV. Bath application of 10 μM d-APV removed the voltage sensitivity of the optic tract-evoked EPSP, reduced its peak amplitude and dramatically shortened EPSP time course (Figure 4, center column, and Figure 5). Subtraction of the responses in d-APV from responses recorded in normal solution revealed the d-APV sensitive component of the optic tract EPSP. This component was nearly absent at hyperpolarized membrane potentials, but increased in both amplitude and duration as transmembrane voltage was depolarized (figure 4, right column).

A plot of EPSP amplitude and half-width against membrane potential for the same cell shows the subthreshold enhancement of these parameters as responses are elicited at more depolarized voltages (Figure 5). D-APV (10 μM) attenuates substantially both the EPSP peak amplitude and half-width, and the steep increase of both parameters as membrane potential is depolarized is reduced significantly by d-APV (Figure 5). I attribute the persistence of a shallow voltage-dependence of EPSP amplitude and half-width after application of the antagonist to remaining voltage-dependent NMDA receptor-mediated components that are not fully blocked by 10 μM d-APV.

When intracellular recordings were made with 4M potassium acetate as the electrolyte, I was unable to observe a consistent relationship between membrane potential and EPSP amplitude (n=7; see below and Discussion). However, optic tract-evoked responses were still reduced by d-APV application. Figure 6 shows a typical optic tract EPSP recorded with a potassium-containing electrode, at membrane potentials between -53 and -77 mV. Responses in normal ACSF and 20 μM d-APV are superimposed. Application of d-APV reduced the EPSP amplitude by an average of 8.5 mV (79%) and half-width by 3.9 ms (25%). In normal ACSF, the EPSP showed none of the subthreshold enhancement seen with cesium-filled electrodes, and both the amplitude and half-width remained essentially constant at membrane potentials between -71 mV and -53 mV.

At membrane potentials negative to -71 mV, the optic tract EPSP in this cell

showed a form of enhancement clearly distinct from the APV-sensitive component described above. At the most hyperpolarized membrane potential tested, the optic tract EPSP increased in duration while its peak amplitude remained unchanged (half width for EPSP marked by open arrow in Figure 6A, 17.3 ms; compare to mean half width of 15.6 ± 0.7 ms for other traces shown). In this and other cells (n=4), optic tract stimulation at sufficiently hyperpolarized membrane potentials led to slow, long-latency depolarizations that could develop into responses clearly resembling low-threshold calcium spikes. This effect was highly sensitive to membrane voltage, stimulation strength, and characteristics of the underlying EPSP, and invariably occurred at voltages identical to those at which low-threshold calcium spikes were elicited by current injection alone. Figure 6B shows responses of an LGN cell to optic tract stimulation at a membrane potential deeply hyperpolarized from rest. The traces were recorded 20 seconds apart in normal solution at identical membrane potentials and shock strengths. In trace B1, the optic tract-evoked EPSP gave rise to a depolarizing potential that accelerated rapidly toward spike threshold, elicited 2 action potentials, and slowly decayed toward baseline. In its time course and evocation by a depolarizing step (EPSP) from hyperpolarized membrane potentials, this response is identical to the low-threshold calcium spike (cf. Figure 1; see also Crunelli et al., 1987; Scharfman et al, 1990). In contrast to low threshold spikes evoked by direct current injection (Figure 1), however, the appearance of this spike was not all-or-none when it was elicited by optic tract stimulation. Trace B2 shows the response of this cell to identical optic tract stimulation 20 seconds later.

Instead of a fully developed calcium spike, this response shows a second rising phase that begins 20 ms post-stimulation, giving a distinct bimodal or humped appearance to the EPSP. In general, optic tract stimuli at hyperpolarized membrane potentials gave rise to responses that ranged from slight broadening of EPSPs to larger calcium currents without fast action potentials to full calcium spikes with action potential bursts.

The size of the calcium current evoked by optic tract stimulation depended on the rate of rise of the EPSP. The inset of figure 6B shows the initial phases of the 2 illustrated EPSPs. Response 1 rose at an initial rate of 125 V/s and gave rise to the full calcium spike, while response 2 increased at 95 V/s and only partially activated the calcium current.

Range of d-APV effects. The effects of d-APV application on the optic tract-evoked EPSP varied among cells. Figure 7 shows responses from 3 different LGN neurons that exemplify the range of effects observed after d-APV application. Note that each EPSP was recorded at a different resting membrane potential; the EPSP with the largest d-APV sensitive component (Figure 7A) was recorded at the most hyperpolarized membrane potential, while smaller effects were seen at more depolarized membrane potentials. The variability in the effects of d-APV included variable reductions in EPSP amplitude, half-width, latency to peak and decay constant (see below).

The effect of d-APV on various parameters of optic tract-evoked EPSPs in my

sample of cells in shown in Figure 8. All EPSPs were recorded at resting membrane potential (between -53 and -72 mV). The amplitude and time course of EPSPs were most consistently affected by d-APV, as shown by the reductions in peak amplitude and half-width (Figure 8, A and B ; Table 1 shows the mean reductions in each of the parameters). The effects on the latency to peak and decay constant were less consistent.

In order to determine whether the synaptic response that remained after NMDA receptor blockade was mediated by non-NMDA receptors, I applied both d-APV and CNQX to the optic tract-evoked EPSP. Figure 9 shows that addition of CNQX in conjunction with d-APV completely abolished the retinogeniculate EPSP. This effect reversed partially after washout of the CNQX and d-APV (n=2).

DISCUSSION

My results indicate that NMDA receptors play a crucial role in synaptic transmission between retinal ganglion cell afferents and postsynaptic cells in the ferret lateral geniculate nucleus. Intracellular recordings of retinogeniculate EPSPs show that this effect is due to direct participation of these receptors in generation of the postsynaptic response to optic tract activity.

I consider it unlikely that my optic tract electrodes stimulated afferents other than those arising from retinal ganglion cells, since no evidence exists for significant afferent pathways in the optic tract other than the retinogeniculate projection. This conclusion is further supported by the observation that d-APV application substantially reduces visual responses in the LGN of intact animals (see below). Furthermore, the observed responses are probably monosynaptic, since intracellular labelling of cat and ferret LGN cells with HRP and fluorescent markers suggests that no collaterals of relay cell axons arborize within the nucleus (Friedlander et al, 1981; Esguerra and Sur, 1987).

Membrane voltage and NMDA receptor activation

The voltage dependence of the d-APV sensitive EPSP component in my slice preparation was most prominent as membrane potentials were depolarized up to spike threshold. These voltages are more hyperpolarized than would be predicted by the negative slope conductance region of the NMDA current observed in isolated

patches (about -60 mV to -30 mV; Mayer and Westbrook, 1987). However, EPSP amplitudes tended to be between 5 and 10 mV measured at the soma, and could have brought the membrane potential transiently into the negative slope conductance region of NMDA receptors. Furthermore, since the EPSP amplitude measured at the soma is likely to be attenuated in amplitude and distorted in its time course by the electrotonic properties of the cell (Koch, 1985; cf. Bloomfield et al, 1987), it is possible that the initial amplitude of the retinogeniculate EPSP is even larger than observed at the soma, and hence the membrane adjacent to retinogeniculate synapses depolarized transiently even more.

The voltage-dependent enhancement of the EPSP was only observed when recorded with cesium-containing electrodes (Figure 4). Since intracellular cesium blocks outward potassium currents (Connors et al., 1982), this result suggests that potassium conductances could be shunting either currents injected through the recording electrode or generated by synaptic activation. Potassium conductances did not appear to directly affect the NMDA receptor current, since I still observed large reductions of the optic tract-evoked EPSP after d-APV application even with potassium-containing electrodes. It is more likely that outward potassium currents blocked attempts to change the membrane voltage at sites of retinogeniculate input by shunting currents injected at the soma through potassium-containing electrodes, and this must be considered as an issue in intracellular analyses of thalamic neurons.

It is also possible that the EPSP would not show a change with membrane

potential because the NMDA and non-NMDA components of the EPSP could vary in opposite directions as membrane voltage is altered, and an increase in one component might cancel a decrease in the other. However, this is unlikely in a cell with a large contribution from NMDA receptors to the EPSP, such as the cell shown in Figure 6 (cf. Figure 4).

While dendritic regions receiving synaptic input appeared to be affected little by current injection through potassium-containing electrodes, the same electrodes easily modulated low threshold calcium conductances. However, this calcium current is a membrance conductance whose distribution does not necessarily coincide with sites of synaptic input. Antidromically activated action potentials in LGN cells can elicit low threshold calcium spikes in the absence of any soma-dendritic action potential components, suggesting that low threshold calcium channels are located close to the axon initial segment, either at the soma or on proximal dendrites (Deschenes et al., 1984; see also Hernandez-Cruz and Pape, 1989).

Synaptic currents and low-threshold calcium currents evoked by synaptic activation

In the present study, optic tract EPSPs evoked at membrane potentials between about -70 mV and spike threshold had a concave falling phase, and did not show the variable late peak that has been described for EPSPs from cat LGN in vitro (Scharfman et al, 1990). However, I did obtain EPSPs with similar late peaks at membrane potentials at which low-threshold calcium currents are prominent (Figure

6B), suggesting that broad or "bimodal" retinogeniculate EPSPs consist of an early synaptic component and a later calcium-dependent membrane component that does not lead to a fully-developed calcium "spike." EPSPs recorded in cat LGN neurons following stimulation of the optic radiations at hyperpolarized voltages show a similar late component that disappears upon depolarization (D. McCormick, personal communication). Importantly, Scharfman et al. also describe "unimodal" EPSPs that resemble the EPSPs I obtain at membrane potentials more depolarized than -70 mV.

I have not determined whether optic tract-evoked low-threshold calcium currents or calcium spikes in ferret LGN are sensitive to d-APV; however, the voltage dependence of the NMDA component of retinogeniculate EPSPs would suggest that this component is very small at the membrane potentials at which low-threshold calcium currents are de-inactivated. I cannot rule out the possibility that NMDA receptor blockade would subtly affect the amplitude of the early EPSP or its rising phase, to which the low-threshold spike seems to be exquisitely sensitive. Indeed, a suggestion consistent with my data is that the large effect of d-APV on the late component of the "bimodal" EPSP observed by Scharfman et al. (1990) is due to rather small effects on the early synaptic component of the EPSP, followed by a considerable secondary effect on the later low-threshold calcium component.

Contribution of NMDA receptors to retinogeniculate transmission

I found that NMDA receptor blockade attenuated the peak amplitude and

duration of the retinogeniculate EPSP in most cells (Figures 3,4,6,7,8). It is unlikely that these reductions are due to nonspecific actions of d-APV on non-NMDA receptors mediating the early phase of EPSPs, since the concentration of d-APV used (in most cases 10-20 μM, in 2 instances 40 μM) is well within the limits of the concentration that is specific for NMDA receptors (e.g. Dingledine, 1986; Coan and Collingridge, 1987). Furthermore, d-APV is considerably more specific as an NMDA receptor antagonist than the racemic mixture dl-APV (Watkins and Olverman, 1987; Lodge et al., 1988; Coleman and Miller, 1988).

The variation in the effect of NMDA receptor blockade from cell to cell under the same concentrations of antagonist suggests that NMDA receptors exist, or at least contribute to retinogeniculate transmission, in varying proportions on different LGN cell classes. While identification of functional cell classes by the usual physiological criteria is impossible in the isolated LGN, my recordings are likely to have been from a mixture of X and Y LGN cells, since the terminal arbors of single retinal X and Y axons overlap in the A laminae of the ferret LGN (Roe et al, 1989). It is possible that morphological differences could be used to distinguish functional cell classes in LGN slices (Friedlander et al., 1981; Humphrey and Weller, 1988). my results also raise the possibility that the lack of effect of d-APV on retinogeniculate EPSPs observed by Crunelli et al. (1987) in the rat LGN are due to variable contributions of NMDA receptors to retinogeniculate EPSPs.

The variability in the influence of d-APV that I observe in the ferret LGN <u>in vitro</u> is consistent with results of iontophoresis experiments performed in the intact

cat, for which a range of sensitivities of the visual responses of LGN cells to EAA receptor blockade is also reported. In these studies, this variation appears to be loosely associated with functional class, as revealed by temporal properties of LGN cell responses to visual stimulation. Heggelund and Hartveit (1990) reported that the visual responses of lagged cells are reduced by the NMDA antagonist CPP, while nonlagged cell responses are preferentially blocked by the non-NMDA antagonist DNQX. Iontophoresis experiments in the cat LGN performed in our laboratory partially support this dissociation; in our hands the visual responses of lagged LGN cells are attenuated more by d-APV than the responses of nonlagged cells, but CNQX has roughly equal effects on lagged and nonlagged cells (Kwon et al, 1991). Whether or not the different sensitivities of lagged and nonlagged cells to d-APV indicate a pharmacological distinction between unique LGN cell classes, or differential participation of NMDA receptors during different response modes of the same cell, remains an open question (Kwon et al., 1991).

Functional consequences

The attenuation of single-shock optic tract responses by d-APV supports the hypothesis that NMDA receptors play a significant role in single synaptic events and conventional visual processing in the retinogeniculate pathway. The involvement of NMDA receptors in retinogeniculate transmission fits well with other evidence indicating that a crucial function of the mammalian lateral geniculate nucleus is to regulate the flow of retinal information to visual cortex (e.g. Sherman and Koch,

1986). My results suggest that NMDA receptors can gate visual transmission by modulating EPSP amplitudes and time courses near spike threshold, depending on changes in membrane voltages of LGN neurons. Depolarization and consequent activation of large NMDA receptor-mediated synaptic currents could lead to nonlinear increases in spike frequency, while hyperpolarization could reduce spiking in a nonlinear fashion. These changes in the membrane potential of LGN neurons may be produced by summation of EPSPs due to repetitive retinal input itself, or by activity in extraretinal afferents such as the corticogeniculate feedback projection (Esguerra and Sur, 1990).

REFERENCES

Artola, A., and Singer, W. (1987). Long-term potentiation and NMDA receptors in rat visual cortex. Nature 330, 649-652.

Bloomfield, S. A, Hamos, J. E., and Sherman, S. M. (1987). Passive cable properties and morphological correlates of neurones in the lateral geniculate nucleus of the cat. J. Physiol. 383, 653-692.

Cline, H. T., Debski, E. A., and Constantine-Paton, M. (1987) N-methyl-D-aspartate antagonist desegregates eye-specific stripes. Proc. Natl. Acad. Sci. 84, 4342-4345.

Coan, E. J., and Collingridge, G. L. (1987). Characterization of an N-methyl-D-aspartate receptor component of synaptic transmission in rat hippocampal slices. Neuroscience 22, 1-8.

Coleman, P. A., and Miller, R. F. (1988). Do N-methyl-D-aspartate receptors mediate synaptic responses in the mudpuppy retina? J. Neurosci. 8, 4728-2733.

Connors, B. W., Gutnick, M. J., and Prince, D. A. (1982). Electrophysiological properties of neocortical neurons in vitro. J. Neurophysiol. 48, 1302-1320.

Crunelli, V., Kelly, J. S., Leresche, N., and Pirchio, M. (1987). On the excitatory post-synaptic potential evoked by stimulation of the optic tract in the rat lateral geniculate nucleus. J. Physiol. 384, 603-618.

Deschenes, M., Paradis, M., Roy, J. P., and Steriade, M. (1984). Electrophysiology of neurones of lateral thalamic nuclei in cat: resting properties and burst discharges. J. Neurophysiol. 51, 1196-1219.

Dingledine, R. (1986). NMDA receptors: what do they do? TINS 9, 47-49.

Esguerra, M., Kwon, Y. H., and Sur, M. (1989). NMDA and non-NMDA receptors mediate retinogeniculate transmission in cat and ferret LGN in vitro. Soc. Neurosci. Abstr. 15, 175.

Esguerra, M., and Sur, M. (1990). Corticogeniculate feedback gates retinogeniculate transmission by activating NMDA receptors. Soc. Neurosci. Abstr. 15, 159.

Fox, K., Sato, H., and Daw, N. (1990). The effect of varying stimulus intensity on NMDA-receptor activity in cat visual cortex. J. Neurophysiol. 64, 1413-1428.

Friedlander, M. J., Lin, C.-S., Stanford, L. R., and Sherman, S. M. (1981). Morphology of functionally identified neurons in lateral geniculate nucleus of the

cat. J. Neurophysiol. 46, 80-129.

Hahm, J., Langdon, R. B., and Sur, M. (1990). NMDA antagonists disrupt normal ON/OFF sublaminar segregation of ferret retinogeniculate axons. Soc. Neurosci. Abstr. 16, 1128.

Hartveit, E., and Heggelund, P. (1990). Neurotransmitter receptors mediating excitatory input to cells in the cat lateral geniculate nucleus. II. Nonlagged cells. J. Neurophysiol. 63, 1361-1372.

Heggelund, P., and Hartveit, E. (1990). Neurotransmitter receptors mediating excitatory input to cells in the the cat lateral geniculate nucleus. I. Lagged cells. J. Neurophysiol. 63, 1347-1360.

Humphrey, A. L., and Weller, R. E. (1988). Structural correlates of functionally distinct X-cells in the lateral geniculate nucleus of the cat. J. Comp. Neurol. 268, 448-468.

Jahnsen, H., and Llinas, R. (1984). Electrophysiological properties of guinea- pig thalamic neurones: an in vitro study. J. Physiol. 349, 205-226.

Kauer, J. A., Malenka, R. C., and Nicoll, R. A. (1988). A persistent postsynaptic

modification mediates long-term potentiation in the hippocampus. Neuron 1, 911-917.

Kemp, J. A., and Sillito, A. M. (1982). The nature of the excitatory transmitter mediating X and Y cell inputs to the cat dorsal lateral geniculate nucleus. J. Physiol. 323, 377-391.

Koch, C. (1985). Understanding the intrinsic circuitry of the cat's lateral geniculate nucleus: electrical properties of the spine-triad arrangement. Proc. Roy. Soc. Lond. 225, 365-390.

Kwon, Y. H., Esguerra, M., and Sur, M. (1991). NMDA and non-NMDA receptors mediate visual responses of neurons in the cat's lateral geniculate nucleus. J. Neurophysiol., in press.

Lodge, D., Davies, S. N., Jones, M. G., Millar, J., Manallack, D. T., Ornstein, P. L., Verberne, A. J. M., Young, N., and Beart, P. M. (1988). A comparison between the in vivo and in vitro activity of five potent and competitive NMDA antagonists. Brit. J. Pharm. 95, 957-965.

MacDermott, A. B., and Dale, N.(1987). Receptors, ion channels, and synaptic potentials underlying the integrative actions of excitatory amino acids. TINS 10,

280-284.

Mayer, M. L., and Westbrook, G. L. (1987). The physiology of excitatory amino acids in the vertebrate central nervous system. Prog. Neurobiol. 28, 197-276.

McCormick, D.A., and Feeser, H. R. (1990). Functional implications of burst firing and single spike activity in lateral geniculate nucleus neurons. Neuroscience 39, 103-113.

Roe, A. W., Garraghty, P. E., and Sur, M. (1989). Terminal arbors of single ON-center and OFF center X and Y retinal ganglion cell axons within the ferret's lateral geniculate nucleus. J. Comp. Neurol. 288, 208-242.

Scharfman, H. E., Lu, S.-M., Guido, W., Adams, P. R., and Sherman, S. M. (1990). N-methyl-D-aspartate receptors contribute to excitatory postsynaptic potentials of cat lateral geniculate neurons recorded in thalamic slices. Proc. Natl. Acad. Sci. 87, 4548-4552.

Sherman, S.M., and Koch, C. (1986). The control of retinogeniculate transmission in the mammalian lateral geniculate nucleus. Exp. Brain Res. 63, 1-20.

Sillito, A. M., Murphy, P. C., Salt, T. E., and Moody, C. I. (1990a). Dependence of

retinogeniculate transmission in cat on NMDA receptors. J. Neurophysiol. 63, 347-355.

Sillito, A. M., Murphy, P.C., and Salt, T. E. (1990b). The contribution of the non-N-methyl-D-aspartate group of excitatory amino acid receptors to retinogeniculate transmission in the cat. Neuroscience 34, 273-280.

Steriade, M., and Llinas, R. (1988) The functional states of the thalamus and the associated neuronal interplay. Physiol. Rev. 68, 649-742.

Watkins, J. C., and Olverman, H. J. (1987) Agonists and antagonists for excitatory amino acid receptors. TINS 10, 265-272.

Table 1
Parameters of EPSPs evoked in LGN cells by stimulation of the optic tract, and the effect of d-APV. All values are shown as mean ± s.e.; n=14 cells. See also Figure 8, and the text for details.

	Normal	d-APV	Mean % Reduction
Peak (mV)	5.69 ± 0.67	3.87 ± 0.60	33.02 ± 5.28
Half-Width (ms)	22.84 ± 3.44	16.63 ± 3.67	28.36 ± 7.48
Latency to Peak (ms)	6.85 ± 1.86	7.82 ± 3.69	8.19 ± 12.43
Decay Constant (ms)	50.76 ± 23.6	31.42 ± 9.44	7.13 ± 15.39

FIGURE LEGENDS

Figure 1. Responses of a neuron in the ferret LGN to intracellular current injection. Left: The cell's membrane potential was held at -54 mV by injection of dc current. A superimposed 0.1 nA x 120 ms depolarizing pulse elicits a train of action potentials which persists over the period of current injection. Latency to threshold for first spike, 1.1 ms. Mean interspike interval, 22.9 ms (44 Hz). Right: Membrane potential held at -91 mV. Injection of 0.1 nA at this membrane potential elicits a broad depolarizing potential capped by a high-frequency burst of 4 action potentials. Mean interspike interval, 2.3 ms (434 Hz). Latency to first spike, 32.4 ms. This cell's resting potential was -65 mV; input resistance was 83 MΩ. Unless otherwise specified, all intracellular records in this and subsequent figures were obtained using electrodes filled with 4M potassium acetate.

Figure 2: Intracellular recording of an LGN cell response to NMDA. Upper chart recorder trace represents voltage, lower trace injected current (0.5 nA hyperpolarizing pulses). Application of a drop of 10 μM NMDA to the slice surface (drop volume < 100 pL) elicited a long (> 1 min) depolarization and action potentials which rapidly inactivated (*). The cell's input resistance decreased dramatically in the presence of NMDA.

Figure 3. Effect of d-APV on the retinogeniculate EPSP. Left: Optic tract evoked

responses in normal ACSF (Control) and after addition of d-APV to the perfusion solution. Right: APV-sensitive components derived by subtraction of each response in d-APV from the control trace. For these traces and all following figures, solid arrowheads indicate time of optic tract stimulation. Scale bars apply to both parts of the figure.

Figure 4. Application of d-APV attenuates a voltage-dependent component of the retinogeniculate EPSP. Left: EPSPs evoked by electrical stimulation of the optic tract. Membrane potential was varied by intracellular current injection. Stimulation at most depolarized voltage elicited action potentials, which are shown clipped to save space. Note increase in EPSP amplitude and width with progressive depolarization. Center: Optic tract evoked EPSPs from the same neuron, recorded during perfusion with ACSF containing 10 μM d-APV. Responses show considerably less variation with membrane potential than in normal ACSF. Right: d-APV sensitive component of the optic tract evoked EPSP. Traces were obtained by subtracting the response in d-APV from the control response at the same membrane potential. The control response that included action potentials was not included in the subtractions. Membrane voltages and scale bars apply to all 3 sets of traces.

Figure 5. Voltage dependence of the EPSP peak and half-width and effect of d-APV. The values in the graphs are derived from traces in Figure 4. Peak amplitudes are measured from average baseline voltage in the 5 ms preceding optic tract stimulation. Half-widths were measured by recording the width of the EPSP at

a voltage representing half the peak amplitude. Each set of traces has been fitted with a 2nd order polynomial function.

Figure 6. A: Example of an optic tract-evoked EPSP that was sensitive to d-APV, but did not show voltage dependence when recorded with a potassium-filled electrode. Optic tract-evoked responses in normal ACSF are shown superimposed on responses in 20 uM d-APV. Membrane potentials are as indicated at left. The open arrow on the trace at -77 mV shows broadening of the EPSP, presumably due to a low-threshold calcium current that is partially activated by the synaptic component of the EPSP. B: Records from a different cell, showing that at hyperpolarized membrane potentials, optic tract stimulation activated a low-threshold depolarizing current. Two optic tract-evoked EPSP's recorded in normal ACSF are shown superimposed. In trace B1, optic tract stimulation evoked a large depolarizing potential capped by a high-frequency burst of action potentials. The time course and voltage dependence of this response resemble that of the low-threshold calcium current described in LGN cells from other species. Trace B2 was collected 20 seconds after B1; the EPSP shows a prolonged time course that fails to develop into a full calcium spike. Membrane potential and optic tract stimulation strength are identical for both traces. Inset: Rising phases of EPSP B1 and B2 at higher gain and sweep speed. EPSP 1 rises at an initial rate of 1250 V/s; EPSP 2 rises at 950 V/s. Scale bar in inset, 1 mV x 2 ms.

Figure 7. Diversity of effects of d-APV on retinogeniculate EPSPs. A-C: Optic tract

evoked responses from 3 different LGN cells are shown. Upper traces: Dashed lines indicate responses in control ACSF; solid lines are responses after addition of 20 μM d-APV. Lower traces: APV-sensitive components derived by subtraction of the APV-attenuated response from control.

Figure 8. Histograms showing the distribution of d-APV effects on characteristics of retinogeniculate EPSPs. Peak amplitudes and half widths were measured as described in the legend to Fig. 5. Time to peak was measured from the EPSP take-off point. Decay constant was determined by fitting a single-term exponential (see Methods) to the region between the EPSP peak and return to initial baseline voltage.

Figure 9. Simultaneous blockade of NMDA and non-NMDA receptors reversibly abolishes the optic tract-evoked EPSP. Traces were obtained by recording first in normal ACSF (control), then successively after addition of 20 μM d-APV, addition of 5 uM CNQX to the APV solution, and wash to normal ACSF. The entire procedure required 2 hours of stable recording. The amplitude of optic tract stimulation was kept constant for all traces.

Figure 1

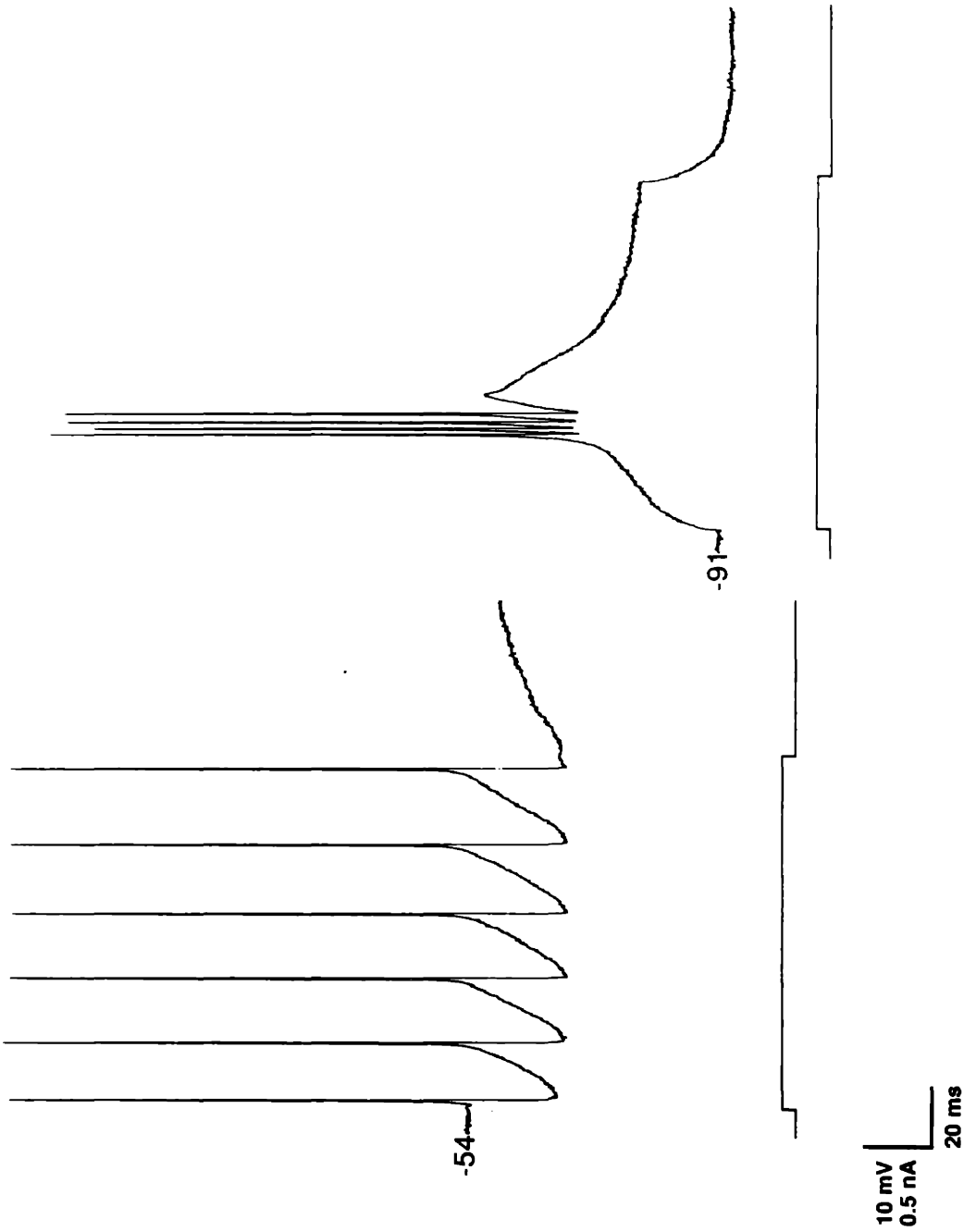

Figure 2

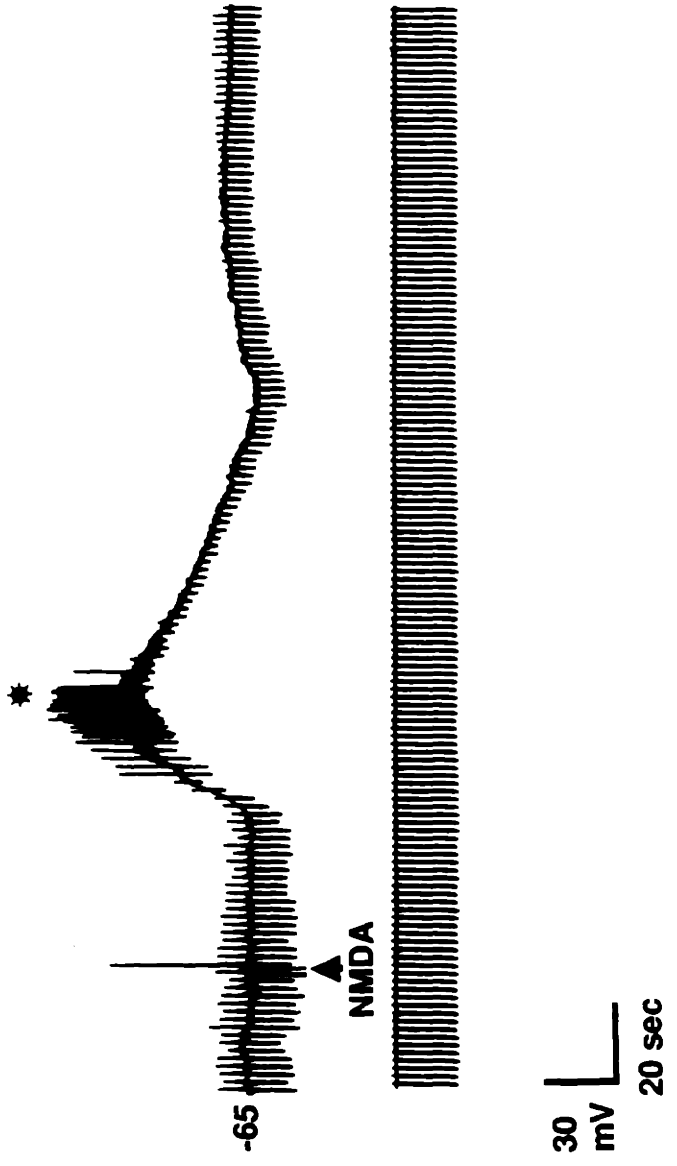

Figure 3

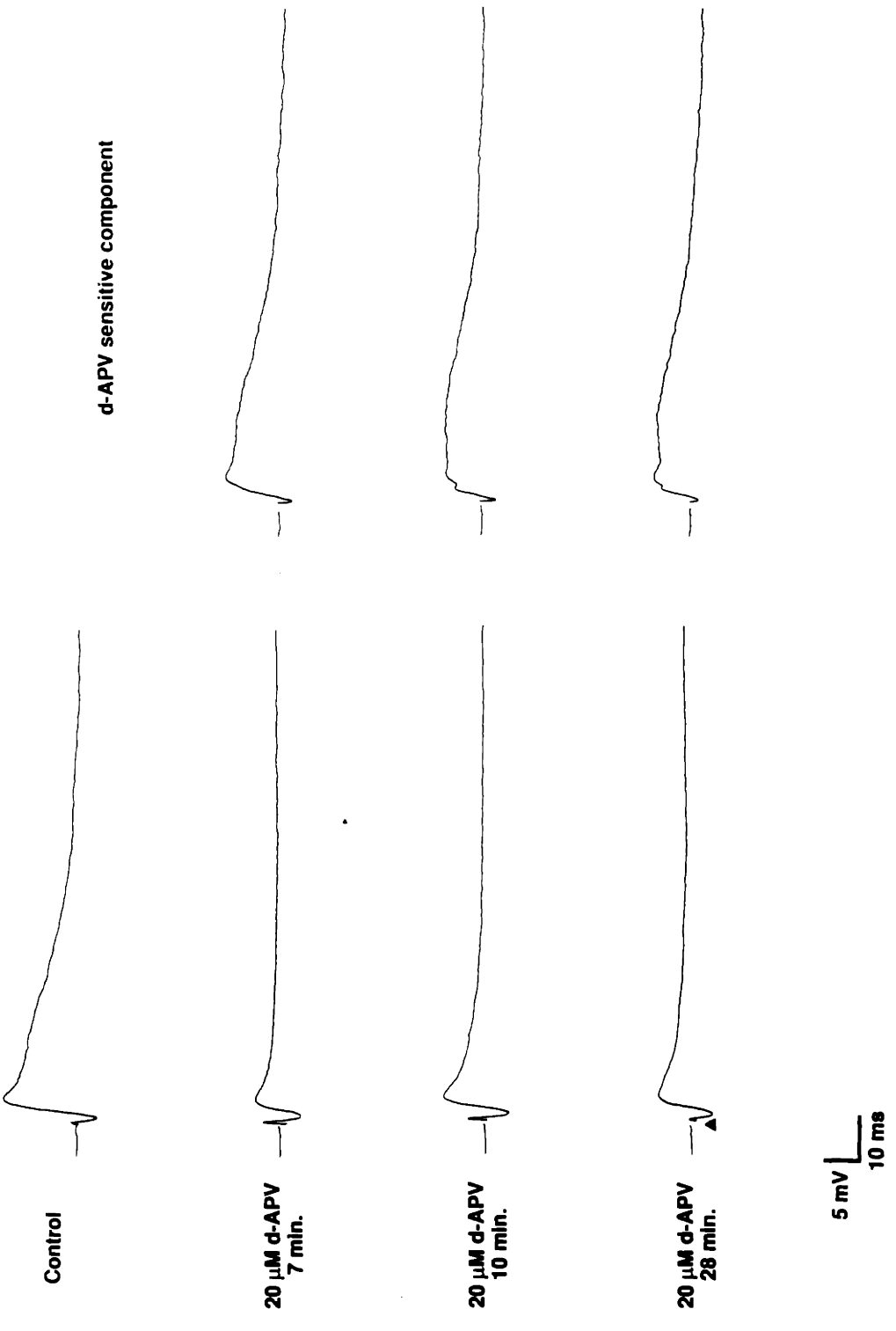
d-APV sensitive component
Control
20 µM d-APV
7 min.
20 µM d-APV
10 min.
20 µM d-APV
28 min.
5 mV
10 ms

Figure 4

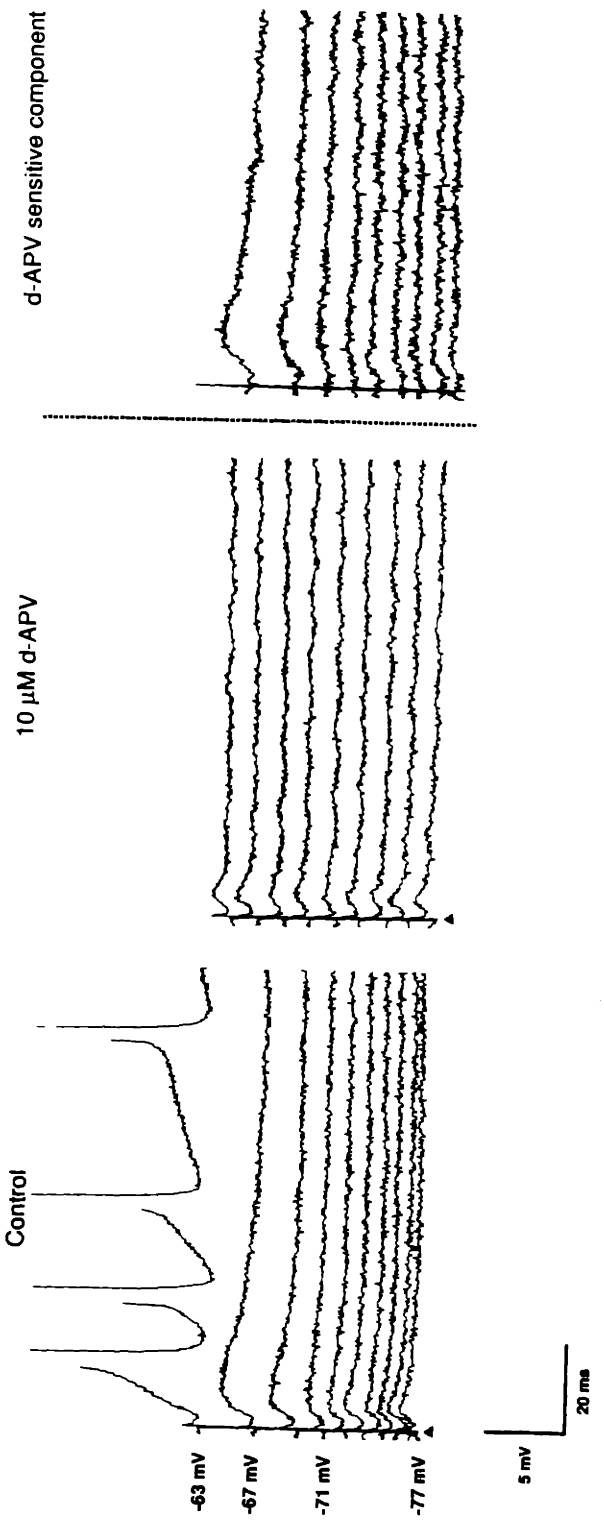
d-APV sensitive component
10 µM d-APV
Control
-63 mV
-67 mV
-71 mV
-77 mV
5 mV
20 ms

Figure 5

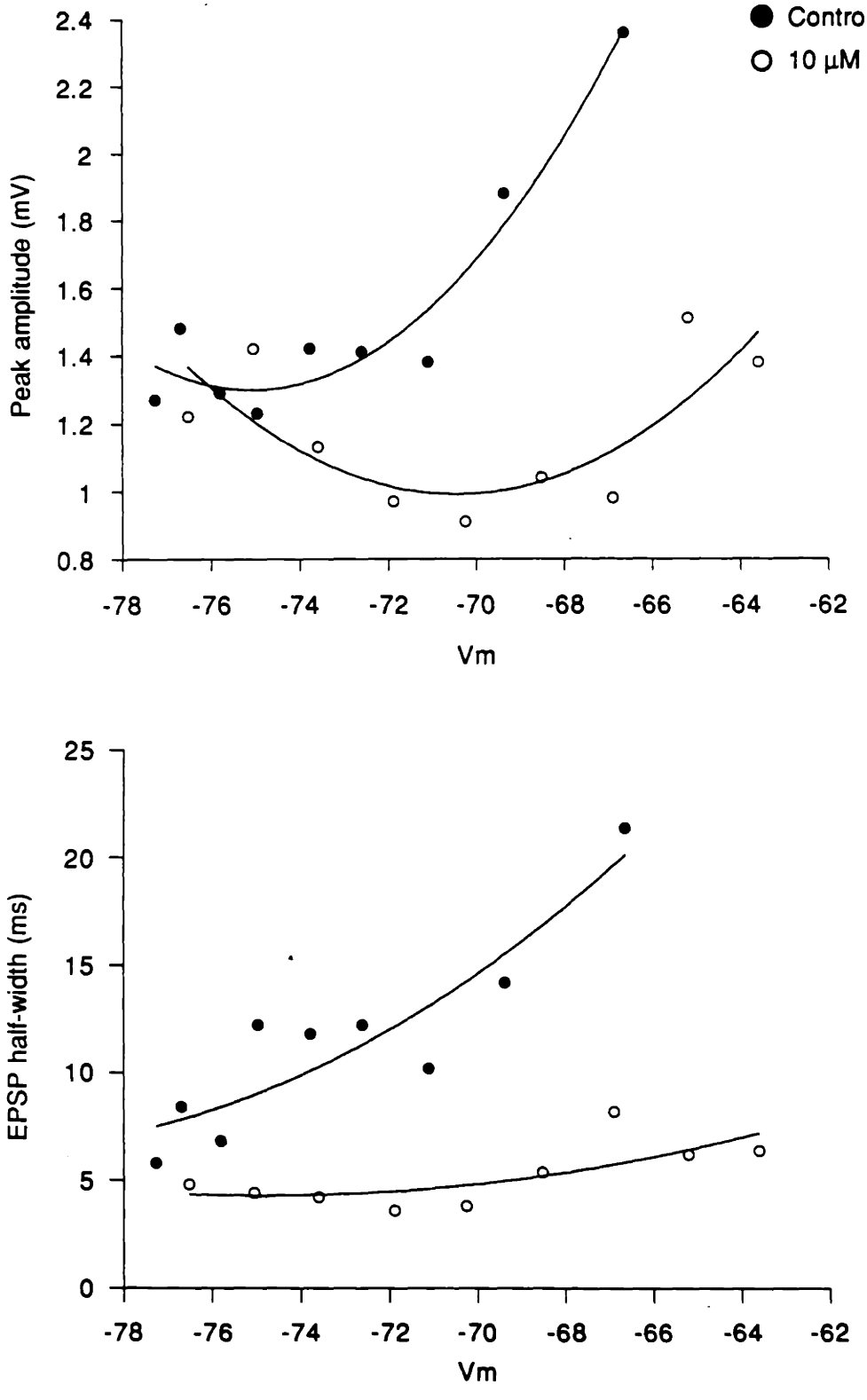
Control
10 µM d-APV
Peak amplitude (mV)
2.4
2.2
2
1.8
1.6
1.4
1.2
1
0.8
-78
-76
-74
-72
-70
-68
-66
-64
-62
Vm
EPSP half-width (ms)
25
20
15
10
5
0
-78
-76
-74
-72
-70
-68
-66
-64
-62
Vm

Figure 6

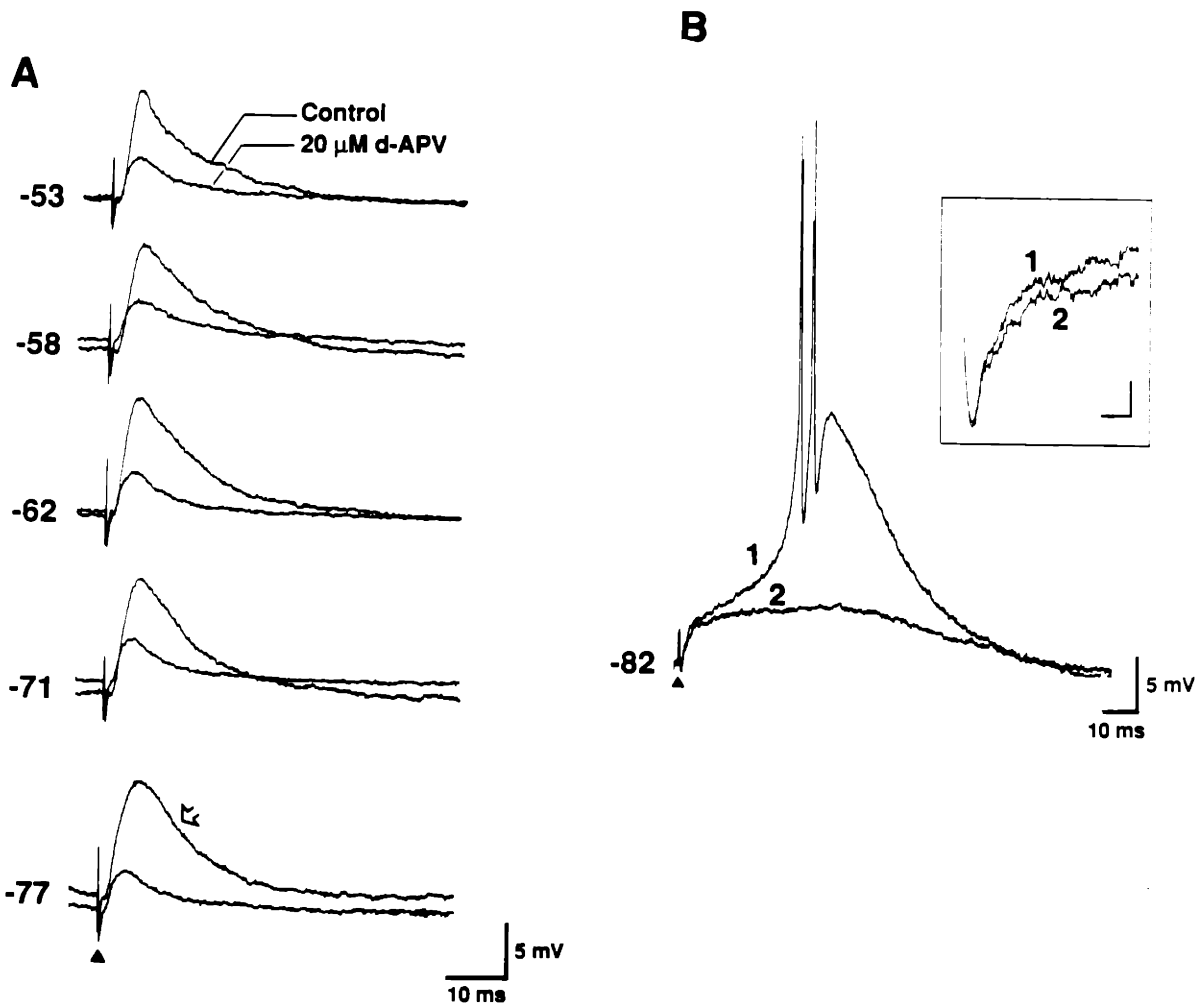

Figure 7

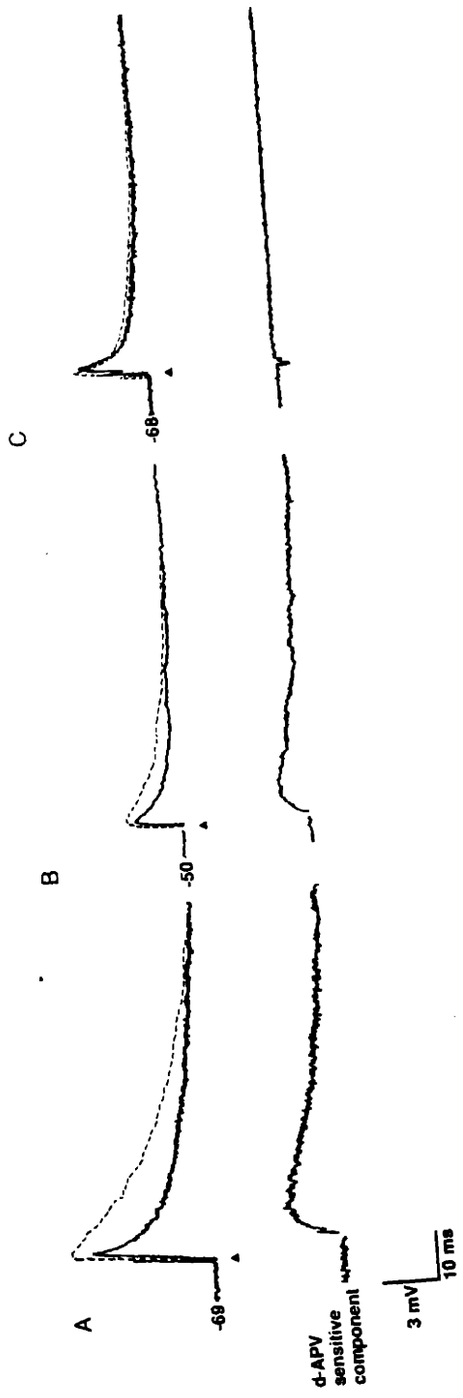

Figure 8

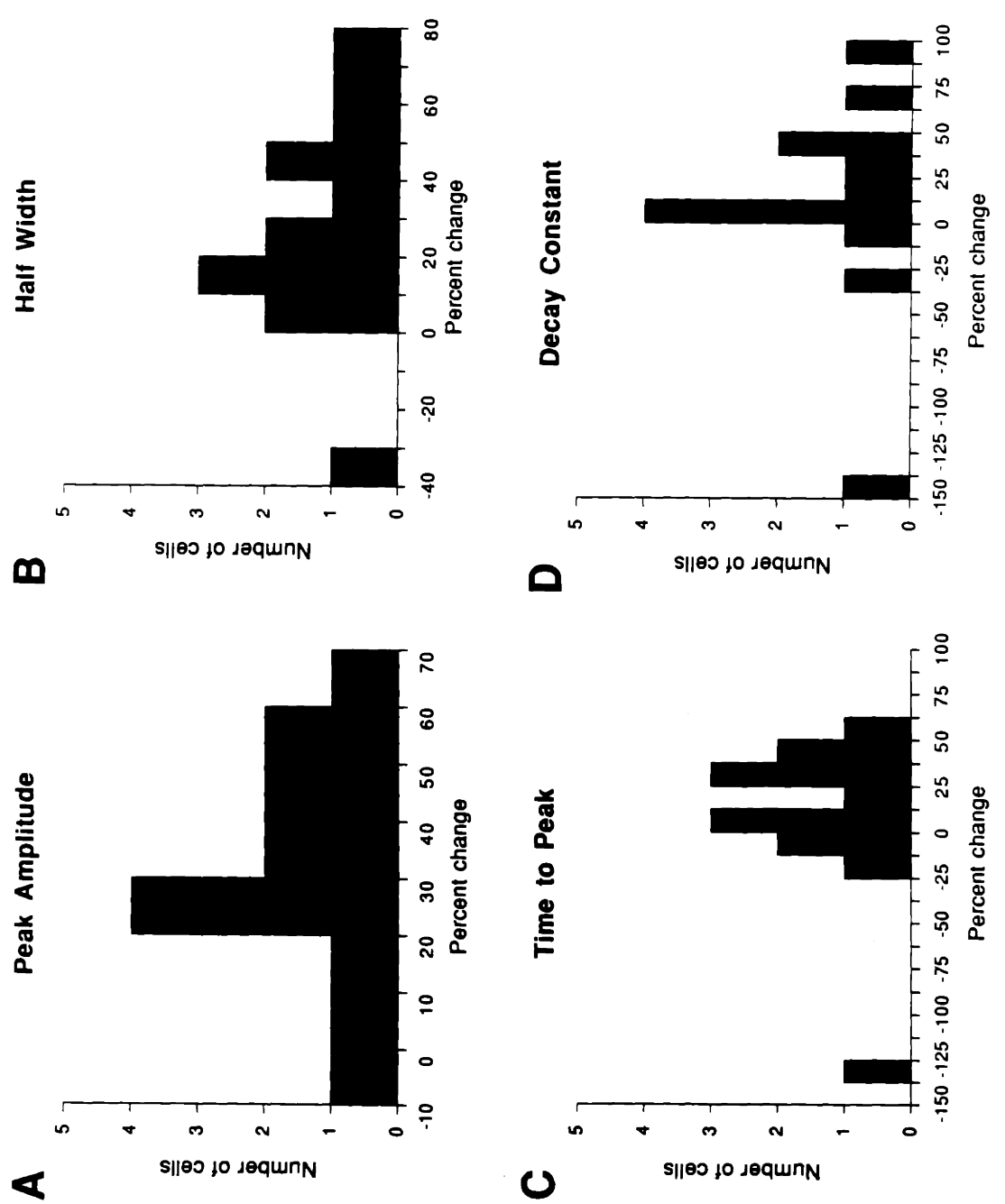

Esguerra et al.

Figure 8

Figure 9

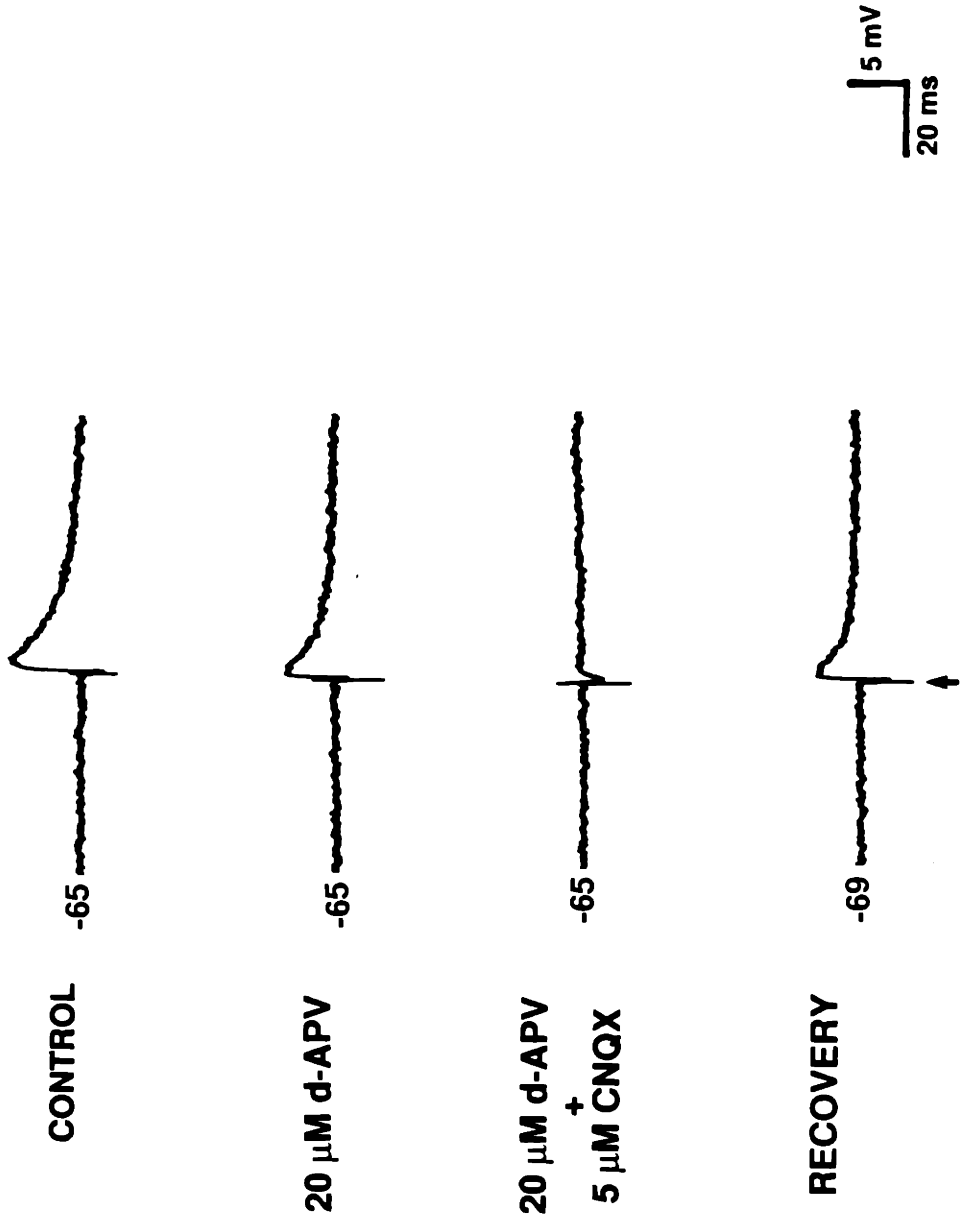
5 mV
20 ms
CONTROL
-65
20 μM d-APV
-65
20 μM d-APV
+
5 μM CNQX
-65
RECOVERY
-69

Chapter 4

Synaptic responses to stimulation of the cortical feedback projection in the ferret lateral geniculate nucleus *in vitro*.

ABSTRACT

Corticofugal afferents were activated by stimulation of the optic radiations in isolated slices of ferret lateral geniculate nucleus (LGN). Optic radiation stimulation elicited both excitatory and inhibitory postsynaptic responses in the LGN. The excitatory responses were monosynaptic and appeared to be similar to optic tract-evoked postsynaptic potentials in amplitude and duration. In contrast to retinogeniculate EPSPs, optic radiation-evoked responses could be divided into "fast" and "slow" types based on the time courses of their activation. Most corticogeniculate EPSPs were attenuated by blockade of NMDA receptors; one EPSP was apparent only in low-magnesium medium, and was blocked completely by normal levels of extracellular magnesium. I propose that a possible role of the corticofugal projection is to produce local dendritic depolarizations that can modulate nearby sites of retinogeniculate input.

INTRODUCTION

In the preceding chapter of this thesis, I demonstrated that changes in the membrane voltage of LGN cells can enhance the efficacy of the retinogeniculate EPSP by the activation of NMDA receptors. An important question remains open: at sites of retinogeniculate input, what physiological influences on LGN cells could depolarize the membrane to activate NMDA receptors to cause enhancement of the retinogeniculate EPSP? In this chapter, I propose that the corticofugal feedback projection from visual cortex to the LGN is capable of this modulation.

Part I of this Chapter describes the characteristics of the EPSP evoked by electrical stimulation of corticofugal afferents in the optic radiations. Part II reports on the effects of concurrent stimulation of retinal and cortical afferents.

Anatomy of the cortical feedback projection

In the cat, the cortical projection to the LGN comprises the axons of layer VI pyramidal cells in areas 17, 18, and 19 of the visual cortex (Guillery, 1967). These axons represent about half of the cells in layer 6 (Gilbert and Kelly, 1975); thus each cell in the LGN may receive input from as many as 10 or more corticothalamic fibers (Sherman and Koch, 1988). The corticogeniculate projection appears to be retinotopically organized and in register with the visual map produced by ascending retinogeniculate afferents in both cats (Updyke, 1975; Robson, 1983)

and ferrets (Claps and Casagrande, 1990). In ferrets, the corticogeniculate fibers enter the LGN from the anterior border of the nucleus, passing first through the perigeniculate nucleus. There appear to be several populations of these axons with diverse morphologies and patterns of termination. The terminal fields of single corticogeniculate axons innervate all layers of the LGN, as well as interlaminar zones (Claps and Casagrande, 1990).

Physiological consequences of corticogeniculate pathway activity

To date, behavioral and physiological experiments performed in vivo have not provided a unified description of the effects of visual cortex blockade and stimulation on responses of LGN neurons. In some studies, inactivation of visual cortex, which strongly modulates responses in superior colliculus and pulvinar, appears to have no effect on LGN visual responses (Richard et al, 1975; Baker and Malpeli, 1977). On the other hand, when effects are reported, there is some dispute over their direction. In the extensive study by Kalil and Chase (1970), cooling area 17 lowered the background firing rate of LGN cells and their responses to stationary spots of light, while receptive field organization remained unaffected. The most dramatic effect of cortical cooling was on LGN cell responses to moving bars. The responses of both ON and OFF center LGN cells to moving bars was dramatically increased. Cortical ablation also appears to enhance the responses of LGN cells to moving bars by removing length tuning, which presumably derives from the length-summating receptive fields of the cells in layer 6 of cortex (Sillito and

Murphy, 1987). Both these studies support an inhibitory role of the cortical feedback projection. A study by Schmielau and Singer (1977) suggests that corticofugal feedback mediates a strong facilitation of LGN cell responses by the non-dominant eye. Both excitatory and inhibitory effects were reported by Geisert et al. (1981), who found that cooling elicited either or both of these effects in 86% of recorded LGN cells. Similarly, both excitatory and inhibitory effects were found in a study that used exotic visual stimuli to activate the corticogeniculate projection (Marrocco et al, 1982). The apparent conflict among these results may arise because cortical feedback fibers synapse with both principal cells and inhibitory interneurons in the LGN, as shown physiologically with intracellular recordings made in vivo (Ahlsen et al., 1982) and by ultrastructural analysis (Wilson et al. 1984; Weber and Kalil, 1983). The conditions under which either inhibitory or excitatory actions would predominate remain unknown.

In this chapter I describe the synaptic responses that electrical stimulation of the corticofugal projection evokes in cells of ferret LGN maintained in vitro.

The major findings of this part of the study may be summarized as follows:

1) Stimulation of the optic radiations can lead to expression of EPSPs and IPSPs recorded at the cell body of LGN cells.

2) Excitatory responses to optic radiation stimulation can be of 2 types: a fast EPSP that peaks less than 5 ms after stimulation, and a slow EPSP peaking at about

25 ms after stimulation.

3) Recordings made in the absence of Mg^{2+} suggest that some corticofugal EPSPs are masked in normal levels of Mg^{2+} and do not contribute to the membrane potential observed at the soma. Since physiological levels of Mg^{2+} can block NMDA receptor channels, this result implicates NMDA receptors in corticofugal transmission.

4) Suppression of cortical afferent stimulation responses by NMDA receptor antagonists suggests that NMDA receptors contribute to the optic-radiation evoked EPSP. The attenuation with d-APV was not well correlated with either EPSP rise time or membrane potential, suggesting that sites of cortical input to LGN cells are electrically distant from the intracellular recording site.

5) In their time courses and amplitudes, EPSPs evoked by optic radiation are similar to those evoked by optic tract stimulation.

METHODS

Slice preparation

Slices of ferret lateral geniculate nucleus in the parasagittal plane were prepared as described in the **General Methods** chapter. For experiments involving electrical stimulation of the optic radiations, each slice was trimmed to leave at least 500 μm of white matter intact anterior to the LGN; I made no attempt to ablate the perigeniculate nucleus in this preparation.

Afferent stimulation

I placed bipolar platinum-iridium stimulation electrodes on the white matter about 100 μm anterior to the inner edge of lamina A. In order to cause as little damage to fibers as possible, the wires were not driven through the white matter but placed on the surface of the slice. This arrangement gave strong synaptic responses with acceptably small artifacts at current levels of .1 to 1.0 mA, corresponding to between 2 and 20 V between the stimulating wires.

Antidromic excitation

Stimulation of the optic radiations can lead to antidromic activation of action potentials in LGN cells because the axons of relay neurons exit the nucleus through the optic radiations (Claps and Casagrande, 1990). Antidromic activation was

characterized by narrow action potentials with a brief latency; ability to follow high rates of stimulation without jitter or failure; and rapid rise times, i.e. lack of slow somatic or dendritic charging (Figure 1A, arrow). Cells which responded to optic radiation stimulation with only antidromic spikes were excluded from this part of the study.

RESULTS

Stimulation of the optic radiations was attempted in 22 slices of ferret LGN. For any given cell, the stimulation paradigm elicited one of four types of responses, which are exemplified in Figure 1. An antidromic, nonsynaptic action potential response is shown in Figure 1A. The action potential arises directly from the stimulus artifact, and shows no sign of a slow charging transient or inflection which would indicate invasion of the dendrites and soma by synaptic current. The antidromic spike is followed by an afterhyperpolarization with rapid rise time and slower decay. Such afterhyperpolarizations followed antidromic spikes in an all-or-none manner. Antidromic stimulation was also characterized by nearly 100% reliability of response, by lack of variability in timing of the response (lack of jitter), and by ability to follow high rates of stimulation. In all cells (n=17), a high intensity shock to the optic radiations could evoke such antidromic action potentials; in some cells, low voltages (ca. 2 V) evoked antidromic spikes, suggesting that the stimulating electrodes were directly in the path of the exiting

relay cell axons. These cells were not included in EPSP analysis, since the action potential and afterhyperpolarization obscured components of the synaptic potential.

The synaptic responses observed after optic radiation stimulation were of 3 types. Figure 1B shows a purely excitatory (depolarizing) response which rises following a short delay after stimulation (arrow). The response decays to baseline with a slow time course. These EPSPs (n = 15) usually gave rise to action potentials if evoked near threshold. Optic radiation stimulation also led to purely inhibitory synaptic events (Figure 1C; n=2), which did not include any sign of depolarizing or excitatory components at resting potentials. Since it is possible that this pure inhibition represents direct stimulation of axons arising in the perigeniculate nucleus of the thalamic reticular complex (see Discussion), the 2 cells that showed such responses were not included in the present study. Finally, in 2 cells, optic radiation stimulation elicited mixed excitatory and inhibitory responses (Figure 1D). These responses were characterized by a short excitatory component followed by a longer duration inhibitory component (IPSP), and most likely represent a direct excitatory input from the corticofugal afferents paired with a disynaptic feed-forward inhibition by intrinsic geniculate interneurons. Since I wished to investigate the influence of the excitatory component of corticogeniculate feedback, in both cases where I observed EPSP-IPSP paired responses I blocked the IPSPs by addition of 5-10 μM bicuculline methiodide to the perfusion medium.

In the cells in which excitatory synaptic responses to optic radiation stimulation were observed (including the 2 cells recorded in the presence of bicuculline), optic

radiation-evoked EPSPs varied somewhat in their amplitude and time course. Table 1 summarizes measurements of EPSPs from 17 LGN cells held at resting potential. The peak amplitude represents the height of the response relative to the pre-stimulation baseline voltage. Half-width is the width of the response between the points on the rise and fall of the EPSP corresponding to half the peak amplitude. Latency to the EPSP peak was measured from the foot of the EPSP to peak amplitude. The rise time of the EPSP was estimated by measuring the time required for the response to rise from 10% to 90% of its peak value. While EPSP amplitudes varied over a small range (1-10 mV), the temporal characterisitics of these EPSPs showed considerable variability. I examined more closely the distributions of latencies and rise times of EPSPs following optic radiation stimulation.

Fast and Slow EPSPs in response to optic radiation stimulation

Measurements of the rise times of optic radiation evoked EPSPs indicated that these responses fell into 2 groups, which I shall term "slow" and "fast" EPSPs. Figure 2A shows examples of these 2 classes of EPSP. The 10-90% rise time of the fast EPSP (left) was 2.6 ms. The slow EPSP at -59 mV (right) had a 23.6 ms rise time. Stimulation of the optic radiations while this cell was held at a depolarized membrane potential (-55 mV) did not significantly shorten the rise time of this EPSP, indicating that the low-threshold calcium current, which inactivates at depolarized potentials, did not contribute to lengthening of the EPSP (see below and Chapter 2 for further description of synaptically evoked low-threshold spikes). The

histograms in Figure 2B show the distributions of latencies and rise times of optic radiation evoked EPSPs from 13 LGN cells held at initial membrane potentials between -65 and -55 mV. The histograms clearly indicate a bimodal distribution of EPSP rise times and suggests a bimodal latency distribution. The EPSP rise time distribution shows modes at 3 and 25 ms, while latencies peak at 5 and 29 ms.

Low threshold calcium spikes

Stimulation of the optic radiations with cells held at hyperpolarized membrane potentials infrequently elicited low-threshold calcium spikes (n = 3). As I have described previously for responses to optic tract stimulation (Chapter 3), low-threshold spikes appeared only at membrane potentials hyperpolarized from rest, and only developed into a full spike when activated by a depolarizing input. The low-threshold spikes increased in latency with hyperpolarization, and inactivated again at deeply hyperpolarized levels, as described previously (Figure 3).

NMDA receptor contribution to the corticogeniculate EPSP

The effect of d-APV application (20 μM) on components of the the optic-radiation evoked EPSP varied widely. Application of d-APV (20 μM) reduced EPSP peak amplitudes by an average of 37.8%, ranging between 3% and 77% reduction (n = 5 out of 6 cells tested). An example of the largest reduction of optic radiation-evoked EPSP amplitude is shown in Figure 4. In one cell, the EPSP amplitude increased dramatically after d-APV application. The effect of d-APV on

the time course of EPSPs was also highly variable. Latency to peak was reduced 23.5% (n=2/6), half-width by 62.5% (n=2/6), and 10-90% rise time reduced by 36.7% (n=3/6). In the remaining cells, each of these measures was lengthened by d-APV.

The magnitude of APV reduction of OR-evoked EPSPs correlated weakly with 10%-90% rise times (r=-0.57, n=5), with larger APV effects ending to associate weakly with shorter rise times. There was also a weak tendency toward larger d-APV reductions of the EPSP at more hyperpolarized membrane potentials (r=0.49, n=5). These trends suggest that somatic membrane voltage and EPSP rise time are poor predictors for the amount of NMDA receptor activation in a corticogeniculate EPSP.

OR-evoked EPSPs showed voltage-sensitive enhancement of the half-width, but not the peak of the EPSP (n=3). Figure 5A shows optic radiations-evoked EPSPs from an LGN cell recorded with a 4 M cesium acetate electrode and held at membrane voltages between -14 and -73 mV. The EPSP amplitude decreases progressively with depolarization until it reverses between -14 and -25 mV, while the latency and rise time increase (Figure 4B), consistent with a progressive flattening of the EPSP as the membrane potential is depolarized from -73 mV. The half-width of the EPSP for this cell shows a slight enhancement in the -50 to -30 mV voltage range; for the other 2 cells, the increase in half-width occurred at even more depolarized levels (not shown).

The participation of NMDA receptors in OR EPSPs suggests that these responses

should also be sensitive to the concentration of magnesium in the extracellular fluid (Ascher et al., 1988; Ascher and Nowak, 1988). I tested the effects of magnesium removal on optic radiation-evoked EPSPs recorded in one cell from the ferret LGN (Figure 6). In order to save time, these recordings were begun in ACSF from which Mg++ had been removed and replaced with equimolar sodium to maintain osmotic balance. The medium also contained 10 μM bicuculline methiodide to block inhibitory transmission. Under these initial conditions, optic radiation stimulation evoked a small EPSP. Optic tract stimulation gave rise to a larger response. Addition of Mg++ to the bath at physiological concentrations (1.2 mM) abolished the OR-evoked response, while only slightly attenuating the optic tract evoked EPSP. The continued presence of a robust retinogeniculate EPSP indicates that the OR EPSP was not attenuated by general deterioration of the cell. Because 10μM bicuculline was continuously present under both conditions, this effect was also unlikely to be due to unmasking of a $GABA_A$ receptor-mediated inhibitory component.

Comparison of corticogeniculate and retinogeniculate EPSPs

The amplitude and time courses of optic tract-evoked and optic radiation-evoked (OR) EPSPs in the same cell were compared. I measured the peak amplitude, half-width, 10-90% rise time, and latency to peak of 6-7 consecutive EPSPs from each of 11 cells in which both optic tract and optic radiation stimulation elicited responses. For each measure I derived a ratio of OR to OT response for EPSP's

paired by order of presentation. A ratio of 1 for any measure indicates that the OR and OT responses were identical along this measure. Figure 7 shows histograms constructed from the distributions of these ratios. The distributions for peak amplitude, half-width, and 10%-90% rise time have major modes about a ratio of 1, indicating that the majority of OR and OT EPSPs are similar along these dimensions. Two deviations from this similarity are apparent. First, the latency to peak of OR EPSP's tended to be shorter than for OT EPSPs; note the rightward skew of the latency distribution. Second, the 10%-90% rise time distribution has a small second mode at about 2, indicating that a small population of optic radiation evoked EPSPs has rise times about double those of optic tract EPSP's.

DISCUSSION

These results confirm the prediction that the corticogeniculate projection can have a direct excitatory influence on cells of the lateral geniculate nucleus (Ahlsen et al., 1982; Koch, 1987). This excitation takes the form of EPSPs that cover a small range of amplitudes and a wide range of time courses. In particular, corticogeniculate EPSPs comprise at least 2 populations, one that rises rapidly toward peak amplitude, and another that rises with a much slower time course. The time course of the response to cortical input can have a profound effect on voltage-dependent modulation of retinal activity and spike output. By holding cells at depolarized levels for shorter or longer periods, the cortical EPSP could be maintaining cells in one of the firing modes described in Chapter 2 on signaling modes of LGN cells. Finally, some active membrane conductances, such as the low threshold calcium current, are directly influenced by the rate of a voltage change as well as its amplitude (Chapters 2 and 3). The 2 populations of corticogeniculate EPSPs could arise by several mechanisms, which I discuss below.

Diverse populations of corticogeniculate afferents. The 2 EPSP types may represent different populations of corticogeniculate axon terminals, one close to the soma producing fast EPSPs, and another population farther from the soma producing slow EPSPs. Ultrastructural evidence (Wilson et al., 1984) indicates that RSD axon terminals in the cat LGN, which are believed to arise from corticogeniculate axons,

tend to appose dendritic shafts distal to presumed sites of retinal input. The electrotonic properties of a long dendritic arbor could account for the long rise time and duration of slow EPSPs; EPSP amplitudes would also be attenuated by these properties. A variant on this interpretation is that the EPSPs represent input from distinct populations of cortical layer VI neurons. There is evidence for distinct classes of corticogeniculate axons based on single axon morphology and patterns of projection in the monkey (Lund et al., 1975), cat (Updyke, 1975; Robson, 1983), and ferret (Claps and Casagrande, 1990). Different morphological subclasses of cortical afferents could also have physiological properties that would account for the diversity of EPSPs elicited by optic radiation stimulation.

Variable convergence of corticogeniculate inputs to LGN cells. The large numbers of corticogeniculate axons (10 to 40 times more than in the retinal projection: Updyke, 1975; Robson, 1983) suggests that there is a large amount of convergence of corticogeniculate input to LGN cells. If the slicing procedure were to leave different numbers of cortical axons intact for different cells, then their responses could appear to be of different size. A larger number of intact axons could lead to a larger postsynaptic response if the inputs are stimulated simultaneously. A larger complement of axons might also have a wider distribution of conduction velocities and dispersion on dendrites, with the result being an apparent lengthening of the EPSP rise time and duration. This hypothesis assumes that the ensemble of axons converging on a single LGN cell travel close together through the site of stimulation; local injections of anterograde tracers suggest that

this is the case (Claps and Casagrande, 1990). It also assumes that the response to synchronous activity of many spatially and temporally separated synaptic inputs would be manifest as a single EPSP recorded at the cell body. Except for cells giving rise to paired EPSP-IPSP response, we saw no evidence for polymodal epsps that could arise from activity in afferents with different latencies; instead I observed monolithic EPSPs with uninterrupted rise and fall courses. However, temporally or spatially dispersed inputs may still give rise to somatic transients with smooth time courses, as has been shown with models of multiple inputs to spinal motor neurons (Walmsley and Stuklis, 1989). Furthermore, retinogeniculate afferents make several thousand contacts with postsynaptic cells in the LGN (Roe et al., 1989), but the response recorded at the cell body takes a smoothly rising and decaying course (See Chapter 3).

Synaptic currents with different time courses The time course of the slow EPSP might be interpreted as reflecting the slow rise of an EPSP mediated primarily by NMDA receptor activation. If this were the case, then we would expect slow EPSPs to be exquisitely sensitive to blockade by d-APV. However, NMDA antagonists appeared to affect equally both fast and slow EPSPs, suggesting that differential distribution of excitatory amino acid receptors cannot account for their different temporal properties.

Morphology of postsynaptic cells A final possibility is that different corticogeniculate EPSPs are the results of transformations of similar inputs by neurons with different morphologies. Cells in the lateral geniculate nucleus of cats

have been classified morphologically by use of Golgi staining (Guillery, 1966) and intracellular injection of physiologically identified single neurons (Friedlander et al., 1981). These classes differ in the sizes of their somata; numbers, diameters, and lengths of dendritic branches; and in the distribution of inputs to spines or dendritic shafts. Koch (1985) and others have postulated that the passive characteristics derived from the morphology of a neuron, together with its distribution of active conductances, can profoundly influence the somatic expression of currents injected into the dendrites. Since ferret LGN cells are also of heterogeneous morphologies (Esguerra et al., 1987), it is possible that the classes of EPSPs observed here represent different processing of synaptic inputs by cells of different anatomical, and perhaps functional classes.

Inhibitory functions of the corticogeniculate projection

I have investigated here only the role of exitatory inputs to the LGN. Anatomical and physiological evidence suggest that the cortex can also exert a powerful inhibitory influence on LGN cells indirectly through its connections to intrinsic interneurons and the perigeniculate nucleus (Dubin and Cleland, 1977). Electron micrographs show that corticofugal fibers synapse onto profiles that resemble the dendrites and axons of inhibitory interneurons (Weber and Kalil, 1983), suggesting that cortical input could produce feedforward inhibition similar to that seen for optic tract stimulation (Crunelli and Leresche, 1991). Another source of inhibitory influence on LGN cells is the perigeniculate nucleus, a sheet of GABA-containing cells anterior to the inner border of the LGN (Linden et al.,

1981). Its neurons send inhibitory terminals directly into the LGN. A possible source of inhibitory responses observed in this study was direct stimulation of these inhibitory axons; this could explain the presence of IPSPs that did not show an initial depolarizing component. The responses could also be the result of indirect inhibition produced by stimulation of collaterals of corticogeniculate axons that terminate in the PGN (Claps and Casagrande, 1990).

In the absence of visual stimulation, I was unable to support or reject the hypothesis that the pattern of inhibition and excitation by corticogeniculate input is determined by the relative alignment of cortical and LGN cell receptive fields (Tsumoto et al, 1978). The large stimulating electrodes used here would most likely have stimulated a population of cortical afferents whose aggregate receptive field exceeds the 3 degree boundaries reported by these authors. Thus it is not surprising that we were able to observe both excitatory and inhibitory effects of corticogeniculate stimulation.

Role of NMDA receptors in the corticofugal EPSP

The sensitivity of the corticogeniculate EPSP to d-APV strongly suggests that NMDA receptors participate in corticogeniculate as well as retinogeniculate transmission. The presence of NMDA receptors at sites of corticothalamic input has been described also for optic radiation evoked EPSPs in the cat lateral geniculate nucleus in vitro (Scharfman et al, 1990) and for lateral thalamic nuclei in vivo (Deschenes and Hu, 1990). The apparently complete blockade of a corticogeniculate EPSP by normal levels of extracellular magnesium (Figure 6) suggests that at least

some EPSPs are mediated in their entirety by NMDA receptors. Furthermore, under these conditions single shocks to the optic radiations and injection of current at the soma did not elicit enough depolarization to relieve the magnesium blockade of NMDA receptors. This conclusion would imply that in normal function, high frequency stimulation or another source of depolarization such as modulatory transmitters would be necessary to activate NMDA receptors at sites of corticogeniculate input. High frequency stimuli are necessary to observe some NMDA components of responses in hippocampal neurons (Collingridge et al., 1988); a similar mechanism may operate for the cortical input to LGN cells.

An alternative explanation for the sensitivity of this EPSP to magnesium concentration is that stimulation elicited an EPSP that was so attenuated by the presence of magnesium and by the membrane properties of the cell that it was too small to observe at the cell body. Since sites of corticofugal input are farther from the soma than are sites of retinal input (Wilson et al. 1984), optic radiation-evoked EPSPs may be subject to more passive attenuation than optic tract evoked responses. This interpretation raises the possibility that cortical inputs modulate voltage locally in the dendritic arbor, without significant direct effects on somatic membrane potential. This possibility was discussed by Koch (1987), in which he proposes that one role of the corticogeniculate projection is to enhance transmission of visual information by depolarizing sites of retinogeniculate input, thereby activating the large currents carried by NMDA receptors.

REFERENCES

Ahlsen, G., Grant, K., and Lindstrom, S. (1982). Monosynaptic excitation of principal cells in the lateral geniculate nucleus by corticofugal fibers. Brain Res. 234, 454-458.

Artola, A., and Singer, W. (1987). Long-term potentiation and NMDA receptors in rat visual cortex. Nature 330, 649-652.

Ascher, P., Bregestovski, P., and Nowak, L. (1988). N-methyl-D-aspartate-activated channels of mouse central neurones in magnesium-free solutions. J. Physiol. 399, 207-226.

Ascher, P., and Nowak, L. (1988). The role of divalent cations in the N-methyl-D-aspartate responses on mouse central neurones in culture. J. Physiol. 399, 247-266.

Baker, F.H., and Malpeli, J.G. (1977). Effects of cryogenic blockade of visual cortex on the responses of lateral geniculate neurons in the monkey. Exp. Brain Res. 29, 433-444.

Bromberg, M.B., Penney, J.B., Stephenson, B.S. and Young A.B. (1981) Evidence

for glutamate as the neurotransmitter of corticothalamic and corticorubral pathways. Brain Res. 215, 369-374.

Claps, A., and Casagrande, V. A. (1990). The distribution and morphology of corticogeniculate axons in ferrets. Brain Res. 530, 126-129.

Collingridge, G. L., Herron, C. E., and Lester, R. A. J. (1988). Frequency-dependent N-methyl-D-aspartate receptor-mediated synaptic transmission in rat hippocampus. J. Physiol. 399, 301-312.

Cotman, C.W., Monaghan, D.T., Ottersen O.P. and Storm-Mathisen, J. (1987). Anatomical organization of excitatory amino acid receptors and their pathways. TINS 10, 273-280.

Crick, F. H. C. (1984). The function of the thalamic reticular complex: the searchlight hypothesis. Proc. Natl. Acad. Sci. USA 81, 4586-4590.

Crunelli, V., Kelly, J. S., Leresche, N., and Pirchio, M. (1987). On the excitatory postsynaptic potential evoked by stimulation of the optic tract in the rat lateral geniculate nucleus. J. Physiol. 384, 603-618.

Crunelli, V., and Leresche, N. (1991). A role for $GABA_B$ receptors in excitation and inhibition of thalamocortical cells. TINS 14, 16-21.

Deschenes, M., and Hu, B. (1990). Electrophysiology and pharmacology of the corticothalamic input to lateral thalamic nuclei: an intracellular study in the cat. Eur. J. Neurosci. 2, 140-152.

Dubin, M. W., and Cleland, B.G. (1977). Organization of visual inputs to interneurons of lateral geniculate nucleus of the cat. J. Neurophysiol. 40, 410-427.

Esguerra, M., Kwon, Y. H., and Sur, M. (1989). NMDA and non-NMDA receptors mediate retinogeniculate transmission in cat and ferret LGN in vitro. Soc. Neurosci. Abstr. 15, 175.

Fonnum, F., Fosse, V.M. and Allen, C.N. (1984). Identification of excitatory amino acid pathways in the mammalian nervous system. In Excitotoxins, K. Fuxe, P.J. Roberts, and R. Schwarcz, eds., pp. 3-18, Plenum, New York.

Friedlander, M. J., Lin, C.-S., Stanford, L. R., and Sherman, S. M. (1981). Morphology of functionally identified neurons in lateral geniculate nucleus of the cat. J. Neurophysiol. 46, 80-129.

Geisert, E.E., Langsetmo, A., and Spear, P.D. (1981). Influence of the cortico-geniculate pathway on response properties of cat lateral geniculate neurons.

Brain Res. 208, 409-415.

Gilbert, C.,D., and Kelly, J. P. (1975). The projections of cells in different layers of the cat's visual cortex. J. Comp. Neurol. 163, 81-106.

Guillery, R.W. (1966). A study of Golgi preparations from the dorsal lateral geniculate nucleus of the adult cat. J. Comp. Neurol. 128, 21-50.

Guillery, R.W. (1967). Patterns of fiber degeneration in the dorsal lateral genicualt nuclus of the cat following lesions in the visual vortex. J. Comp. Neurol. 130, 197-222.

Heggelund, P. and Hartveit, E. (1989). Lagged and non-lagged X-cells in the cat lateral geniculate nucleus receive retinal input through different glutamate receptors. Soc. Neurosci. Abstr. 15, 175.

Honore, T., Davies, S. N., Drejer, J., Fletcher, E. J., Jacobsen, P., Lodge, D., and Nielsen, F. E. (1988). Quinoxalinediones: potent competitive non-NMDA glutamate receptor antagonists. Science 241, 701-703.

Horikawa, K., and Armstrong, W. E. (1988). A versatile means of intracellular labeling: injection of biocytin and its detection with avidin conjugates. J. Neurosci.

Meth. 25, 1-11.

Humphrey, A. L., and Weller, R. E. (1988) Structural correlates of functionally distinct X-cells in the lateral geniculate nucleus of the cat. J. Comp. Neurol. 268, 448-468.

Jackson, C. A., and Hickey, T. L. (1985).Use of ferrets in studies of the visual system. Lab. Animal Sci. 35, 211-215.

Jahnsen, H., and Llinas, R. (1984). Ionic basis for the electroresponsiveness and oscillatory properties of guinea-pig thalamic neurones in vitro. J. Physiol. 349, 227-247.

Jahnsen, H., and Llinas, R. (1984). Electrophysiological properties of guinea-pig thalamic neurones: an in vitro study. J. Physiol. 349, 205-226.

Kalil, R. E., and Chase, R. (1970) Corticofugal influence on activity of lateral geniculate neurons in the cat. J. Neurophysiol. 33, 459-474.

Kemp, J. A., and Sillito, A. M. (1982). The nature of the excitatory transmitter mediating X- and Y- cell inputs to the cat dorsal lateral geniculate nucleus. J. Physiol. 323, 377-391.

Koch, C. (1987) The action of the corticofugal pathway on sensory thalamic nuclei: an hypothesis. Neuroscience 25, 399-406.

Kwon, Y. H., Esguerra, M., and Sur, M. (1989). Off-center cells in the cat lateral geniculate nucleus are senitive to NMDA receptor blockade. Soc. Neurosci. Abstr. 15, 175.

Marrocco, R. T., McClurkin, J. W., and Young, R. A. (1982). Modulation of lateral geniculate nucleus cell responsiveness by visual activation of the corticogeniculate pathway. J. Neurosci. 2, 256-263.

Mayer, M. L., and Westbrook, G. L. (1987). The physiology of excitatory amino acids in the vertebrate central nervous system. Prog. Neurobiol. 28, 197-276.

McCormick, D. A. (1989). Cholinergic and noradrenergic modulation of thalamocortical processing. TINS 12, 215-221.

Monaghan, D.T., Yao, D. and Cotman, C.W. (1983). L-[3H]glutamate binds to kainate, NMDA-, and AMPA-sensitive binding sites: an autoradiographic analysis. Brain Res. 340, 378-383.

Murphy, P.C., and Sillito, A.M. (1987). Corticofugal feedback influences the generation of length tuning in the visual pathway. Nature 329, 727-729.

Olverman,H.T., Monaghan,D.T., Cotman, C.W., and Watkins, J.C. (1986) [3H]CPP, a new competitive ligand for NMDA receptors. Eur. J. Pharmacol. 131, 161-162.

Richard, D., Gioanni, Y., Kitsikis, A., and Buser, P. (1975). A study of geniculate unit activity during cryogenic blockade of the primary visual cortex in the cat. Exp. Brain Res. 22, 235-242.

Robson, J. A. (1983). The morphology of corticofugal axons to the dorsal lateral geniculate nucleus in the cat. J. Comp. Neurol. 216, 89-103.

Salt, T. E., and Eaton, S. A. (1989). Function of non-NMDA receptors and NMDA receptors in synaptic responses to natural somatosensory stimulation in the ventrobasal thalamus. Exp. Brain Res. 77, 646-652.

Scharfman, H. E., Lu, S.-M., Guido, W., Adams, P.R., and Sherman, S.M. (1990). N-methyl-D-aspartate receptors contribute to excitatory postsynaptic potentials of cat lateral geniculate neurons recorded in thalamic slices. Proc. Natl. Acad. Sci. 87, 4548-4552.

Schmielau, F., and Singer, W. (1977). The role of visual cortex for binocular interactions in the cat lateral geniculate nucleus. Brain Res. 120, 354-361.

Sherman, S. M. and Koch, C. (1988). The control of retinogeniculate transmission in the mammalian lateral geniculate nucleus. Exp. Brain Res. 63, 1-20.

Singer, W. (1977). Control of retinogeniculate transmission by corticofugal and ascending reticular pathways in the visual system. Physiol. Rev. 57, 390-420.

Steriade, M., and Deschenes, M. (1984) The thalamus as a neuronal oscillator. Brain Res. Rev. 8, 1-63.

Steriade, M., and Llinas, R. (1988) The functional states of the thalamus and the associated neuronal interplay. Physiol. Rev. 68, 649-742.

Stryker, M. P., and Zahs, K. R. (1983). ON and OFF sublaminae in the lateral geniculate nucleus of the ferret. J. Neurosci. 3, 1943-1951.

Thomson, A.M. (1986). A magnesium-sensitive post-synaptic potential in rat cerebral cortex resembles neuronal responses to N methyl aspartate. J Physiol. 370, 531-549.

Tsumoto, T., Creutzfeldt, O. D., and Legendy, C. R. (1978). Functional organization

of the corticofugal system from visual cortex to lateral geniculate nucleus in the cat. Exp. Brain. Res. 32, 345-364.

Updyke, B.V. (1975). The patterns of projection of cortical areas 17, 18, and 19 onto the laminae of the dorsal lateral geniculate nucleus in the cat. J. Comp. Neurol. 163, 377-396.

Weber, A. J., and Kalil, R. E. (1983). The percentage of interneurons in the dorsal lateral geniculate nucleus of the cat and observations on several variables that affect the sensitivity of horseradish peroxidase as a retrograde marker. J. Comp. Neurol. 220, 336-346.

Wilson, J. R., Friedlander, M. J., and Sherman, S. M. (1984). Ultrastructural morphology of identified X- and Y-cells in the cat's lateral geniculate nucleus. Proc. Roy. Soc. Lond. B 221, 411-436.

Table 1. Optic radiation EPSPs evoked at resting potential

			EPSP			10%-90%
Cell	Vm	n	Amplitude	Half-Width	Latency	Rise Time
1	-64	8	10.6 ± 0.4	26.1 ± 1.3	2.1 ±.1	1.4 ± 0.0
2	-63	8	1.3 ± 0.1	23.6 ± 11.9	33.7 ± 18.3	32.0 ± 18.2
3	-66	8	2.2 ± 0.4	51.7 ± 12.3	30.5 ± 11.5	25.0 ± 12.1
4	-68	6	9.26 ± 0.7	142.3 ± 12.1	64.7 ± 16.9	35.8 ± 6.2
5	-59	4	1.8 ± 0.7	21.4 ± 11.6	27.9 ± 9.1	21.2 ± 9.2
6	-62	8	1.3 ± 0.2	20.6 ± 22.1	33.4 ± 13.7	29.3 ± 14.3
7	-63	8	2.5 ± 0.7	31.5 ± 14.6	26.7 ± 13 .6	19.5 ± 13.1
8	-57	8	5.9 ± 0.3	83.7 ± 8.0	25.9 ± 6.6	16.8 ± 5.9
9	-65	8	8.7 ± 1.2	85.4 ± 28.4	1.8 ± 0.6	0.5 ± 0.2
10	-49	8	5.8 ± 0.6	20.3 ± 0.9	6.1 ± 1.1	3.4 ± 0.5
11	-56	15	4.0 ± 0.4	23.5 ± 8.7	6.7 ± 1.1	4.8 ± 0.7
12	-72	8	2.4 ± 0.3	3.2 ± 0.4	1.8 ± 0.4	1.2 ± 0.3
13	-59	16	4.2 ± 1.0	8.8 ± 4.1	3.9 ± 1.3	2.7 ± 1.6
14	-62	6	5.2 ± 0.8	5.2 ± 0.5	2.0 ± 0.2	1.2 ± 0.1
15	-70	8	1.9 ± 0.2	65.1 ± 28.0	5.8 ± 0.9	4.6 ± 1.0
16	-69	2	7.4 ± 1.3	13.7 ± 1.5	2.2 ± 0.1	1.2 ± 0.1
17	-73	16	4.9 ± 0.6	57.2 ± 5.9	24.8 ± 3.6	21.8 ± 3.6

All values are expressed as mean ± S.D.

FIGURE LEGENDS

Figure 1. The four types of responses observed after stimulation of optic radiations in the ferret lateral geniculate nucleus. The responses of four different cells to single shocks are shown. A. Antidromic spike activation by optic radiation stimulation. The action potential appears with a short latency, almost coincident with the stimulation artifact. The spike's rising phase (arrow) shows no sign of discontinuities indicative of a slow somatic or dendritic charging transient. B. Excitatory postsynaptic potential elicited by optic radiation stimulation. The rising phase of the EPSP started with a small delay (0.55 ms) after stimulation. This EPSP showed no sign of a following IPSP. EPSP measures were peak amplitude: 6.2 mV; half-width, 20.4 ms; latency to peak (from foot of EPSP), 5.2 ms; 10-90% rise time, 3.8 ms. C. Example of a cell in which optic radiation stimulation evoked a unitary IPSP. The hyperpolarizing response begins without signs of a previous depolarizing potential. IPSP peak: 5.0 mV; half width: 24.9ms. D. An EPSP-IPSP pair. Stimulation evoked a small depolarization that is immediately followed by a slightly longer IPSP. Labels at left of traces indicate membrane potential. Open triangles indicate times of optic radiation stimulation. The scale bar applies to all parts of the figure.

Figure 2. Two populations of corticogeniculate EPSPs in the ferret LGN. A. A "fast-rising" EPSP elicited by optic radiation stimulation. This response reaches its

peak 3.2 ms after the start of the EPSP, with a 10-90% rise time of 2.6 ms. **B**. A "slowly rising" EPSP elicited from another LGN cell held at 2 different transmembrane potentials. At -59 mV, this response reaches its peak after 43.0 ms with a 10-90% rise time of 23.6 ms. Depolarizing the membrane potential by 7 mV with current injection slightly decreases latency and rise time to 26.1 ms and 14.4 ms respectively. Scale bar also applies to A. **C**. Histogram showing bimodal distribution of optic radiation-evoked EPSP latencies. This histogram was constructed by measuring the latency to peak of 10 consecutive optic-radiation evoked EPSPs from each of 14 cells held at resting potential (between -55 and -65 mV). Counts of latency values were placed in 5 ms-wide bins. Nearly half of the latencies observed were between 5 and 10 ms. The distribution has a small second mode at 25-30 ms. **D**. Distribution of 10-90% rise time measurements for the same 140 EPSPs. Bin width, 5 ms. This distribution has 2 modes, one at 0-5 and the other at 25-30 ms.

Figure 3. Low-threshold calcium spikes evoked by optic radiation stimulation in a ferret LGN cell. Corticofugal afferent stimulation (open arrow) elicited a short-latency low-threshold spike and action potential in this LGN cell when the membrane voltage was held at -63 mV (left). The rising phase of the underlying EPSP is visible as the inflection between stimulation and initiation of the action potential (arrow). At -68 mV, the optic radiation EPSP evoked a low-threshold spike with a longer latency; this response did not elicit action potentials. At -71 mV, the low-threshold spike is only partially activated by the optic radiation EPSP. The

arrowhead indicates the inflection point between the underlying EPSP and the rising phase of the partially activated low-threshold spike.

Figure 4. Blockade of NMDA receptors with d-APV attenuates optic-radiation evoked EPSPs. The upper (thicker) trace is an EPSP elicited by stimulation of the optic radiations in normal ACSF. Lower trace is the response to identical stimulation 20 minutes after addition of 20 μM d-APV to the bathing medium. The medium contained normal levels of magnesium (1.2 mM) in both cases.

Figure 5. Voltage sensitivity of optic-radiation evoked EPSP in a ferret LGN cell. A. EPSPs at different membrane potentials. The optic radiation was electrically stimulated with single shocks while membrane potential was adjusted to the indicated levels by injection of hyperpolarizing or depolarizing current. The recording electrode contained 4M cesium acetate. Note progressive reduction of EPSP amplitude with depolarization, and reversal between -14 and -25 mV. B. For EPSPs shown in A, the amplitude, latency to peak, 10-90% rise time, and width at half peak amplitude were plotted against pre-stimulation membrane potential. Latency and rise time increase progressively with depolarization, while the peak amplitude and half-width decrease, indicating a flattening of the EPSP envelope as the membrane approaches reversal potential.

Figure 6. Effect of magnesium concentration on an optic radiation evoked EPSP in

ferret LGN. In normal ACSF containing 1.2 mM magnesium (right), stimulation of the optic radiations at 2 different membrane potentials elicited no clear excitatory or inhibitory response in this cell. In the same cell, removal of the magnesium revealed a small EPSP in response to optic radiation stimulation. To prevent osmotic effects on the synaptic response, magnesium sulfate was replaced with equimolar sodium sulfate. Open triangles indicate the time of optic radiation stimulation. Fast vertical deflections are the stimulus artifacts.

Figure 7. Comparison of optic tract- (OT) and optic radiation-evoked (OR) EPSPs in cells of the ferret LGN. Six consecutive EPSPs elicited by stimulation of the optic radiation and the optic tract in 11 LGN cells were collected and measured. Cells were held at resting potential for these measurements. The response magnitude ratios were calculated by aligning corresponding EPSPs from the optic radiation and optic tract stimulation series (i.e., first OR stimulus with first OT stimulus, second OR with second OT, etc.) and dividing OR measurement by the OT measurement. A ratio of 1 therefore indicates equal amplitudes of a measure for the OR and OT responses; a value <1 indicates the OR response was smaller along this dimension, and values >1 indicate the value for OR stimulation was larger than that of the OT response. This process was carried out for measurements of EPSP amplitude, latency to peak, width at half of peak amplitude, and 10-90% rise time. The distributions were constructed with 0.5 mV bins for peak amplitude, and 0.5 ms bins for latency, half-width, and rise time. Note bimodal distribution of OR/OT rise time ratio.

Figure 1

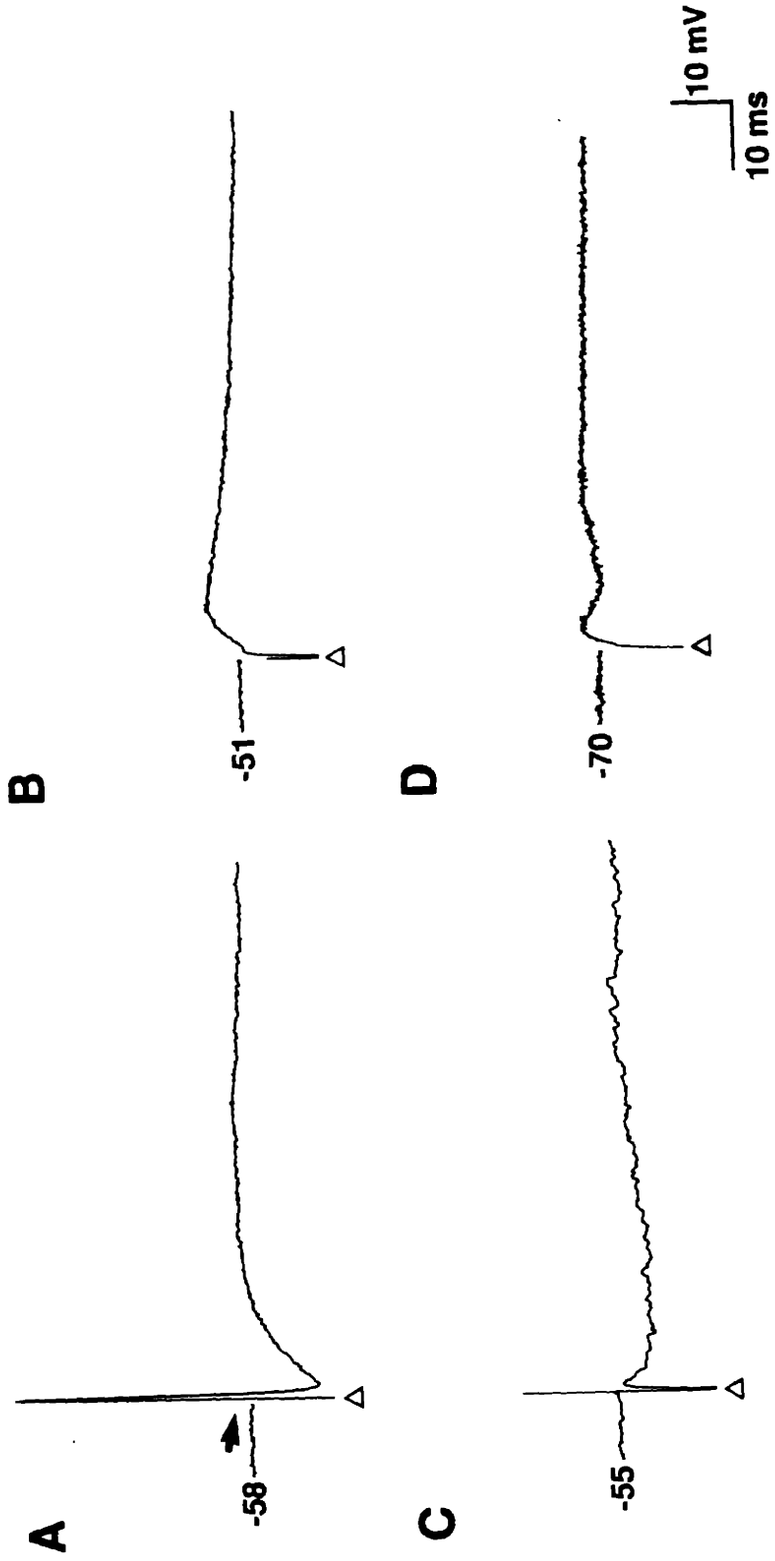

Figure 2

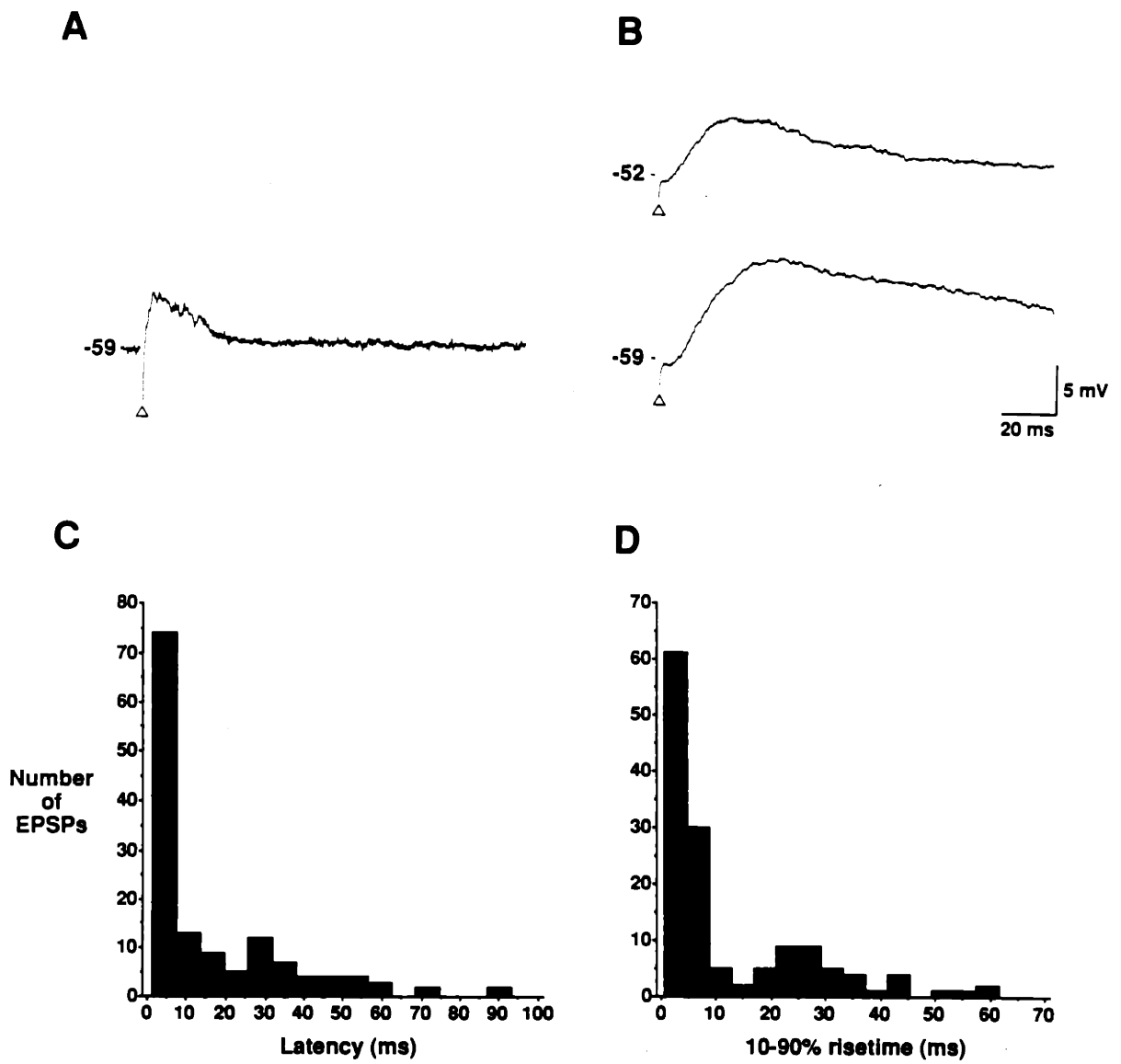
A
-59
B
-52
-59
5 mV
20 ms
C
Number of EPSPs
0 10 20 30 40 50 60 70 80 90 100
Latency (ms)
D
0 10 20 30 40 50 60 70
10-90% risetime (ms)

Figure 3

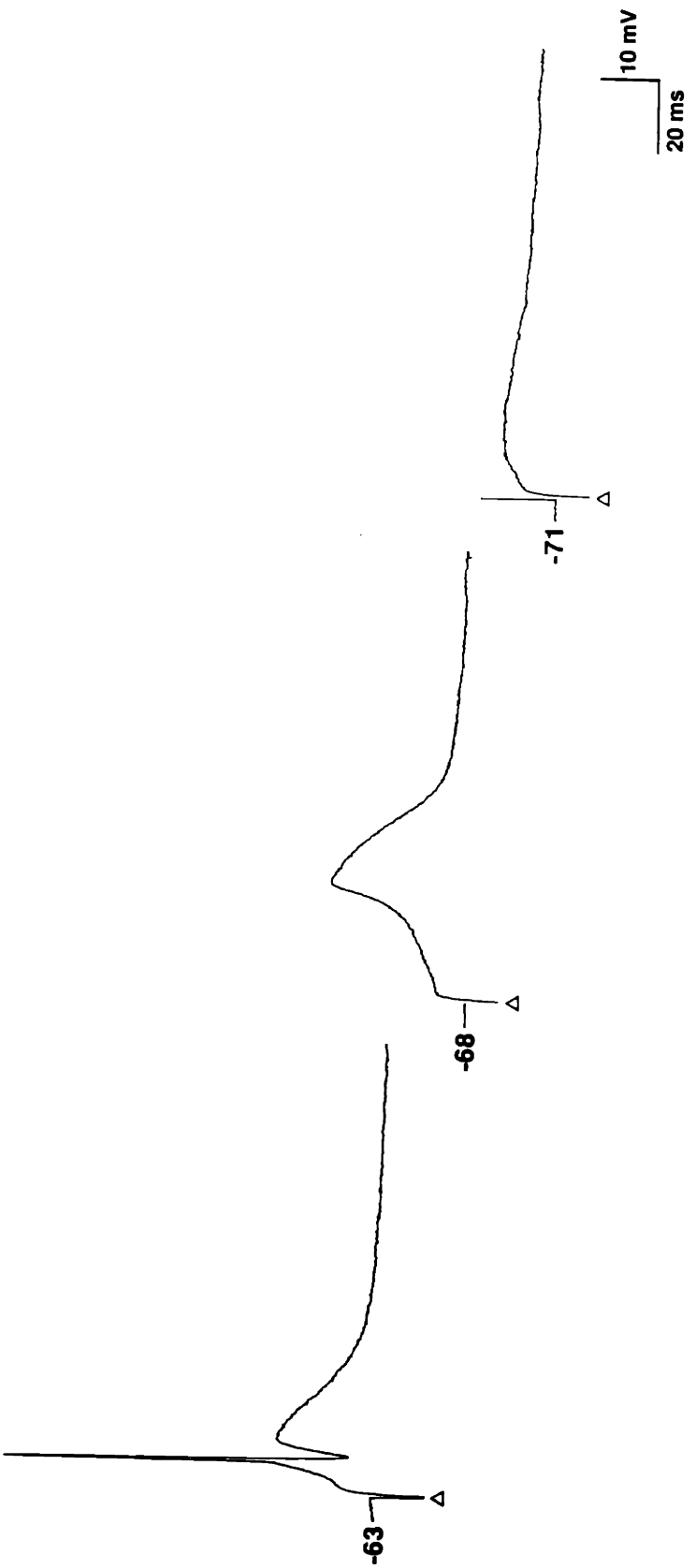

Figure 4

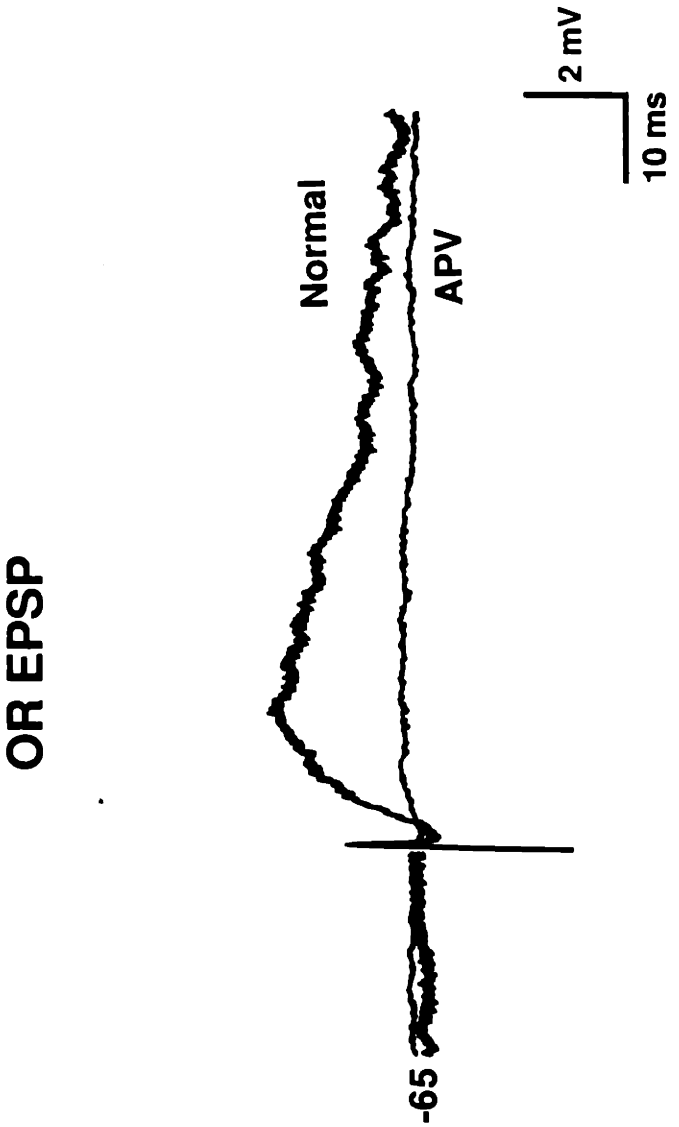

Figure 5

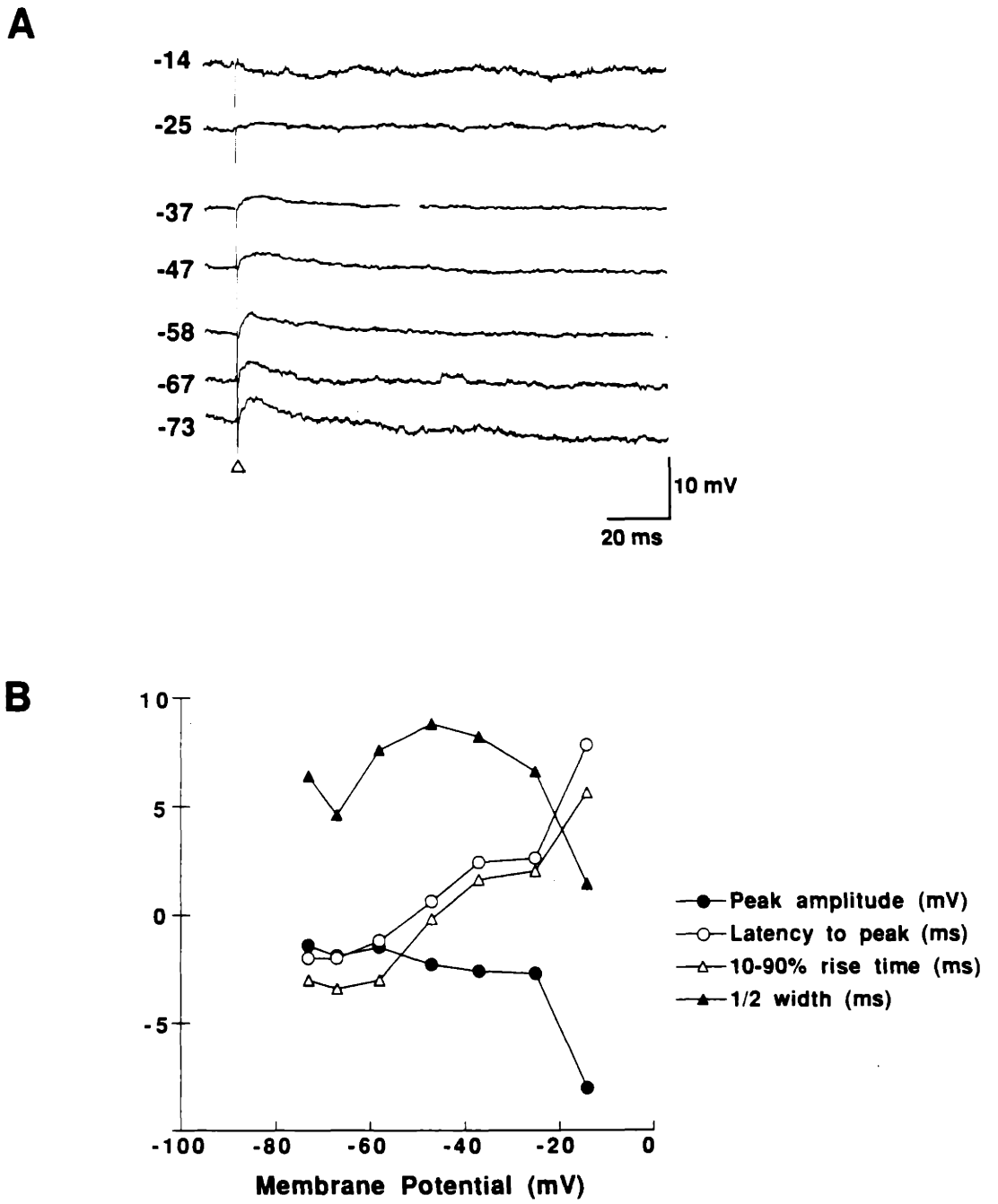
A
-14
-25
-37
-47
-58
-67
-73
10 mV
20 ms
B
10
5
0
-5
-100
-80
-60
-40
-20
0
Membrane Potential (mV)
Peak amplitude (mV)
Latency to peak (ms)
10-90% rise time (ms)
1/2 width (ms)

Figure 6

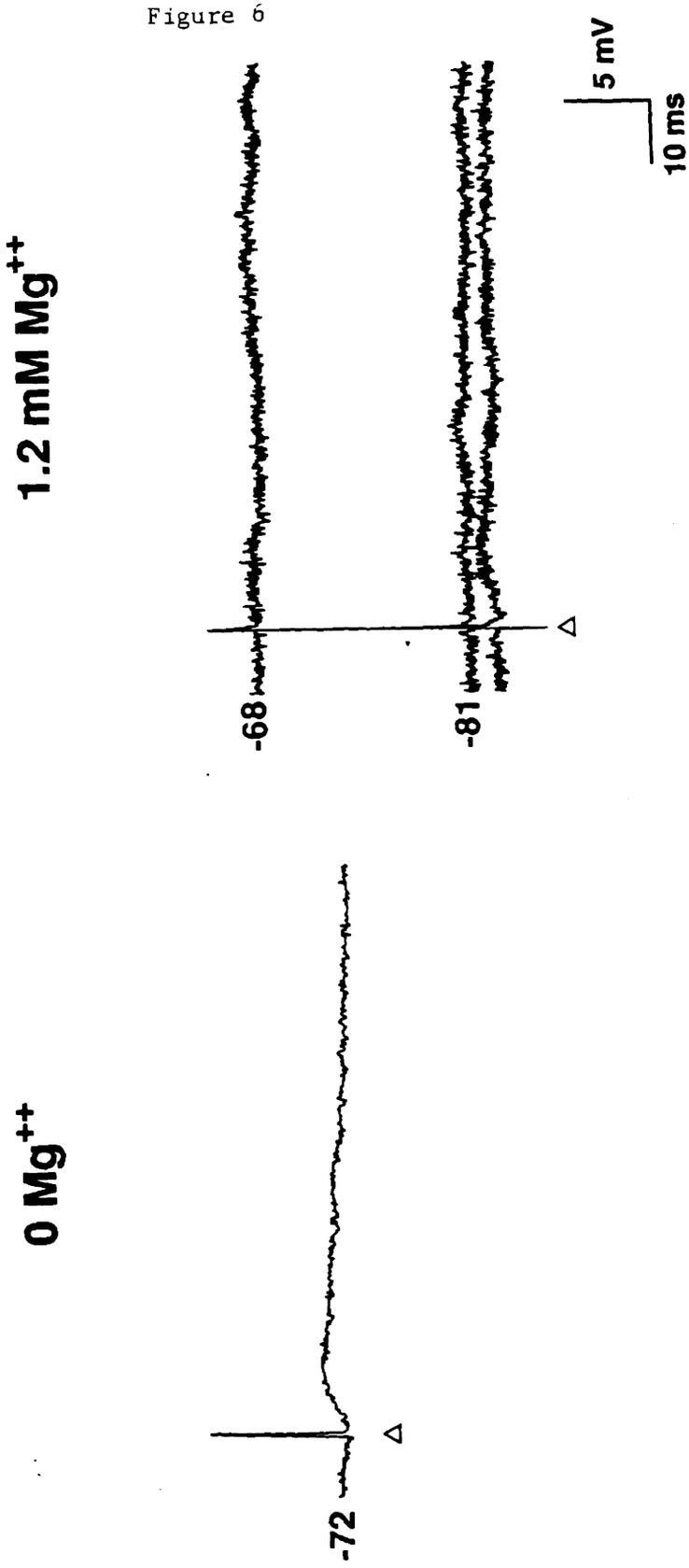

Figure 7

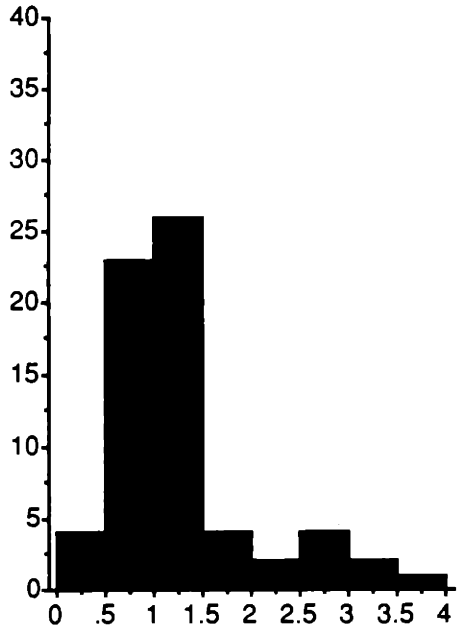

OR / OT : EPSP Amplitude

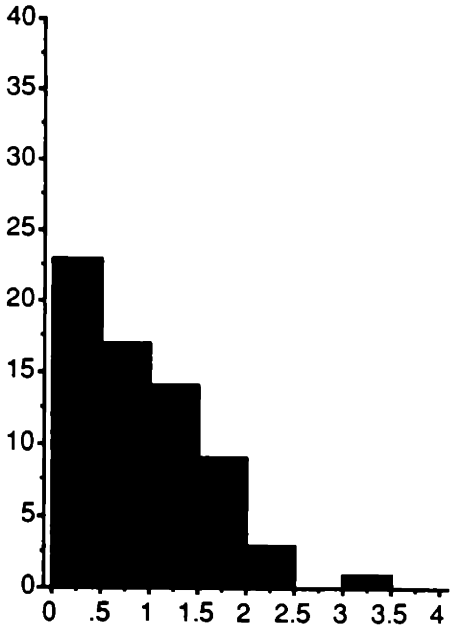

OR/OT: Latency to
EPSP Peak

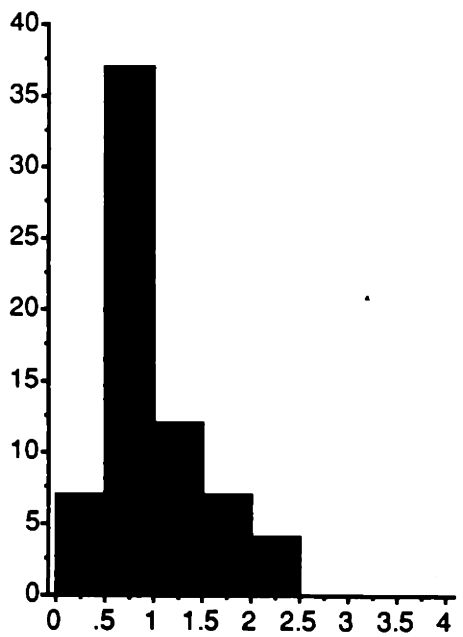

OR/OT: EPSP Half- Width

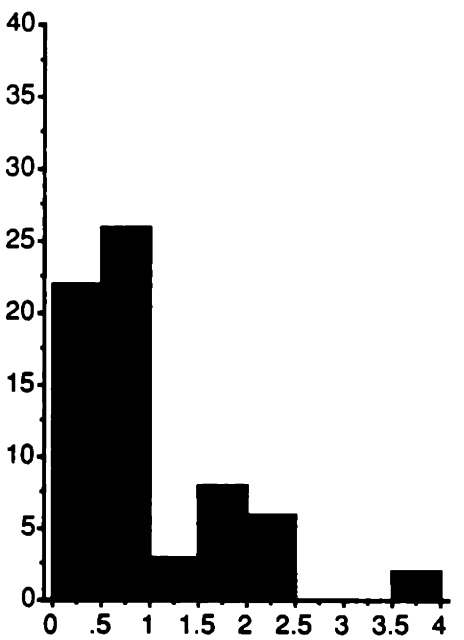

OR / OT : EPSP
10 -90 % Rise Time

Chapter 5

Corticogeniculate feedback can modulate retinogeniculate transmission by activating NMDA receptors

ABSTRACT

Chapters 2 and 3 of this thesis discussed the role of membrane voltage in modulation of the synaptic responses of cells in the lateral geniculate nucleus (LGN). In this chapter, I address a specific mechanism that has been proposed as a modulator of LGN cell membrane voltage during normal function. I tested the hypothesis that activity in the large cortical feedback pathway to the LGN enhances the efficacy of retinogeniculate transmission by activation of the NMDA class of excitatory amino acid receptors. I made intracellular recordings from slices of the ferret lateral geniculate nucleus (LGN) while stimulating independently the retinal and cortical afferent pathways. Because the LGN was isolated from ascending monoaminergic and cholinergic pathways, the observed responses reflected only the contributions of the two major excitatory pathways and intrinsic interneurons. In 4 of 9 cells tested, activation of the corticofugal projection reliably enhanced optic tract evoked EPSP amplitude and time course. This enhancement was larger than the algebraic sum of the 2 component EPSPs, and larger than the voltage dependent enhancement evoked by current injection at the soma. This EPSP enhancement was highly sensitive to blockade by the NMDA receptor antagonist d-APV. These results suggest that the visual cortex is capable of modulating its own input by controlling the efficacy of transmission through the lateral geniculate nucleus.

INTRODUCTION

The mammalian lateral geniculate nucleus (LGN) is currently regarded as a "gatekeeper" for visual information rather than as a simple relay between the retina and visual cortex (Sherman and Koch, 1986). This view attempts to reconcile the known visual response properties of LGN cells with their intrinsic membrane properties, which have been described over the last 10 years. In particular, thalamic cells show at least 2 modes of firing, a "tonic" mode, in which sensory information is transmitted to the visual cortex with high fidelity; and a "burst" or oscillatory mode, which appears unsuited for visual information processing and probably plays a role in sleep and arousal (Steriade and Llinas, 1988). Switching of the LGN cell from one of these modes to the other would constitute "gating" of visual information to cortex by altering the quality and quantity of information flow. While the specific behavioral significance of these mechanisms remains the subject of speculation (see Crick, 1984), the phenomenon of gating could shed light on a possible function of the massive feedback projection from visual cortex to LGN.

Another proposed form of gating depends on activation of large NMDA receptor currents at sites of retinogeniculate input (Koch, 1987). It has been demonstrated by anatomical (Monaghan et al., 1983; Fonnum et al., 1984; Cotman et al., 1987) and physiological methods (Kemp and Sillito, 1982; Crunelli et al., 1987; Kwon et al., 1991; see also Chapter 3 of this dissertation) that both NMDA and non-NMDA excitatory amino receptors are present on LGN cells; some studies suggest that the

receptor subtypes are differentially distributed among functional cell classes (Heggelund and Hartveit, 1990; Hartveit and Heggelund, 1990; Kwon et al., 1991). The NMDA receptor has attracted particular interest because its activation depends on membrane voltage. Due to a voltage-dependent magnesium block, the NMDA receptor-linked channel passes large inward current only when the transmitter binds and the local membrane potential is simultaneously depolarized to about -50 mV or less (Mayer and Westbrook, 1987). Thus a long-duration EPSP (from a nonretinal source) concurrent with retinogeniculate input could result in enhanced synaptic NMDA receptor activation and increase spike output in nonlinear fashion. Given that NMDA receptors are present at sites of retinal input to LGN cells, we must consider what excitatory inputs could produce the depolarization necessary to cause their activation.

The largest extraretinal excitatory input to LGN cells arises from layer VI of the visual cortex. Anatomical and physiological studies have demonstrated that this projection is retinotopically organized (Ahlsen et al., 1982; Robson, 1983), and EM reconstruction has shown that cortical fibers make excitatory synapses directly onto distal portions of LGN cell dendrites (Wilson et al., 1984; Weber et al., 1989).

It has been postulated that activity in the corticothalamic projection can activate the NMDA class of glutamate receptors at retinogeniculate synapses, thereby increasing the neuronal throughput (Koch, 1987). I examined whether cortical feedback activity produces depolarization sufficient to activate NMDA receptors at sites of simultaneous retinal input and thereby gate retinogeniculate processing. I

tested this hypothesis by studying the effects of glutamate receptor antagonists on responses of LGN cells to synchronous retinal and cortical afferent stimulation.

I report here that single shocks to cortical afferents can under some conditions enhance the amplitude of concurrent optic tract-evoked EPSPs. The summed response after such concurrent excitation is larger than the arithmetic sum of the component EPSPs, suggesting nonlinear interaction of synaptically activated conductances. The summed EPSP response during paired stimulation is highly sensitive to blockade by d-APV, which strongly suggests that it is the result of NMDA receptor activation.

Portions of these results have been previously presented in abstract form (Esguerra et al. 1989, Esguerra and Sur 1990).

METHODS

Preparation of LGN slices

Slices of the lateral geniculate nucleus were prepared from adult ferrets as described in the General Methods section of this dissertation.

Afferent stimulation

Bipolar platinum-iridium stimulating electrodes were placed on the optic tract (OT) at the outer edge of the slice, and in the optic radiations (OR) about 100 uM anterior to the inner border of lamina A (Figure 1). The optic radiations electrodes were placed along a path emanating from the optic tract electrodes perpendicular to laminar borders. Two constant current sources (Grass Instruments, Quincy MA) delivered single-shock electrical stimuli at currents of 0.1-0.8 mA, 0.05-0.08 ms duration at 0.5 Hz. These currents corresponded to stimulation voltages between 2 and 20 V when measured with a high impedance AC probe. The current sources were driven by separate channels of a Grass stimulator, so that stimulus amplitude, duration, delay, and polarity could be varied independently. The stimulator channels in turn were independently triggered by a microprocessor-driven timer (Winston Electronics) with a 0.1 ms resolution.

Intracellular recording

In healthy 400 μm slices of ferret LGN, the optic tract, optic radiations, and eye-specific laminae were clearly visible under both transillumination and epi-illumination, and recording and stimulating electrodes were easily placed in any of these regions. To increase the probability of recording postsynaptic responses to paired OT-OR stimulation, recordings were made in the A-laminae close to the line passing between the two stimulating electrodes, since optic tract and optic radiation afferents are known to enter the nucleus at more or less right angles to the laminar boundaries (Roe et al., 1989; Claps and Casagrande, 1990).

Drug presentation and ionic manipulations

The NMDA receptor antagonist d-2-amino 5-phosphonovaleric acid (d-APV, 10-40 uM; Cambridge Research Biochemicals, Valley Stream, NY) was introduced via the bathing solution by switching to a second ACSF reservoir to which the drug had been added in known concentrations. When $MgSO_4$ was omitted from the bath, it was replaced with equimolar Na_2SO_4 to maintain pH and osmolarity.

RESULTS

Paired stimulation was attempted in 22 slices of ferret LGN. From these, I obtained responses to paired corticogeniculate and retinogeniculate stimulation from 9 cells. In 8 of these cases, a clear EPSP could be evoked from stimulation of both the optic tract and the optic radiations. In the remaining cell, optic radiation shocks evoked an EPSP discernible at the cell body only when Mg++ was removed from the bathing medium.

Responses to optic tract stimulation

Retinogeniculate EPSPs evoked by optic tract stimulation of the cells used for this study were similar to those obtained in the larger study of optic tract-evoked synaptic potentials. These responses are summarized for 8 cells in Table 1. When evoked at starting membrane potentials between -79 and -43 mV, optic tract EPSP amplitudes ranged between 1.2 and 9.7 mV. No obvious inhibitory potentials could be observed after optic tract stimulation in the cells used for this study.

Responses to optic radiation stimulation

The parameters of EPSPs evoked by cortical afferent stimulation in this study were similar to those obtained in the previous study of optic radiation-evoked

responses. The responses to cortical afferent stimulation alone of the cells included in this study are summarized in Table 2. The amplitudes of the evoked EPSPs ranged between 0.7 and 12.7 mV, at membrane potentials between -79 and -43 mV. Of the 9 cells recorded, 6 responded with "fast rising" EPSPs (10-90% rise time < 15ms), and 3 cells responded with "slow" EPSPs (10-0% rise time > 15 ms; see Chapter 4 for further discussion of these classes of responses). All of the synaptic responses observed after OR stimulation in this study gave rise only to EPSPs; no inhibitory potentials were observed in the soma at any of the membrane voltages tested.

Responses to paired stimulation of the optic tract and optic radiations

I presented paired optic tract and optic radiations stimuli to the LGN cell under study by switching on the 2 independent stimulator channels, while ensuring that all stimulation parameters for each location were identical to those used to collect the unitary response data. The responses to paired afferent stimulation were compared with the response predicted by simple algebraic summation of the peak amplitudes of the EPSPs elicited by stimulation of each pathway alone. Concurrent stimulation of the 2 excitatory pathways in normal ACSF (n=8) led to either enhancement or reduction of the response relative to the algebraic sum. Of seven cells tested at membrane potentials fixed at various levels between -63 and -43 mV, 4 showed an

enhancement of the paired EPSP relative to the predicted value (average increase over prediction, 52.5%). An example of such an enhancement is shown in Figure 2. On the left of Figure 2 are shown the responses to unitary stimulation of the optic tract (top) and the optic radiation (bottom). Shown superimposed on the right side of the figure are the response predicted by linear summation of the unitary responses ("arithmetic sum") and the actual response obtained by paired stimulation of the 2 afferent pathways ("paired stimulation"). Optic radiation stimulation preceded optic tract stimulation by 6 ms in this case. The paired stimulation response is larger than the linear prediction (53% enhancement), indicating nonlinear summation of the unitary EPSPs.

Three cells tested with paired stimulation at fixed membrane potentials between -65 and -52 mV responded with EPSPs smaller than that predicted by simple linear summation of the unitary EPSPs (average reduction, 33%). An example of such a reduction is shown in Figure 3. The responses to unpaired stimulation of the optic tract and optic radiations are shown on the left; on the right is the response to paired stimulation superimposed for comparison over the linear sum of the unitary EPSPs. In this case, the paired EPSP is 15% smaller than predicted by linear summation. The responses to paired stimulation on these 8 cells are summarized in Table 3.

The starting membrane potential was not a reliable predictor for whether the paired stimulation response would be larger or smaller than the response predicted by linear summation. The relative enhancement or inhibition due to paired

stimulation for each of 8 cells is plotted against initial membrane potential in Figure 4A. The responses of cells tested at a single membrane potential (closed circles) and the responses of one cell tested at 4 different voltages (open circles) are shown. Paired stimulation led to either enhancement (points above the horizontal 0% line) or attenuation (points below the line) of the response relative to that predicted by linear summation. When enhancement and attenuation were considered separately, there was a slight tendency for each effect to increase with more depolarized membrane potentials (dashed lines; r= +0.66 for enhanced responses, r= -0.51 for attenuation).

Effect of EPSP rising phase on responses to paired stimulation

As I reported in a previous chapter, the responses of LGN cells to optic radiation stimulation appear to fall into 2 classes, slowly-rising and fast-rising, based on the distribution of their 10%-90% rise times. I tested the hypothesis that more slowly rising EPSPs contribute more to voltage dependent enhancement of the summed response than do fast-rising EPSPs by comparing EPSP rise times with the degree of response enhancement or inhibition after paired stimulation. In Figure 4B, the relative enhancement or inhibition by paired stimuli are plotted against the rise time of the optic radiation-evoked EPSP. The shape of the rising phases of either the optic tract-evoked or the optic-radiation evoked EPSP, expressed as 10%-90% rise times, did not correlate well with the magnitude of effect of paired stimulation.

Therefore, I am unable to support the hypothesis that slowly-rising EPSPs influence membrane potential more effectively than do fast-rising EPSPs.

Comparison of intracellular current injection with synaptic stimulation

In 4 cells, I attempted to simulate the effect of paired optic tract and optic radiation evoked EPSPs by injecting large depolarizing currents through the recording electrode and stimulating the optic tract alone. The current was adjusted so that the somatic membrane potential coincided with the peak of EPSPs elicited earlier by optic radiation stimulation. The optic tract EPSPs observed under these conditions were always of smaller amplitude than those evoked atop a corticogeniculate EPSP (Figure 5), indicating that somatic injection of current is an inadequate model for activation of distal synaptic currents.

Contribution of NMDA receptors to paired stimulation response

Effect of d-APV application Since each of the components comprising the paired response is itself partly mediated by NMDA receptor activation, the paired response should also show strong sensitivity to NMDA receptor blockade. Specifically, if NMDA receptors are making a large contribution to the nonlinear enhancement of summated EPSPs, the response to paired stimulation with NMDA receptors blocked should approximate a linear summation. The responses of 5 cells to paired

stimulation were tested in normal ACSF and during bath application of 20 μM d-APV. Figure 2B shows the response of an LGN cell to stimulation of the optic tract and optic radiations alone in the presence of 20 μM d-APV (left). The response to pairing of these 2 stimuli was compared with the algebraic sum of the 2 APV-attenuated components. With NMDA receptor blockade, the paired stimulation response was still slightly enhanced when compared to the algebraic sum of the d-APV attenuated optic tract and optic radiation evoked EPSPs (Figure 2B, right). The peak of the paired stimulation response was 32% larger than the peak of the algebraic sum; in the absence of d-APV, the enhancement of the peak of the paired response was 55% (Figure 2A).

The effect of d-APV on the paired-stimulation responses of all 5 cells is summarized in Table 4. For one of the 5 cells, application of d-APV caused a frank reversal of the paired response into an IPSP.

Effect of altered magnesium concentration. The effect of paired stimulation was tested on one LGN cell before and after removal of Mg++ from the bathing medium. Due to the activation of strong barrages of action potentials by near-threshold afferent stimulation in the low magnesium medium, it was impossible to compare EPSP components at the same membrane potentials for the paired stimulation paradigm. The voltage range tested in low magnesium medium was -80 to -60 mV; normal EPSPs were collected in a more depolarized range (-50 to -35 mV). The results are suggestive of a lack of voltage-dependent enhancement by

paired stimulation in the absence of magnesium, while the addition of magnesium appears to enable a voltage dependent modulation of the paired response at a more depolarized level. Since it was impossible to test EPSPs at the same potentials in the absence of Mg++ due to the aforementioned action potential discharges, it remains unknown whether the responses in low Mg++ medium would have showed a similar voltage dependence in this range. Recording in this range requires intracellular blockade of action potentials by QX-314 or similar anesthetics (Connors et al., 1982); such materials were unavailable to me at the time of this experiment.

Timing of OR and OT stimulation

I investigated in 2 cells the importance of the relative timing of the optic radiation stimulus and optic tract stimulus in producing a nonlinear enhancement of the response to paired stimulation. The results indicate that enhancement occurs when the optic radiation stimulus precedes the optic tract stimulus by between 2 and 6 ms; with longer delays, the optic tract stimulus is relatively unaffected by the preceding cortical afferent activity. Figure 6 shows the effect of altered delays between optic radiation and optic tract stimulation on 4 measures of an EPSP evoked in response to paired stimulation. The EPSP peak, latency, and 10%-90% rise time measures reach asymptotes at delays longer than 6 ms; these levels correspond to the same measures for optic tract EPSPs elicited singly for this cell (not shown), suggesting that the preceding stimulus was incapable of significant

modulation of this response when the interstimulus interval exceeded ~6 ms.

DISCUSSION

Summary

The results of this study may be summarized as follows:

1. Concurrent stimulation of the retinogeniculate and corticogeniculate pathways can lead to nonlinear summation of the component EPSPs. This nonlinear summation is expressed as either an increase or decrease of the paired-stimulation response when compared to the response predicted by linear summation of the component EPSPs. The result suggests that co-activation of 2 excitatory pathways to single LGN cells activates nonlinear synaptic mechanisms.

2. The actual direction of the response (nonlinear enhancement or attenuation) was not predicted by starting membrane potential. However, when enhancing or attenuating responses were considered separately, each showed a slight tendency to increase with depolarization. The result suggests that two separate mechanisms participate in modulation of synaptic responses by concurrent inputs. Selection of the inhibitory or excitatory mechanism is independent of membrane voltage; however, the magnitude of the effect may depend on voltage.

3. The degree of nonlinear enhancement of the paired response appeared to be independent of the type of EPSP evoked by optic radiation stimulation, suggesting that the populations of afferents responsible for these classes of EPSPs can both modulate synaptic responses in LGN cells.

4. Injection of depolarizing current pulses through the recording electrode that depolarized the local membrane to levels attained by the peak of the optic radiation EPSP, did not enhance optic tract responses to the degree they were enhanced by optic radiation stimulation. This result indicates that the interactions necessary for modulation of synaptic responses by concurrent stimulation must be occurring at locations that are electrically distant from the recording site. The space clamp achieved with a sharp electrode containing potassium as electrolyte probably does not extend beyond the soma of LGN cells (cf. Johnston and Brown, 1982), so these interactions must be occurring near sites of synaptic input in the dendritic arbor.

5. Application of d-APV strongly reduced the amplitude of the responses evoked by paired stimulation, indicating participation of NMDA receptors in this response. In the presence of d-APV, the amplitude of the paired stimulation responses were closer to those modeled by linear EPSP summation. This interpretation is weakly supported by the voltage dependent enhancement of one paired-stimulation evoked EPSP recorded in the presence of Mg, which disappeared when Mg was removed from the medium.

6. The modulation of EPSP amplitude by pairing of retinogeniculate and corticogeniculate stimulation occurred when the optic radiation stimulus preceded optic tract stimulation by 2 to 6 ms.

Taken together, these results indicate that activity in the cortical projection to the LGN can lead to depolarizations sufficient to activate NMDA receptors at retinogeniculate synapses. I propose that one function of the corticothalamic projection is to modulate the gain of retinogeniculate transmission by increasing EPSP amplitude at membrane potentials near the action potential threshold.

Limitations of linear (algebraic summation) as a model for EPSP summation

The above conclusion is based largely on the observation that paired stimulation can lead to responses larger than that predicted by a simple linear summation of the component EPSPs. I used algebraic summation of the optic tract and optic radiation evoked EPSPs as observed at the soma to derive our prediction for EPSP summation in the absence of voltage-dependent or other nonlinear influences. This simple model assumes that postsynaptic potentials observed at the soma are similar in amplitude and time course to voltage changes that would be measured at sites of synaptic input. Such high fidelity transmission of EPSPs requires that the cell be electrotonically compact, i.e. that its linear membrane properties do not cause significant attenuation of voltage changes at dendrites. Data from LGN neurons

identified physiologically and morphologically in vivo (Bloomfield et al., 1987), seem to suggest that LGN cells are electrically compact. However, the passive membrane parameters derived from their experiment are lower than those reported from in vitro preparations, probably due to the difficulty of maintaining a stable intracellular impalement in vivo. Thus Bloomfield et al. may have underestimated the electrotonic length of LGN cell dendrites. Linear (algebraic) summation of EPSPs is therefore probably an inadequate model for simulating EPSPs recorded at the soma. The algebraic summation procedure also ignores the role of active synaptic and membrane conductances in shaping EPSPs observed at the soma. Preliminary results from a simulation of synaptic input to a passive (linear) compartmental model of an LGN cell suggests that the presence of just 2 synaptic conductances radically alters the expression and summation of distal synaptic currents as observed from the soma (D. Smetters, unpublished observations).

Timing dependence in paired stimulation

The time dependence of the paired stimulation modulation (2-6 ms) was unexpectedly brief, given the somewhat longer duration of optic radiation EPSPs measured at the soma (half-widths between 3 and 140 ms). However, it is possible that the voltage changes activated at sites of corticogeniculate input are of brief duration, and the potential observed at the soma has been attenuated in amplitude and lengthened in its time course by the electrotonic properties of the intervening membranes (Rall, 1977). Thus the time dependence of the paired response may

actually reflect a brief period of overlap of the synaptic potentials evoked by optic tract and optic radiation stimuli. An alternative explanation is that the synaptic responses are shortened by active membrane conductances, possibly active or shunting inhibition, which act locally to attenuate EPSPs without being observed directly at the somatic recording site (Poggio and Torre, 1978).

Which EPSP is potentiated?

I have interpreted these results as reflecting a corticogeniculate enhancement of retinogeniculate synaptic responses. However, since NMDA receptors are present at sites of retinal and cortical input (Scharfman et al., 1990), it is possible that any local depolarizing influence could activate the NMDA current at both these sites. I did not test whether a stimulation paradigm with the optic tract stimulus first would lead to effects similar to those reported here.

In most cases the optic radiation stimulus preceded the optic tract stimulus by several milliseconds. If the presynaptic stimulus is brief and low-frequency, as in this study, then transmitter is likely to be released in short bursts. Since NMDA receptor activation requires both depolarization and transmitter binding, it is possible that the first EPSP will not be potentiated by the second because the transmitter released by the first stimulus would no longer be present in the synaptic cleft. Mechanisms for glutamate reuptake are known to be among the fastest uptake systems in the brain (Fonnum, 1984); since the neurons in this preparation maintain their physiological properties for many hours, these metabolic mechanisms must also

be operating normally.

Functional consequences

These results indicate that a possible role of the corticogeniculate projection is to excite specifically regions of membrane in the vicinity of retinogeniculate synapses. In combination with release of neurotransmitter from active retinal terminals, this can lead to large increases in the synaptic response to visual stimulation, and a higher probability of action potential generation. Since corticofugal terminals are arranged retinotopically in the LGN (Robson, 1983), activity in subsets of cortical afferents can potentially lead to enhancement of specific parts of the visual representation. This is in contrast to modulatory influences arising from the brainstem, which lack spatial resolution and give rise to more diffuse enhancement of thalamic activity (McCormick, 1989). The distal location of corticogeniculate terminals in the dendritic arbor of LGN cells (Wilson et al., 1984) suggests that in some cases the cortical projection may not contribute significantly to membrane voltage at the soma, while still being able to influence the synaptic efficacy of retinal inputs.

Two hypotheses concerning the role of the corticofugal projection in visual processing may be derived from these results. The first is that this projection acts as a variable gain regulator to provide the basis for a neural filter for selective attention. The cortex may be able to produce small, sharply defined loci of increased activity in the lateral geniculate nucleus. The specificity of the corticofugal

map would ensure that this area of activity remain small and focused. Its patterns of activity would then encode not features, but rather levels of activity or "conspicuity" in the visual system (Koch and Ullman, 1985).

A second hypothesis is that the corticofugal input has a predictive function, whereby it tests for particular configurations of features in the visual scene. Predictions about the motion or contours of objects in the scene would be made by higher visual areas such as MT. These centers would send their predictions to specific locations in layer 6, which in turn would excite specific locations in the geniculate representation. Successful matches of prediction with retinal input would activate the mechanisms described here, and an enhanced representation of that portion of the visual scene transmitted to the visual cortex.

REFERENCES

Ahlsen, G., Grant, K., and Lindstrom, S. (1982). Monosynaptic excitation of principal cells in the lateral geniculate nucleus by corticofugal fibers. Brain Res. 234, 454-458.

Bloomfield, S. A., Hamos, J. E., and Sherman, S.M. (1987). Passive cable properties and morphological correlates of neurones in the lateral geniculate nucleus of the cat. J. Physiol. 383, 653-692.

Claps, A., and Casagrande, V.A. (1990). The distribution and morphology of corticogeniculate axons in ferrets. Brain Res. 530, 126-129.

Connors, B. W., Gutnick, M. J., and Prince, D. A. (1982). Electrophysiological properties of neocortical neurons in vitro. J. Neurophysiol. 48, 1302-1320.

Cotman, C.W., Monaghan, D.T., Ottersen O.P. and Storm-Mathisen, J. (1987). Anatomical organization of excitatory amino acid receptors and their pathways. TINS 10, 273-280.

Crick, F. H. C. (1984). The function of the thalamic reticular complex: the searchlight hypothesis. Proc. Natl. Acad. Sci. 81, 4586-4590.

Crunelli, V., Kelly, J. S., Leresche, N., and Pirchio, M. (1987). On the excitatory post-synaptic potential evoked by stimulation of the optic tract in the rat lateral geniculate nucleus. J. Physiol. 384, 603-618.

Esguerra, M., Kwon, Y. H., and Sur, M. (1989). NMDA and non-NMDA receptors mediate retinogeniculate transmission in cat and ferret LGN in vitro. Soc. Neurosci. Abstr. 15, 175.

Esguerra, M., and Sur, M. (1990). Corticogeniculate feedback gates retinogeniculate transmission by activating NMDA receptors. Soc. Neurosci. Abstr. 16, 159.

Fonnum, F. (1984). Glutamate: a neurotransmitter in mammalian brain. J.

Neurochem. 42, 1-11.

Fonnum, F., Fosse, V.M. and Allen, C.N. (1984). Identification of excitatory amino acid pathways in the mammalian nervous system. In Excitotoxins, K. Fuxe, P.J. Roberts, and R. Schwarcz, eds., pp. 3-18, Plenum, New York.

Hartveit, E., and Heggelund, P. (1990). Neurotransmitter receptors mediating excitatory input to cells in the cat lateral geniculate nucleus. II. Nonlagged cells. J. Neurophysiol. 63, 1361-1372.

Heggelund, P., and Hartveit, E. (1990). Neurotransmitter receptors mediating excitatory input to cells in the the cat lateral geniculate nucleus. I. Lagged cell. J. Neurophysiol. 63, 1347-1360.

Johnston, D., and Brown, T.H. (1983). Interpretation of voltage-clamp measurements in hippocampal neurons. J. Neurophysiol. 50, 464-486.

Kalil, R. E., and Chase, R. (1970). Corticofugal influence on acitvity of lateral geniculate neurons in the cat. J. Neurophysiol. 33, 459- 474.

Kemp, J. A., and Sillito, A. M. (1982). The nature of the excitatory transmitter mediating X- and Y- cell inputs to the cat dorsal lateral geniculate nucleus. J.

Physiol. 323, 377-391.

Koch, C. (1987) The action of the corticofugal pathway on sensory thalamic nuclei: an hypothesis. Neuroscience 25, 399-406.

Koch, C., and Ullman, S. (1985). Shifts in selective visual attention: towards the underlying neural circuitry. Human Neurobiol. 4, 219-227.

Kwon, Y. H., Esguerra, M., and Sur, M. (1991). NMDA and non-NMDA receptors mediate visual responses of neurons in the cat's lateral geniculate nucleus. J. Neurophysiol., in press.

Mayer, M. L., and Westbrook, G. L. (1987). The physiology of excitatory amino acids in the vertebrate central nervous system. Prog. Neurobiol. 28, 197-276.

McCormick, D. A. (1989). Cholinergic and noradrenergic modulation of thalamocortical processing. TINS 12, 215-221.

Monaghan, D.T., Yao, D. and Cotman, C.W. (1983). L-[3H]glutamate binds to kainate, NMDA-, and AMPA-sensitive binding sites: an autoradiographic analysis. Brain Res. 340, 378-383.

Poggio, T., and Torre, V. (1978) A new approach to synaptic interactions. In Approaches to Complex Systems, R Heim and G. Palm, eds. 89-115. Berlin: Springer Verlag.

Rall, W. (1977). Core conductor theory and cable properties of neurons. In Handbook of Physiology, Section 1: The Nervous System, vol. 1: Cellular Biology of Neurons (E. R. Kandel, ed.) Bethesda: Am. Physiol. Soc. pp 39-98.

Robson, J. A. (1983). The morphology of corticofugal axons to the dorsal lateral geniculate nucleus in the cat. J. Comp. Neurol. 216, 89-103.

Roe, A. W., Garraghty, P. E., and Sur, M. (1989). Terminal arbors of single ON-center and OFF center X and Y retinal ganglion cell axons within the ferret's lateral geniculate nucleus. J. Comp. Neurol. 288, 208-242.

Scharfman, H. E., Lu, S.-M., Guido, W., Adams, P. R., and Sherman, S. M. (1990). N-methyl-D-aspartate receptors contribute to excitatory postsynaptic potentials of cat lateral geniculate neurons recorded in thalamic slices. Proc. Natl. Acad. Sci. 87, 4548-4552.

Sherman, S. M. and Koch, C. (1986). The control of retinogeniculate transmission in the mammalian lateral geniculate nucleus. Exp. Brain Res. 63, 1-20.

Steriade, M., and Llinas, R. (1988) The functional states of the thalamus and the associated neuronal interplay. Physiol. Rev. 68, 649-742.

Weber, A. J., Kalil, R. E., and Behan, M. (1989). Synaptic connections between corticogeniculate axons and interneurons in the dorsal lateral geniculate nucleus of the cat. J. Comp. Neurol. 289, 156-164.

Wilson, J. R., Friedlander, M. J., and Sherman, S. M. (1984). Ultrastructural morphology of identified X- and Y-cells in the cat's lateral geniculate nucleus. Proc. Roy. Soc. Lond. B 221, 411-436.

Table 1. Measurements of optic tract-evoked EPSPs

Cell	Vm	EPSP Peak Amplitude (mV)	Latency (ms)	10%-90% Risetime (ms)	Half Width (ms)
1	-43	2.1 ± 0.4	22.4 ± 7.2	19.9 ± 6.9	44.0 ± 11.1
2	-65	4.4 ± 1.9	9.0 ± 3.6	6.3 ± 3.0	37.8 ± 10.8
3	-52	3.8 ± 0.8	18.6 ± 4.8	14.1 ± 3.4	47.5 ± 6.6
4	-64	9.7 ± 0.8	39.7 ± 0.0	0.3 ± 0.0	--
5	-57	7.5 ± 0.7	14.0 ± 2.5	7.7 ± 1.0	42.8 ± 4.9
6	-63	4.0 ± 0.5	4.1 ± 0.7	3.4 ± 0.7	11.8 ± 3.0
7	-49	5.8 ± 0.6	5.9 ± 1.1	3.4± 0.5	20.3 ± 1.0
9	-79	1.3	43.4	18.2	19.8
"	-76	1.2	9.6	6.6	12.4
"	-71	2.4	11.8	7.4	18.8
"	-67	4.1	17.2	9.2	29.2

Values for cells 1-7 are shown as mean ± S.D. and represent average of 8 consecutive EPSPs

Means only are shown for cell 9 (n=4 EPSPs)

Vm = baseline voltage at time of optic tract stimulation

Table 2. Measurements of optic radiations-evoked EPSPs

Cell	Vm	EPSP Peak Amplitude (mV)	Latency (ms)	10%-90% Risetime (ms)	Half Width (ms)
1	-43	1.3 ± 2.1	27.9 ± 10.6	26.6 ± 10.4	22.4 ± 9.0
2	-65	10.5 ± 0.5	1.8 ± 0.3	1.2 ± 0.1	25.5 ± 1.7
3	-52	5.6 ± 0.4	29.0 ± 4.8	20.1 ± 4.3	64.9 ± 5.3
4	-64	12.7 ± 0.4	54.7 ± 0.0	0.3 ± 0	--
5	-57	5.9 ± 0.3	24.3 ± 6.6	16.8 ± 6.0	83.6 ± 8.0
6	-63	4.1 ± 1.3	2.0 ± 0.6	0.9 ± 0.2	8.4 ± 1.8
7	-49	4.2 ± 0.6	10.8 ± 0.9	5.5 ± 0.7	23.3 ± 2.3
9	-79	0.7	2	1.2	6.6
"	-76	1.1	2	1.4	10.8
"	-71	1.2	5.6	5	15
"	-67	1.4	8.6	6.2	25.2

Values for cells 1-7 are shown as mean ± S.D. and represent average of 8 consecutive EPSPs

Means only are shown for cell 9 (n=4 EPSPs)

Vm = baseline voltage at time of white matter stimulation

Table 3. Measurements of paired stimulation responses

Cell	Vm	EPSP Peak Amplitude (mV)	Latency (ms)	10%-90% Risetime (ms)	Half Width (ms)
1	-43	4.5 ± 0.5	12.3 ± 3.9	8.8 ± 4.0	42.7 ± 6.5
2	-67	12.70 ± 4	54.7 ± 0.0	0.2 ± 0.0	--
3	-56	5.9 ± 0.3	2.4 ± 6.6	16.8 ± 6.0	83.6 ± 8.0
4	-66	11.9 ± 0.4	45.7 ± 0.0	0.4 ± 0.5	--
5	-55	20.5 ± 0.6	27.7 ± 1.8	8.5 ± 1.0	43.1 ± 0.9
6	-62	11.7 ± 1.4	4.0 ± 0.1	3.3 ± 0.1	8.7 ± 1.1
7	-53	18.1 ± 0.5	7.4 ± 3.7	3.6 ± 0.3	44.3 ± 1.9
9	-80	1.6	10.4	7.8	14.2
"	-79	2.4	7.8	5.2	16.4
"	-77	2.6	10.6	9.2	18
"	-74	6.3	19.8	11	29.8

Values for cells 1-7 are shown as mean ± S.D. and represent average of 8 consecutive responses
Means only are shown for cell 9 (n=4 EPSPs)
Vm = baseline voltage at time of white matter stimulation

Table 4. Effect of d-APV on peak amplitude of paired response

Cell	Normal ACSF	20 μM d-APV	% reduction
2	12.7	2.5	80.31
3	5.9	2.6	55.93
4	11.9	-0.5	104.20
5	20.5	-36.4	277.56
7	18.1	16.3	9.94

All amplitudes are expressed in mV

FIGURE LEGENDS

Figure 1. Schematic representation of slice preparation with dual optic tract and optic radiation stimulation. Bipolar stimulating electrodes were placed on the optic tract (OT) just outside the C laminae and in the optic radiations (OR) about 100 μm from the inner border of lamina A. Recordings were made from cells in line with the two electrodes.

Figure 2. A: Nonlinear enhancement of EPSP in response to paired stimulation of the optic tract and optic radiations in normal ACSF. Left: EPSPs recorded from an LGN cell after isolated stimulation of the optic tract (top) and optic radiations (bottom). Right: Response to paired stimulation of the 2 afferent pathways superimposed on arithmetic sum of the 2 EPSP's shown on the left. Stimulation voltages for paired stimulation paradigm were identical to those used to elicit unitary responses. Optic radiation stimulation preceded optic tract stimulation by 6 ms. The arithmetic sum was constructed on the computer by adding the digitized values at corresponding time points for the 2 component EPSPs. Scale bars apply to all parts of the figure. B: Effect of d-APV on the response to paired stimulation of optic radiations and optic tract. This is the same cell as shown in part A, recorded 30 minutes after introduction of d-APV to the perfusate (final concentration, 20 μM). Left: Responses to unpaired stimulation of optic tract (upper) and optic radiations (lower) in the presence of d-APV. Right: Response to paired

stimulation of the 2 afferent pathways in 20 μM d-APV, superimposed on arithmetic sum of the unitary EPSPs. The optic radiation stimulus preceded the optic tract stimulus by 6 ms.

Figure 3. Reduction of EPSP after paired stimulation. Left: EPSPs elicited by unitary stimulation of optic tract (top) and optic radiations (bottom). Right: Response to paired stimulation, with optic radiation stimulus preceding optic tract stimulus by 6 ms.

Figure 4. Effects of membrane potential and EPSP rise time on enhancement and inhibition by paired stimulation. A: Plot of membrane potential vs. deviation of paired stimulation response from response predicted by algebraic summation of component EPSPs for 8 LGN cells. Seven cells were tested at fixed membrane potentials (closed dots). One cell was tested at 4 different membrane potentials (open dots). Horizontal line indicates 0% change, i.e. paired response amplitude was identical to prediction. Points above line indicate enhancement, points below line relative attenuation by paired response. Dashed lines indicate best linear fits to points above and below 0% line respectively. B: Plot of rise time of the EPSP evoked by optic radiation stimulation vs. deviation of paired response from prediction.

Figure 5. Comparison of effects on retinogeniculate EPSP of depolarization by

intracellular current injection with effect of concurrent optic radiation stimulation. Paired stimulation: The optic tract and optic radiations were stimulated concurrently, with optic radiation stimulus preceding optic tract stimulus by 6 ms. OT only: The optic tract was stimulated in conjunction with injection of DC depolarizing current through the recording electrode. Current was adjusted to bring membrane potential to the same level as the peak of the optic radiation-evoked EPSP (not shown). Stimulation of the optic tract under these conditions elicited an EPSP that was smaller than that evoked by paired stimulation.

Figure 6. Effect of interstimulus timing on measures of the EPSP evoked by paired stimulation of the optic tract and optic radiations. All data are from one LGN cells. Optic radiation stimulus preceded optic tract stimulus by 2, 4, 6, 8, and 10 ms (horizontal axis).

Figure 1

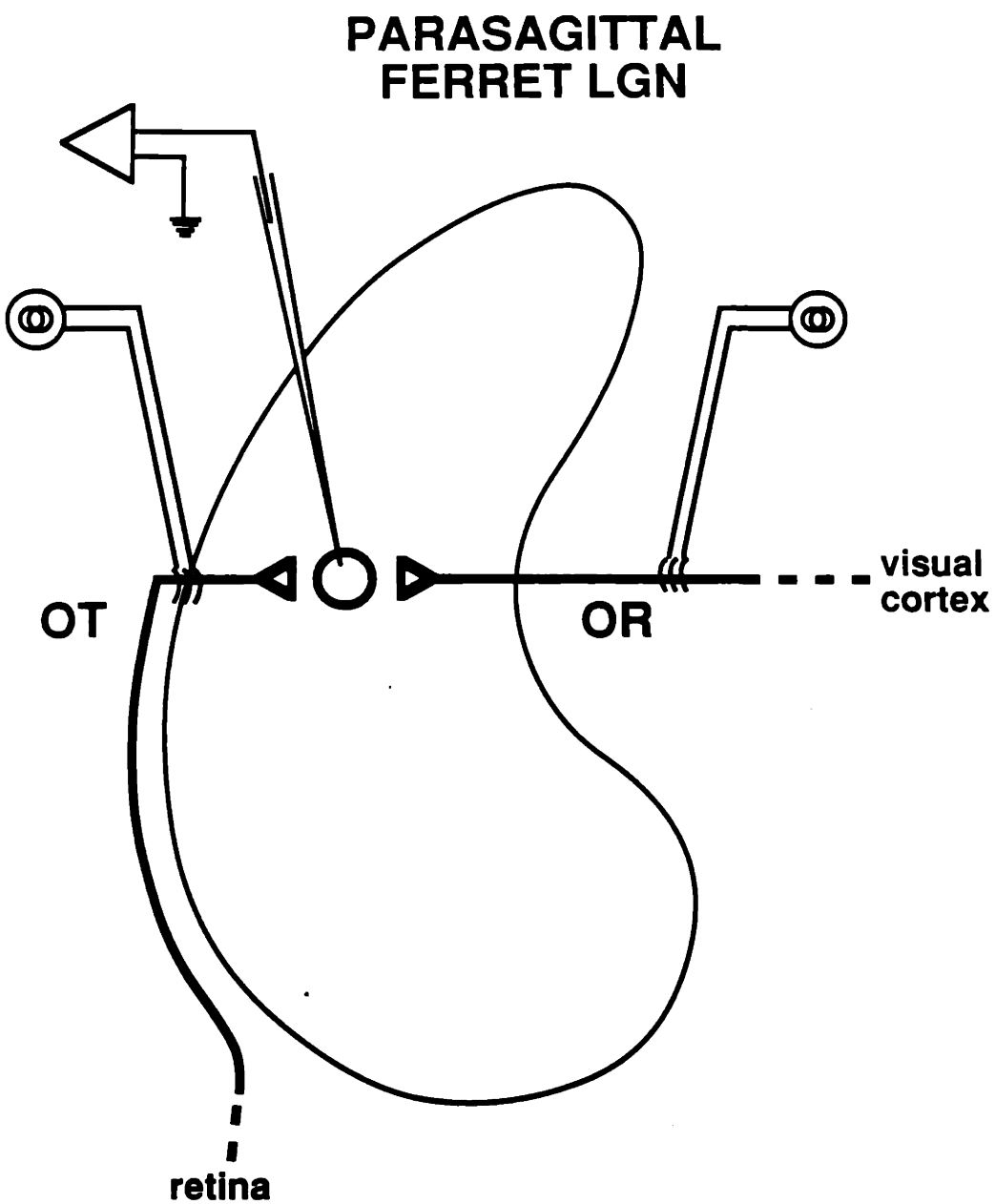

Figure 2

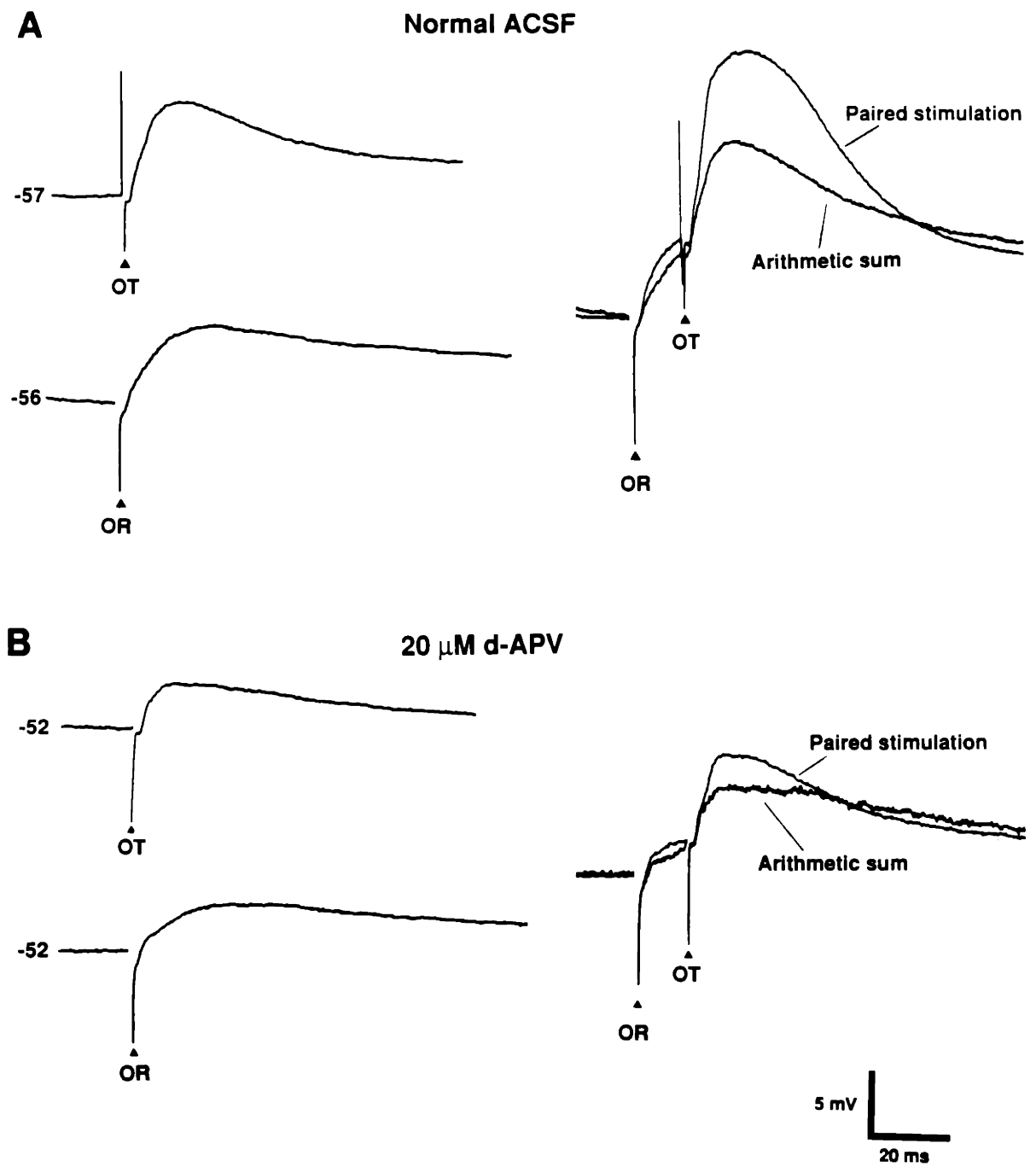
A
Normal ACSF
-57
OT
-56
OR
Paired stimulation
Arithmetic sum
OT
OR
B
20 μM d-APV
-52
OT
-52
OR
Paired stimulation
Arithmetic sum
OT
OR
5 mV
20 ms

Figure 3

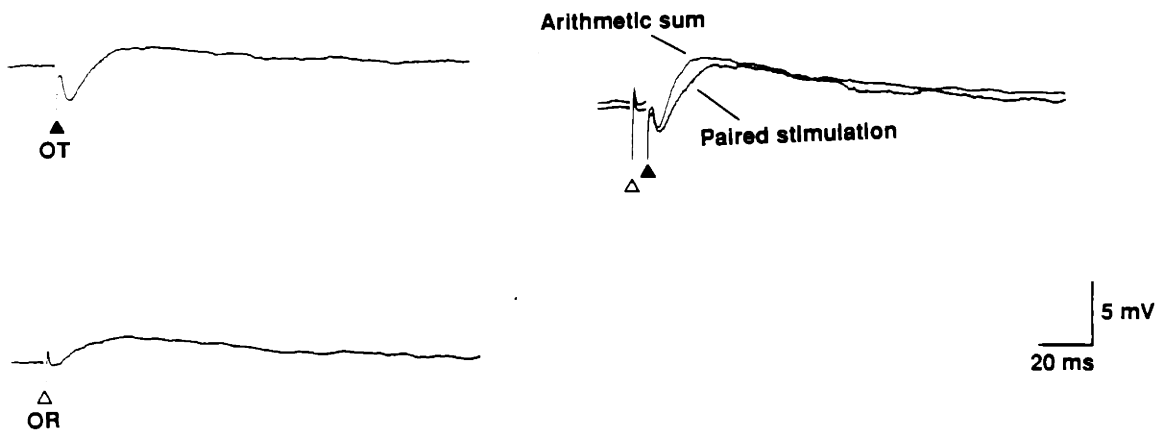

Figure 4

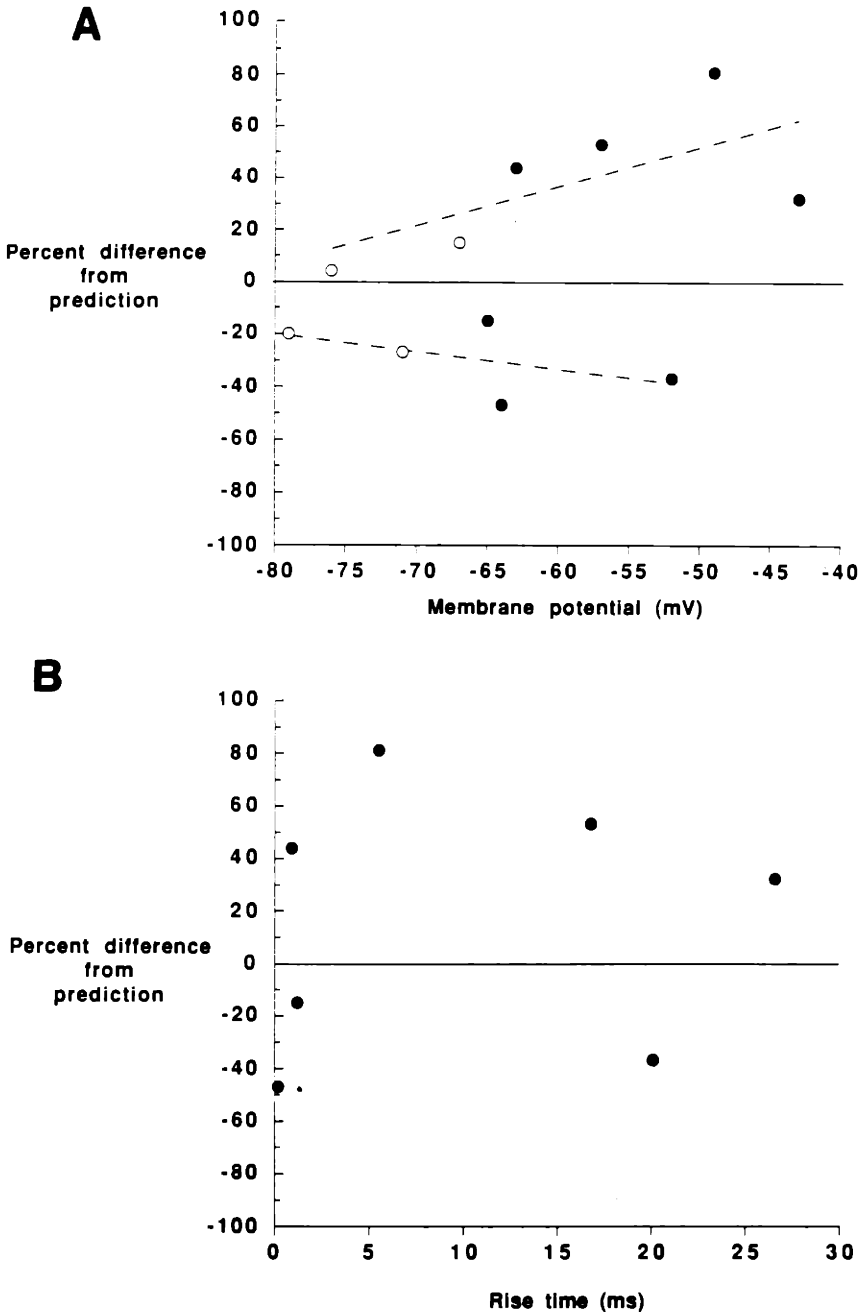
A
100
80
60
40
20
0
-20
-40
-60
-80
-100
Percent difference from prediction
-80 -75 -70 -65 -60 -55 -50 -45 -40
Membrane potential (mV)
B
100
80
60
40
20
0
-20
-40
-60
-80
-100
Percent difference from prediction
0 5 10 15 20 25 30
Rise time (ms)

Figure 5

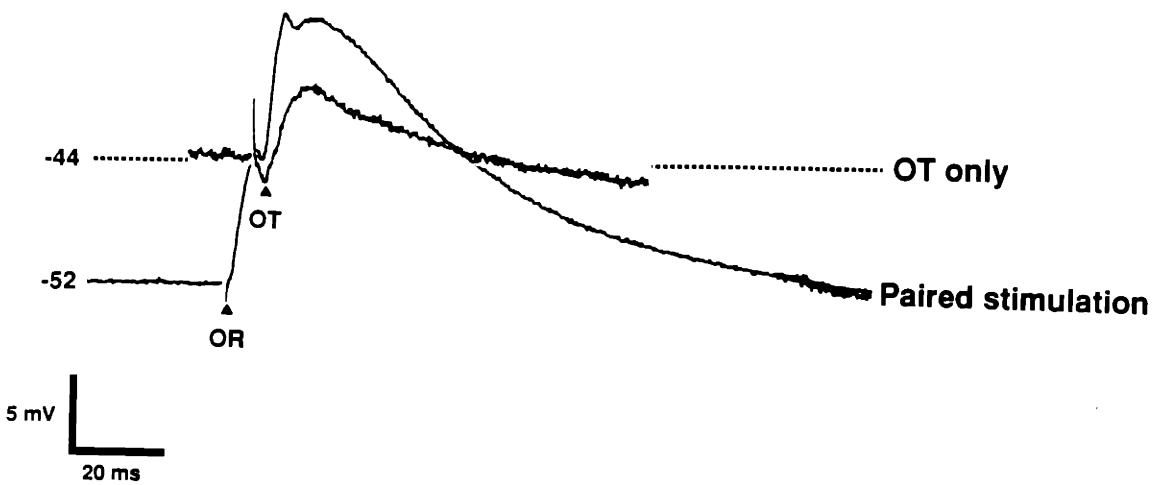

Figure 6

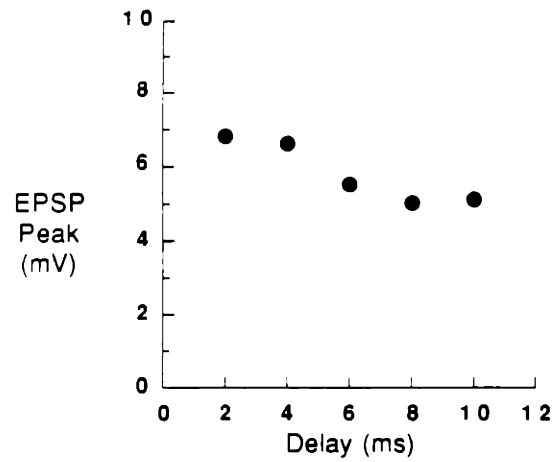
EPSP
Peak
(mV)
10
8
6
4
2
0
0 2 4 6 8 10 12
Delay (ms)

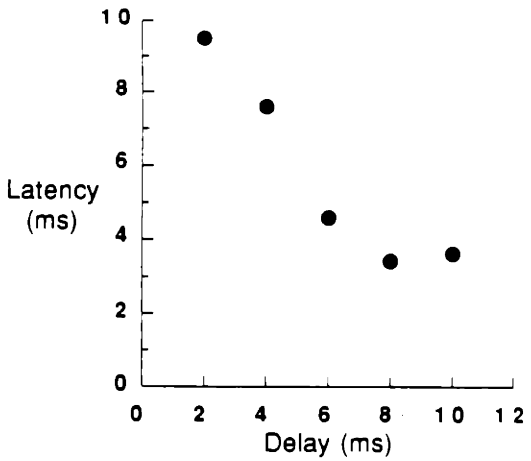
Latency
(ms)
10
8
6
4
2
0
0 2 4 6 8 10 12
Delay (ms)

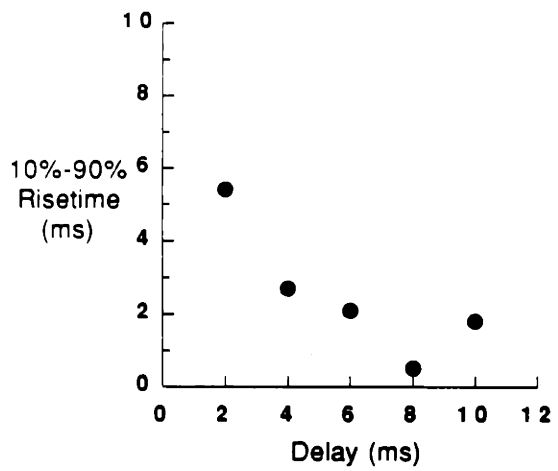
10%-90%
Risetime
(ms)
10
8
6
4
2
0
0 2 4 6 8 10 12
Delay (ms)

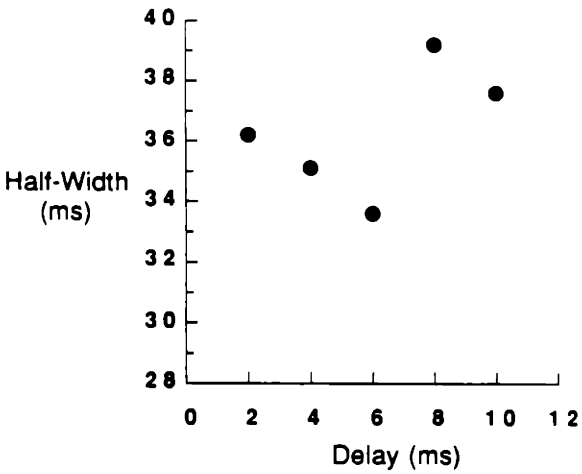
Half-Width
(ms)
40
38
36
34
32
30
28
0 2 4 6 8 10 12
Delay (ms)